Electronic Supplementary Material (ESI) for Polymer Chemistry.

Supporting Information

Xylose-derived thionocarbamates as a synthetic handle towards a functional platform of sugar-based polymers

James R. Runge,[a] Bethan Davies[a] and Antoine Buchard[a,b]*

[a] Department of Chemistry, University of Bath, Claverton Down, Bath BA2 7AY, UK.

[b] Department of Chemistry, University of York, York YO10 5DD, UK.

Email: antoine.buchard@york.ac.uk

Table of Contents

1. Materials and Methods

Unless otherwise stated, all reagents were purchased from either Sigma-Aldrich, Thermo Scientific, Alfa Aesar or Acros Organics and used without further purification. D-xylose was purchased from Carbosynth. All solvents were supplied from VWR chemicals and used without further purification, except for anhydrous solvents, which were purchased from Sigma-Aldrich or Acros Organics and used without further purification. Thin-layer chromatography (TLC) were performed on silica gel and spots visualized with phosphomolybdic acid staining solution (0.1 g mL^{-1} in ethanol). Flash column chromatography was performed either on silica gel (pore size = using a Combi*Flash*® Next Gen 300 from Teledyne equipped with an evaporative light scattering detector (ELSD). RediSep Gold® (20-40 µm particle size, 60 Å pore size) or Bronze® (40-60 µm particle size, 60 Å pore size) disposable silica gel columns were used as the stationary phase. Thiol-ene co-polymerizations were performed in a PhotoRedox TC light box by HepatoChem with a 30 W UV lamp (λ = 365 nm).

^{1}H and ^{13}C{^{1}H} NMR spectra were recorded on a Bruker 400 or 500 MHz instrument and referenced to residual protiated solvent peaks. Spectra were processed and analyzed using the MNova software from Mestrelab. Coupling constants are given in Hertz. The following abbreviations have been used to report splitting patterns (s = singlet, d = doublet, t = triplet, q = quartet and m = multiplet). Polymer conversions were determined by ^{1}H NMR spectroscopy.

Mass spectrometry (MS) analysis was performed on an Agilent QTOF 6545 QTOF with Jetstream ESI spray source coupled to an Agilent 1260 Infinity II Quat pump HPLC with 1260 autosampler, variable wavelength detector (WVD) and column oven compartment. The MS was operated in either positive or negative ionization mode with the gas temperature at 250 °C, the drying gas at 12 L min^{-1} and the nebulizer gas at 45 psi (3.10 bar). The sheath gas temperature and flow were set to 350 °C and 12 L min^{-1} respectively. The MS was calibrated using reference calibrant introduced from the independent ESI reference sprayer. The VCap, Fragmentor, and Skimmer was set 3500, 125 and 45 respectively. All samples were prepared at a concentration of 1 µg mL^{-1} in acetonitrile.

Fourier-transform infrared spectra (FTIR) were recorded on a PerkinElmer Spectrum Two FT-IR spectrometer in the range of 450-4000 cm^{-1} and processed using the PerkinElmer Spectrum software. Data was replotted using OriginPro 2021 software.

Number-average molar masses (M_n) and dispersities ($Đ_M = M_w/M_n$) of polymer samples were determined by **size-exclusion chromatography (SEC)**. This was carried out on an Agilent 1260 Infinity series instrument at 1 mL min^{-1} at 35 °C with a THF eluent using a PLgel 5 µm MIXED-D 300 x 7.5 mm guard column. Detection was carried out using a differential refractive

index (RI) detector (referenced to 11 polystyrene standards of narrow molecular weight, ranging from M_w 615 – 568000 Da). Polymer samples were dissolved at a concentration of 2 mg mL^{-1}.

Glass transition temperatures (T_g) were measured by **differential scanning calorimetry (DSC)** using a MicroSC multicell calorimeter from Setaram employing the Calisto program to collect the data. The measurement cell and the reference cell were both TZero aluminum pans; a mass of 2–10 mg of polymeric material was loaded into the measurement cell with the reference cell empty. The experiment was performed under nitrogen gas and the sample heated and cooled at a rate of 10 °C min^{-1} unless otherwise stated. A second heating and cooling cycle was carried out immediately following completion of the first. The T_g values were taken from the second heating cycle between –60 and 150 °C. Data was processed and analyzed using the TA Universal Analysis software from TA Instruments and plotted using OriginPro 2021 software.

A Setsys Evolution TGA 16/18 from Setaram was used for **thermogravimetric analysis (TGA)**; the Calisto program was employed to collect and process the data. A mass of 10–20 mg of polymeric material was loaded into a 170 µL alumina crucible and the analytical chamber purged with argon (200 mL min^{-1}) for 40 min prior to starting the analysis. The sample was then heated under an argon flow (20 mL min^{-1}) from 30 to 600 °C at a rate of 2 °C min^{-1}. Data was plotted using OriginPro 2021 software. $T_{d,\,5\%}$ refers to the temperature at which 5% mass loss has been achieved and $T_{d,\,max}$ refers to the temperature of the peak of the mass loss derivative.

2. General Synthetic Procedures

2.1 Synthesis of OZT-xylose

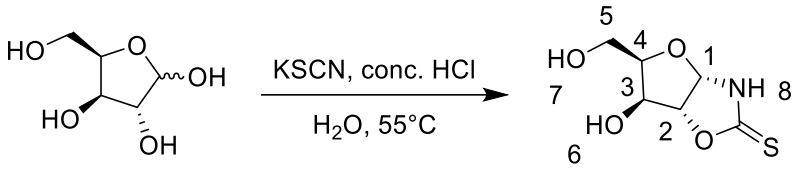

Following an adapted literature procedure:[1] to a round-bottomed flask was charged D-xylose (10.00 g, 66.60 mmol, 1.00 equiv.), potassium thiocyanate (12.95 g, 133.22 mmol, 2.00 equiv.) and DI water (130 mL). The components were stirred until a homogenous solution was obtained after which concentrated hydrochloric acid (32% w/v, 10 mL) was slowly added. The reaction mixture was allowed to stir for 2 hours at room temperature before heating at 55 °C overnight. The solution was concentrated *in vacuo* at 50 °C and the crude product purified *via* silica gel column chromatography (eluent = 100% EtOAc) to yield the xylose-OZT derivative as an off-white solid (9.93 g, 78%). **^{1}H NMR** (400 MHz, $(CD_3)_2SO$): δ 10.76 (s, 1H, H-8), 5.82 (d, *J* = 5.5 Hz, 1H, H-1), 5.52 (d, *J* = 5.1 Hz, 1H, H-6), 5.01 (d, *J* = 5.5 Hz, 1H, H-2), 4.74 (t, *J* = 11.2 Hz, 5.5 Hz, 1H, H-7), 4.16-4.13 (m, 1H, H-3), 3.68-3.62 (m, 2H, H-4, H-5), 3.56-3.48 (m, 1H, H-5'). **^{13}C{^{1}H} NMR** (101 MHz, $(CD_3)_2SO$): δ 188.4 (C=S), 89.9 (C-2), 88.4 (C-1), 80.6 (C-4), 72.3 (C-3), 58.3 (C-5). **MS** *m/z* (ESI+): [$C_6H_9NO_4S+H^+$] theoretical 192.0326, observed 192.0326. **FT-IR** (ATR cm^{-1}): 3423 (O-H stretch), 3144 (N-H stretch), 2980-2887 (C-H (alkane) stretch), 1523 (C-N stretch), 1035 (C=S stretch).

2.2 Synthesis of 10-undecenoic acid anhydride (10-UAA)

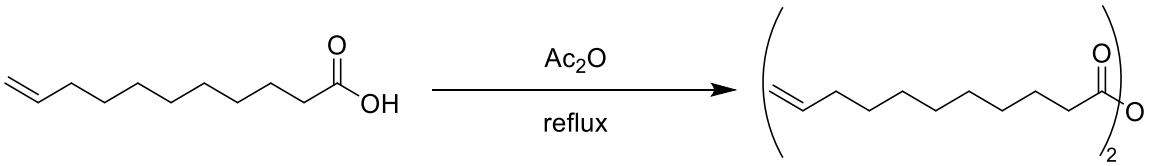

Following an adapted literature procedure:[2] to a round-bottomed flask was charged 10-undecenoic acid (46.68 g, 253 mmol, 1.00 equiv.) and acetic anhydride (119 mL, 1265 mmol, 5.00 equiv.). The components were stirred until a homogeneous solution was obtained. Once fully dissolved, the mixture was heated at reflux for 2.5 hours resulting a pale-yellow solution. The solution was allowed to cool to room temperature and excess acetic acid and acetic anhydride was removed *in vacuo* yielding the product as a pale-yellow oil (46.21 g, 99%). **^{1}H NMR** (400 MHz, $CDCl_3$): δ 5.77 (m, 2H, H-10), 4.87-4.97 (m, 4H, H-11), 2.38-2.42 (m, 4H, H-2), 1.96-2.01 (m, 4H, H-9), 1.57-1.65 (m, 4H, H-3), 1.21-1.38 (m, 21H, H-4-H-8). **^{13}C{^{1}H} NMR**

(101 MHz, CDCl3): δ 169.5 (C-1), 139.0 (C-10), 114.2 (C-11), 35.2 (C-2), 33.8 (C-9), 24.2-29.2 (C-3-C-8) spectroscopic data in accordance with literature.[2]

2.3 Synthesis of 4-pentenoic acid anhydride (4-PAA)

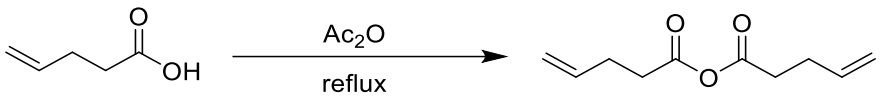

Following an adapted literature procedure:[3] to a round-bottomed flask was charged 4-pentenoic acid anhydride (10.0 g, 99.9 mmol, 1.00 equiv.) and acetic anhydride (45.8 mL, 489.8 mmol, 4.9 equiv.). The components were stirred until a homogenous mixture was obtained. The mixture was heated at reflux for 2.5 hours resulting in a pale-yellow solution. The solution was allowed to cool to room temperature and excess acetic acid and acetic anhydride was removed *in vacuo* yielding the product as an orange oil (9.81 g, 54%). **^{1}H NMR** (400 MHz, $CDCl_3$) δ 5.82-5.72 (m, 2H, H-4), 5.06-4.97 (m, 4H, H-5), 2.53-2.49 (m, 4H, H-2), 2.38-2.32 (m, 4H, H-3). **^{13}C{^{1}H} NMR** (101 MHz, CDCl3) δ 168.6 (C-1) 135.7 (C-4), 116.1 (C-5), 34.4 (C-2), 28.1 (C-3) spectroscopic data in accordance with literature.[3]

2.4 Synthesis of 1a

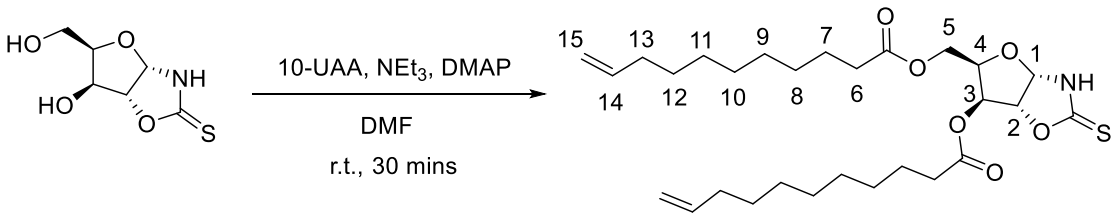

To a 100 mL round-bottomed flask was charged D-xylose-OZT (2.00 g, 10.46 mmol, 1.00 equiv.), 10-undecenoic acid anhydride (9.16 g, 26.15 mmol, 2.50 equiv.) and triethylamine (4.4 mL, 31.38 mmol, 3.00 equiv.). The components were dissolved in anhydrous DMF (40 mL) and stirred until a homogenous solution was obtained. Once fully dissolved, 4-dimethylaminopyridine (DMAP) (0.38 g, 3.13 mmol, 0.30 equiv.) was added and the reaction mixture stirred at room temperature. After 30 minutes, the reaction was quenched by the addition of Amberlyst A-26 OH form resin (10 g) and was stirred for 2 hours. The reaction mixture was diluted with EtOAc (50 m) and the resin removed by vacuum filtration. The resin was further was with EtOAc (2 x 50 mL) and the combined organic phase was transferred to a separating funnel. The organic phase was washed with DI water (3 x 100 mL) to remove excess DMF. The organic phase was collected, dried over $MgSO_4$, filtered, and solvent removed *in vacuo* at 40 °C. The crude product was purified *via* silica gel column chromatography (eluent = 95:5-80:20 Pet Ether:EtOAc) to yield the α,ω-unsaturated OZT diene diester as a colourless waxy solid (1.84 g, 67%). **^{1}H NMR** (400 MHz, $(CD_3)_2SO$)) δ 10.92

(s, 1H, N-H), 5.95 (d, *J* = 5.5 Hz, 1H, H-1), 5.83-5.73 (ddt, *J* = 16.9, 10.2, 6.7 Hz, 2H, H-15), 5.31 (d, *J* = 2.9 Hz, 1H, H-3), 5.26 (d, *J* = 5.6 Hz, 1H, H-2), 5.03 – 4.89 (m, 4H, H-16), 4.26-4.20 (m, 1H, H-5), 4.16-4.09 (m, 2H, H-4, H-5), 2.36-2.27 (m, 4H, H-7), 2.03-1.99 (m, 2H, H-14), 1.54-1.48 (m, 4H, H-8), 1.35-1.24 (m, 21H, H-9-H-13). **$^{13}C\{^{1}H\}$ NMR** (101 MHz, $(CD_3)_2SO$)) δ 188.2 (C=S), 172.5 (C=O), 171.8 (C=O), 138.8 (C-15), 114.6 (C-16), 88.9 (C-1), 87.1 (C-2), 75.5 (C-4), 74.3 (C-3), 60.4 (C-5), 33.2 (C-7), 33.1 (C-14), 28.6-28.2 (C9-13), 24.3 (C-8), 24.1 (C-8'). **MS** *m/z* (ESI+): [$C_{20}H_{45}NO_6S+Na^+$] theoretical 546.2865, observed: 546.2834. **FTIR** (ATR cm^{-1}: 3356 cm^{-1} (N-H stretch), 2925-2851 (C-H (alkane) stretch), 1736 (C=O (ester) stretch), 1479 (C-N stretch), 1161 (C-O (ester) stretch).

2.5 Synthesis of 2a

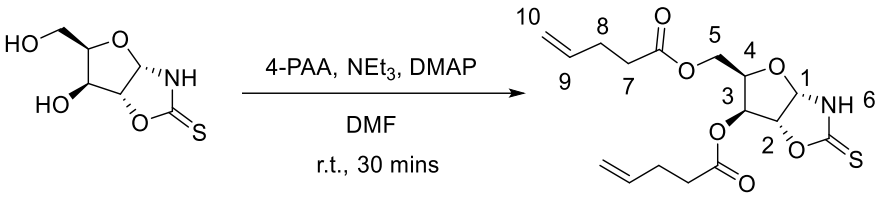

To a 250 mL round-bottomed flask was charged D-xylose OZT (4.00 g, 20.92 mmol, 1.00 equiv.), 4-pentenoic acid anhydride (9.52 g, 52.28 mmol, 2.50 equiv.) and triethylamine (8.8 mL, 62.76 mmol, 3.00 equiv.). The components were dissolved in anhydrous DMF (80 mL) and stirred until a homogenous solution was obtained. Once fully dissolved, 4-dimethylaminopyridine (DMAP) (0.76 g, 6.24 mmol, 0.30 equiv.) was added and the reaction mixture stirred at room temperature. After 30 minutes, the reaction was quenched by the addition of Amberlyst A-26 OH form resin (20 g) and was stirred for 2 hours. The reaction was diluted with EtOAc (2 x 100 mL), and the combined organic phase was transferred to a separating funnel. The organic phase was washed with DI water (3 x 100 mL) to remove excess DMF. The organic phase was collected, dried over $MgSO_4$, filtered, and solvent removed *in vacuo* at 40 °C. The crude product was purified *via* silica gel column chromatography (eluent = 80:20 Pet Ether:EtOAc) to yield the *α,ω*-unsaturated OZT diene diester as a colourless oil (4.92 g, 66%). **^{1}H NMR** (500 MHz, $(CD_3)_2SO$): δ 10.95 (s, 1H, H-6), 5.97 (d, 1H, *J* = 5.1 Hz, H-1), 5.85-5.76 (m, 2H, H-9, H-9'), 5.31 (s, 1H, H-3), 5.26 (d, 1H, *J* = 5.1 Hz, H-2), 5.07-4.97 (m, 4H, H-10, H-10'), 4.29-4.26 (m, 1H, H-5), 4.16-4.11 (m, 2H, H-4, H-5), 2.47-2.40 (m, 4H, H-7, H-7'), 2.31-2.24 (m, 4H, H-8, H-8'). **$^{13}C\{^{1}H\}$ NMR** (125 MHz, $(CD_3)_2SO$): 188.2 (C=S), 171.9 (C=O), 171.2 (C=O), 136.8 (C-9), 136.6 (C-9'), 115.7 (C-10), 115.6 (C-10'), 88.9 (C-1), 87.1 (C-2), 75.6 (C-4), 74.5 (C-3), 60.7 (C-5), 32.5 (C-8), 32.4 (C-8'), 28.3 (C-7), 28.2 (C-7'). **MS** *m/z* (ESI+): [$C_{16}H_{21}NO_6S+Na^+$] theoretical 378.0987, observed 378.0982. **FTIR** (ATR cm^{-1}): 3297 (N-H stretch), 2980-2853 (C-H (alkane) stretch), 1736 (C=O (ester) stretch), 1490 (C-N stretch), 1150 (C-O (ester) stretch), 1039 (C=S stretch).

2.6 General procedure for the S-alkylation of unsaturated OZT *α,ω*-dienes

The respective α,ω-diene (1.00 equiv.) was dissolved in THF (0.5 M) and stirred until homogeneous. Once fully dissolved, the reaction mixture was cooled in an ice bath to 0 °C in an ice bath and the chosen alkyl halide (2.00 equiv.) was slowly added followed by dropwise addition of triethylamine (4.00 equiv.). For compounds **1b-d**, the reaction mixture was allowed to warm to room temperature overnight. For compounds **1e-1h**, the reaction mixture was heated to reflux overnight. After overnight stirring, a white precipitate formed, and excess THF was removed *in vacuo*. The crude residue was taken up in DCM and was washed with water, 1 M $NaHCO_3$, and brine. The organic phase was dried over $MgSO_4$, filtered, and concentrated *in vacuo* at 40 °C. The crude product was purified *via* silica gel flash chromatography (eluent = petroleum ether:EtOAc 100:0 – 80:20) to yield the desired functionalised *α,ω*-diene.

2.6.1 1b

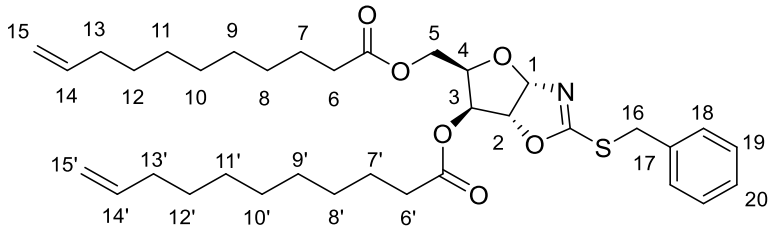

Yield: 40%, **^{1}H NMR** (400 MHz, $CDCl_3$): δ 7.39-7.27 (m, 5H, H-18-H-20), 6.14 (d, 1H, *J* = 5.5 Hz H-1), 5.83-5.76 (ddt, 2H, *J* = 16.1, 10.2, 6.7 Hz, H-14, H-14'), 5.28 (d, 1H, *J* = 3.3 Hz, H-3), 5.01-4.91 (m, 4H, H-15, H-15'), 4.79 (d, 1H, *J* = 5.5 Hz, H-2), 4.34-4.21 (m, 4H, H-5, H-16), 3.98-3.94 (m, 1H, H-4), 2.36-2.29 (m, 4H, H-6, H-6') 2.06-2.01 (m, 4H, H-13, H-13'), 1.63-1.61 (m, 4H, H-7, H-7'), 1.39-1.29 (m, 20H, H-8-H-12, H-8', H-12'). **^{13}C{^{1}H} NMR** (101 MHz, $CDCl_3$): δ 173.4 (C=O), 172.5 (C=O), 170.3 (C-S), 139.1 (C-14), 136.2 (C-17), 129.2 (C-19), 128.8 (C-18), 127.9 (C-20), 114.3 (C-15), 100.2 (C-1), 86.36 (C-2), 75.4 (C-3), 75.1 (C-4), 60.7 (C-5), 36.7 (C-16), 34.2-33.9 (C-6, C-6', C-13, C-13') 29.4-29.0 (C-8, C-8', C-12, C-12'), 24.9 (C-7, C-7'). **MS** *m/z* (ESI+): [$C_{35}H_{51}NO_6S+H^+$] theoretical 614.3510, observed 614.3504. **FTIR** (ATR cm^{-1}): 2926-2855 (C-H (alkane) stretch), 1744 (C=O (ester) stretch), 1598 (C=N stretch), 1133 (C-O (ester) stretch), 699 cm^{-1} (C-S stretch).

2.6.2 1c

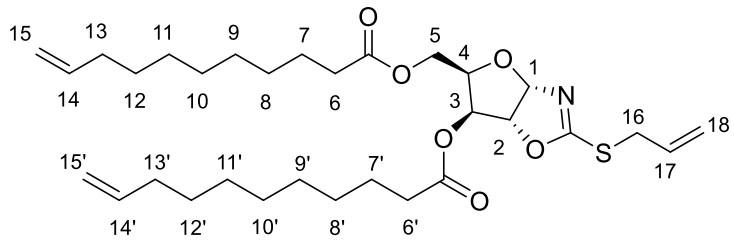

Yield: 70%, **^{1}H NMR** (400 MHz, $CDCl_3$) δ 6.13 (d, 1H, *J* = 5.5 Hz, H-1), 5.96-5.89 (ddt, 1H, *J* = 16.9, 10.0, 6.9 Hz, H-17), 5.84-5.75 (ddt, 2H, J= 16.9, 10.2, 6.7 Hz, H-14, H-14'), 5.34-5.29 (m, 2H, H-18), 5.19-5.16 (m, 1H, H-3), 5.01-4.91 (m, 4H, H-15, H-15'), 4.79 (d, 1H, *J* = 5.5 Hz, H-2), 4.32-4.21 (m, 2H, H-5), 4.03-4.01 (td, 1H, *J* = 6.1, 3.2 Hz, H-4), 3.73-3.68 (m, 2H, H-16), 2.36-2.28 (m, 4H, H-6, H-6'), 2.06-2.01 (m, 4H, H-13, H-13'), 1.63-1.58 (m, 4H, H-7, H-7'), 1.39-1.28 (m, 20H, H-8–H-12, H-8'–H-12'). **^{13}C{^{1}H} NMR** (101 MHz, $CDCl_3$) δ 173.4 (C=O), 172.5 (C=O), 170.2 (C-S), 139.3 (C-14, C-14'), 132.2 (C-17), 119.2 (C-18), 114.3 (C-15, C-15'), 100.2 (C-1), 86.3 (C-2), 75.4 (C-3), 75.2 (C-2), 60.7 (C-5), 35.0 (C-16), 34.1-33.9 (C-6, C-6', C-13, C-13'), 29.4-29.0 (C-8–C-12, C-8'–C-12'), 25.0 (C-7, C-7'). **MS** *m/z* (ESI+): [$C_{31}H_{49}NO_6S$+Na^+] theoretical 586.3173, observed 586.3173. **FT-IR** (ATR) cm^{-1}: 2924-2855 (C-H (alkane) stretch, 1743 (C=O (ester) stretch), 1598 (C=N stretch), 1134 (C-O (ester) stretch), 909 (C=C bend), 634 (C-S stretch).

2.6.3 1d

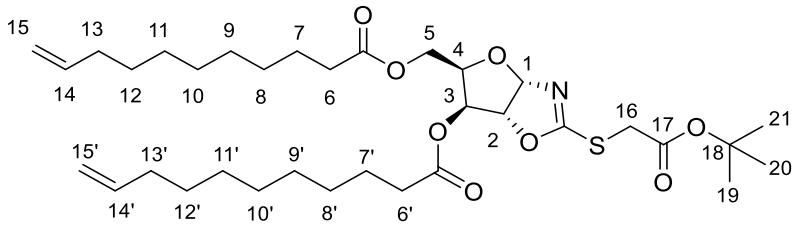

Yield: 40%, **^{1}H NMR** (400 MHz, $CDCl_3$) δ 6.12 (d, 1H, *J* = 5.4 Hz, H-1) 5.86-5.75 (ddt, 2H, *J* = 16.9, 10.3, 6.7 Hz, H-14, H-14') 5.30 (d, 1H, *J* = 3.3 Hz, H-3), 5.01-4.91 (m, 4H, H-15), 4.81 (d, 1H, *J* = 5.5 Hz, H-2), 4.30-4.19 (m, 2H, H-5), 4.04-4.00 (m, 1H, H-4), 3.79 (s, 2H, H-16), 2.36-2.27 (m, 4H, H6, H-6'), 2.06-2.01 (m, 4H, H-13, H-13'), 1.63-1.57 (m, 4H, H-7, H-7'), 1.48 (s, 9H, H-19, H-20, H-21), 1.39-1.28 (m, 20H, H-8-H-12, H8'-H-12'). **^{13}C{^{1}H}** (101 MHz, $CDCl_3$) δ 173.4 (C=O), 172.5 (C=O), 169.5 (C-S), 167.0 (C-17), 139.3 (C-14), 114.3 (C-15), 100.1 (C-1), 86.8 (C-2), 82.9 (C-18), 75.5 (C-3), 75.1 (C-4), 60.7 (C-5), 35.5 (C-16), 34.1-33.9 (C-6, C-6', C-13, C-13'), 29.4-29.0 (C-8-C-12, C-8'-C-12'), 28.1 (C-19, C-20, C-21), 24.9 (C-7, C-7'). **MS** *m/z* (ESI+): [$C_{34}H_{55}NO_8S$+H^+] theoretical 638.3722, observed 638.3722. **FT-IR** (ATR) cm-

[1]: 2935-2855 (C-H (alkane) stretch), 1738 (C=O (ester) stretch), 1603 (C-N stretch), 1133 (C-O (ester) stretch).

2.6.4 1e

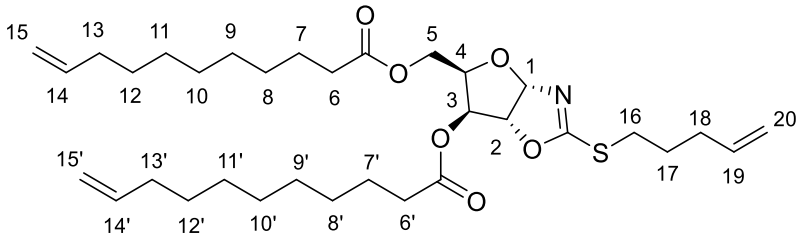

Yield: 45%, **^{1}H NMR** (400 MHz, $CDCl_3$), δ 6.12 (d, 1H, *J* = 5.5 Hz, H-1), 5.86-5.75 (m, 3H, H-14, H-14', H-19), 5.31, (d, 1H, *J* = 3.3 Hz, H-3), 5.14-5.06 (m, 2H, H-20), 5.01-4.96 (m, 4H, H-15, H-15'), 4.78 (d, 1H, *J* = 5.5 Hz, H-2), 4.32-4.21 (m, 2H, H-5, H-5'), 4.03-3.99 (td, 1H, *J* = 6.1, 3.2 Hz, H-4), 3.18-3.07 (m, 2H, H-16), 2.50-2.45 (m, 2H, H-17), 2.36-2.27 (m, 4H, H-6, H-6'), 2.06-2.00 (m, 5H, H-13, H-13', H-18), 1.63-1.57 (m, 4H, H-7, H-7'), 1.40-1.28 (m, 20H, H-8–H-12, H-8'–H-12'). **^{13}C{^{1}H} NMR** (101 MHz, $CDCl_3$) δ 173.4 (C=O), 172.5 (C=O), 170.7 (C-S), 139.3 (C-14, C-14'), 135.6 (C-19), 117.2 (C-20), 114.3 (C-15, C-15'), 100.2 (C-1), 86.2 (C-2), 75.5 (C-3), 75.2 (C-4), 60.7 (C-5), 34.1–33.9 (C-6, C-6' C-13, C-13'), 33.4 (C-17), 31.6 (C-16), 29.4–29.0 (C-8–C-12, C-8'–C-12', C-18), 24.9 (C-7, C-7'). **MS** *m/z* (ESI+): [$C_{33}H_{55}NO_6S+H^+$] theoretical 592.3667, observed 592.363. **FT-IR** (ATR) cm^{-1}: 2926-2853 (C-H (alkane) stretch), 1740 (C=O (ester) stretch), 1599 (C-N stretch), 1135 (C-O (ester) stretch), 908 (C=C bend).

2.6.5 1f

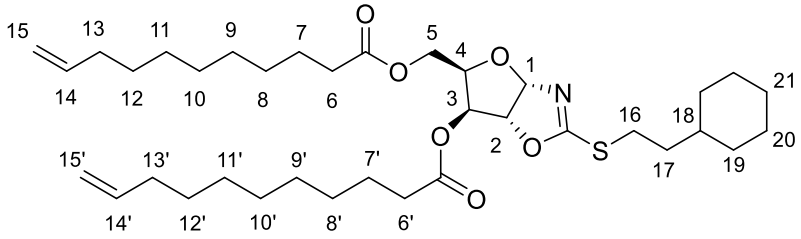

Yield: 44%, **^{1}H NMR** (400 MHz, $CDCl_3$) δ 6.11 (d, 1H, *J* = 5.5 Hz, H-1), 5.86-5.75 (ddt, 2H, *J* = 16.9, 10.2, 6.7 Hz, H-14, H-14'), 5.31 (d, *J* = 3.3 Hz, 1H, H-3), 5.01-4.92 (m, 4H, H-15, H-15'), 4.77 (d, 1H, *J* = 5.4 Hz, H-2), 4.32-4.21 (m, 2H, H-5), 4.03-3.99 (td, 1H, *J* = 6.1, 3.3 Hz, H-4), 3.14-3.02 (m, 2H, H-16), 2.36-2.28 (m, 4H, H-6, H-6'), 2.06-2.01 (m, 4H, H-13, H-13'), 1.74-1.56 (m, 12H, H-7' H-7', Cy), 1.39-1.15 (m, 23H, H-8–H-12, H-8'–H-12', Cy), 0.96-0.83 (m, 3H, Cy). **^{13}C{^{1}H} NMR** (101 MHz, $CDCl_3$) δ 173.4 (C=O), 172.5 (C=O), 171.0 (C-S), 139.2 (C-15, C-15'), 114.3 (C-14, C-14'), 100.2 (C-1), 86.1 (C-2). 75.4 (C-3), 75.2 (C-4), 60.7 (C-5),

37.0 (C-18), 34.2-33.9 (C-6, C-6', C-13, C-13'), 33.1 (C-19), 30.2 (C-16), 29.4-29.0 (C-8–C-12, C-8'–C-12', C-17), 26.6 (C-20), 26.3 (C-21), 24.9 (C-7, C-7'). **MS** *m/z* (ESI+): [$C_{36}H_{59}NO_6S+H^+$] theoretical 634.4136, observed 634.4136. **FT-IR** (ATR) cm^{-1}: 2926-2853 (C-H (alkane) stretch), 1748 (C=O (ester) stretch), 1597 (C-N stretch), 1134 (C-O (ester) stretch), 907 (C=C bend).

2.6.6 1g

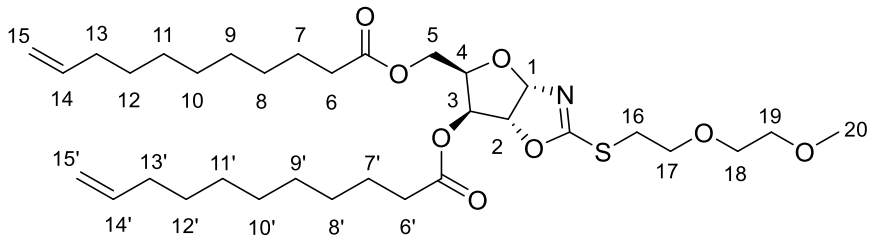

Yield: 37%, **^{1}H NMR** (400 MHz, $CDCl_3$) δ 6.11 (d, 1H, *J* = 5.5 Hz, H-1), 5.85-5.75 (ddt, 2H, *J* = 17.0, 10.2, 6.7 Hz, H-14, H-14'), 5.31 (d, 1H, *J* = 3.2 Hz, H-3), 5.01-4.91 (m, 4H, H-15, H-15'), 4.79 (d, 1H, *J* =. 5.5 Hz, H-2), 4.31-4.22 (m, 2H, H-5), 4.02-3.99 (td, 1H, *J* = 6.1, 3.2 Hz, H-4), 3.76 (t, 2H, *J* = 6.2 Hz, H-17), 3.63-3.54 (m, 4H, H-18, H-19), 3.38 (s, 3H, H-20), 3.34-3.23 (m, 2H, H-16), 2.36-2.27 (m, 4H, H-6, H-6'), 2.06-2.00 (m, 4H, H-13, H-13'), 1.63-1.58 (m, 4H, H-7, H-7'), 1.38-1.28 (m, 20H, H-8-H-12, H-8'-H-12'). **^{13}C{^{1}H} NMR** (101 MHz, $CDCl_3$) δ 173.4 (C=O), 172.5 (C=O), 170.7 (C-S), 139.3 (C-14, C-14'), 114.3 (C-15, C-15'), 100.1 (C-1), 86.4 (C-2), 75.5 (C-4), 75.1 (C-3), 72.0 (C-19), 70.5 (C-18), 69.5 (C-17), 60.7 (C-5), 59.2 (C-20), 34.2-33.9 (C6, C6', C-13, C-13'), 32.2 (C-16), 29.4-29.0 (C-8-C-12, C-8'-C-12'), 24.9 (C-7, C-7'). **MS** *m/z* (ESI+): [$C_{33}H_{55}NO_8S+H^+$] theoretical 626.3722, observed 626.3720. **FT-IR** (ATR) cm^{-1}: 2925-2855 (C-H (alkane) stretch), 1742 (C=O (ester) stretch), 1598 (C-N stretch), 1133 (C-O (ester) stretch), 909 (C=C bend).

2.6.7 1h

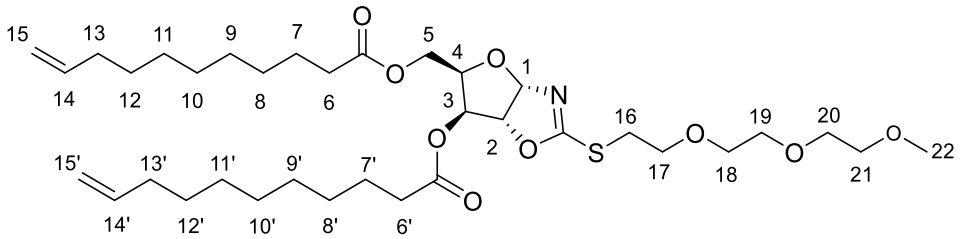

Yield: 40%, **^{1}H NMR** (400 MHz, $CDCl_3$) δ 6.11 (d, *J* = 5.5 Hz, 1H, H-1), 5.85-5.74 (ddt, *J* = 16.8, 10.2, 6.7 Hz, 2H, H-14, H-14'), 5.31 (d, *J* = 3.3 Hz, 1H, H-3), 5.00-4.90 (m, 4H, H-15, H-15'), 4.79 (d, *J* = Hz, 1H, H-2), 4.30-4.20 (m, 2H, H-5), 4.02-3.98 (td, 1H, *J* = 6.0, 3.1 Hz, H-4), 3.75 (t, *J* = 6.0, 3.1 Hz, 2H, H-17), 3.65-3.63 (m, 6H, H-18–H-21), 3.55-3.53 (m, 2H, H-16),

3.37 (s, 3H, H-22), 3.32-3.22 (m, 2H, H-16), 2.35-2.37 (m, 4H, H-6, H-6'), 2.05-2.00 (m, 4H, H-13, H-13'), 1.63-1.57 (m, 4H, H-7, H-7'), 1.38-1.28 (m, 20H, H-8-H-12, H-8'-H-12'). **^{13}C{^{1}H} NMR** (101 MHz, $CDCl_3$) δ 173.4 (C=O), 172.5 (C=O), 170.7 (C-S), 139.3 (C-14, C-14'), 114.3 (C-15, C-15'), 100.1 (C-1), 86.4 (C-2), 75.5 (C-4), 75.1 (C-3), 72.1 (C-17), 70.6-70.4 (C-19–C-21), 69.4 (C-18), 60.6 (C-5), 59.1 (C-22), 34.1-33.9 (C-6, C-6', C-13-C-13'), 32.3 (C-16), 29.4-29.0 (C-8-C-12, C-8'-C-12'), 24.9 (C-7, C-7'). **MS** *m*/z (ESI+) [$C_{35}H_{59}NO_9S+Na^+$] theoretical 692.3803, observed 692.3803. **FT-IR** (ATR cm^{-1}): 2925-2854 (C-H (alkane) stretch), 1745 (C=O (ester) stretch), 1598 (C-N stretch), 1134 (C-O (ester) stretch), 908 (C=C bend).

2.7 General Acyclic Diene Metathesis (ADMET) Polymerisation Procedure

Following an adapted literature procedure[4]: to an oven-dried round-bottomed flask was charged the respective α,ω-diene monomer (1.00 equiv.) and Grubbs second-generation catalyst (0.02-0.05 equiv.). The flask was placed into an oil bath at 90 °C and a dynamic vacuum was applied. After 20 hours, the vacuum was stopped, and the flask was removed from the oil bath and allowed to cool. THF was added to solubilize the residue and reaction was quenched with ethyl vinyl ether (0.5 mL) and stirred at room temperature for 20 minutes. The polymer was precipitated in cold methanol (25 mL) and separated by centrifugation (3500 rpm, 5 minutes). The solid phase was collected, washed twice more with methanol, and dried in a vacuum oven at 70 °C.

2.8 General procedure for the thiol-ene polymerization of xylose-OZT diene diesters

To a dram vial was measured the OZT-diene diester co-monomer (1.00 equiv.) and dissolved in chloroform (0.5 M). Once fully dissolved, the chosen dithiol co-monomer (1.00 equiv.) and Irgacure 819 (0.1 equiv.) were added. The solution was irradiated (λ = 365 nm) for 3 hours before precipitation into cold methanol. The resulting suspension was centrifuged (3500 rpm) for 5 minutes, the supernatant decanted, and the product washed with cold methanol (3 x 10 mL). After drying in a vacuum oven overnight at 70 °C, the co-polymer was isolated as a viscous yellow material or rubbery orange solid.

2.9 General procedure for the S-alkylation of OZT thiol-ene polymers

The respective OZT thiol-ene polymer (1.00 equiv.) was dissolved in THF (0.5 mol L^{-1}) and stirred until a homogenous mixture was obtained. The solution was cooled to 0 °C followed by the slow addition of the chosen R-X compound (0.5-2.00 equiv.) followed by the dropwise

addition of triethylamine (1.00-4.00 equiv.). The reaction mixture was allowed to warm to room temperature overnight. After 24 hours, a white precipitate formed, and an aliquot was taken to determine conversion by ^{1}H NMR spectroscopy. Chloroform was charged to reaction mixture and the solution was added dropwise into cold methanol to precipitate the functionalized polymer and was separated by centrifugation (3500 rpm, 5 minutes). The solid was phase collected, washed twice more with cold methanol, and dried in a vacuum oven at 70 °C to yield the functionalized polymer.

3. NMR Spectra of Compounds

3.1 Small Molecules

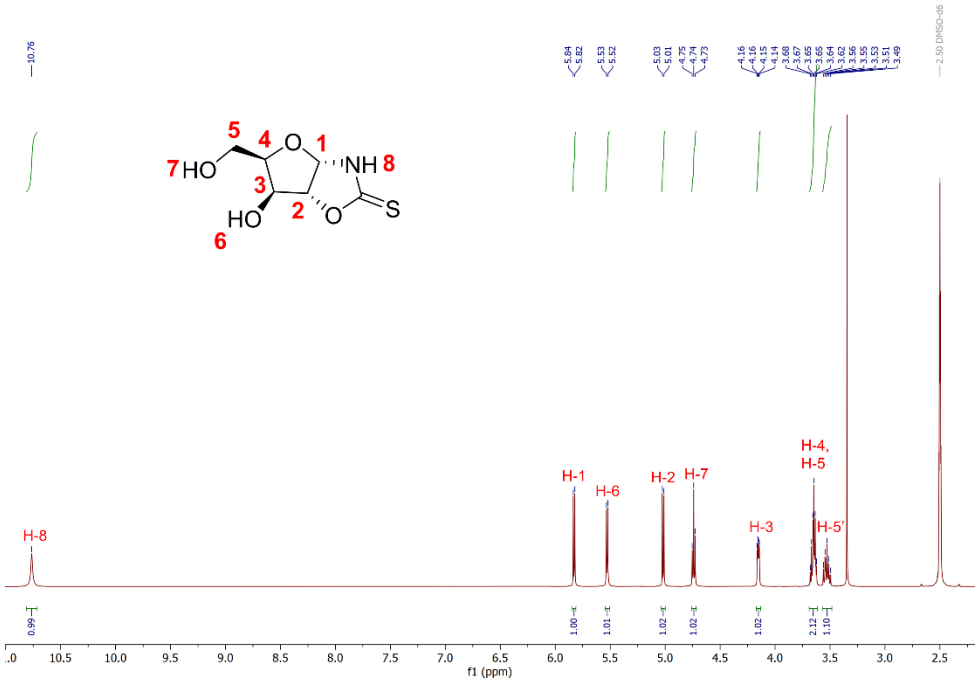

Figure S1: ^{1}H NMR spectrum of OZT-xylose (residual $(CD_3)_2SO$ signal at 2.50 ppm).

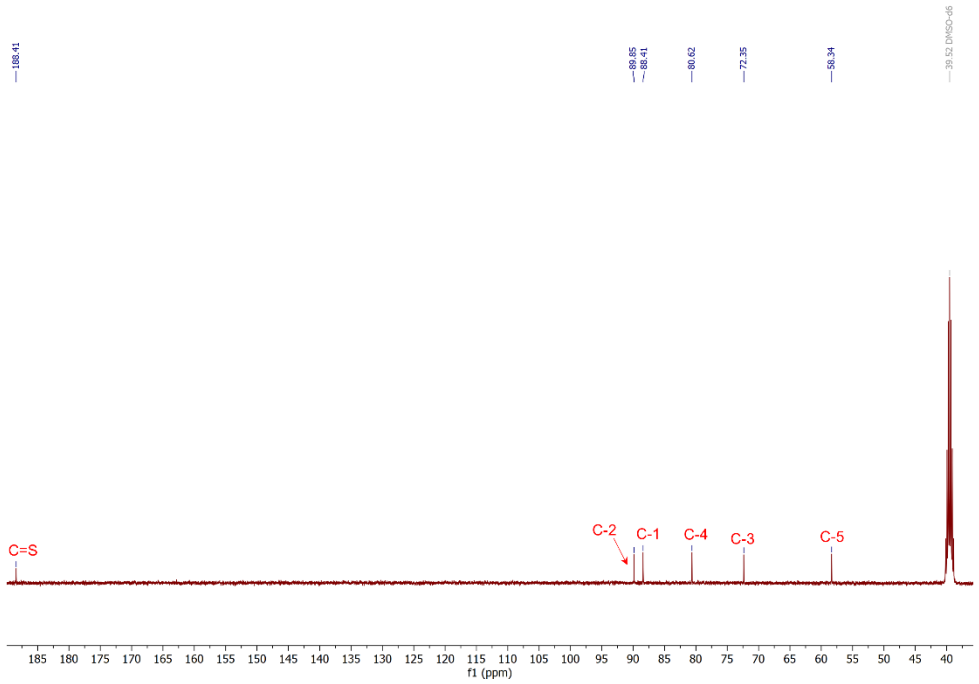

Figure S2: $^{13}C\{^{1}H\}$ NMR spectrum of OZT-xylose (residual $(CD_3)_2SO$ signal at 39.5 ppm).

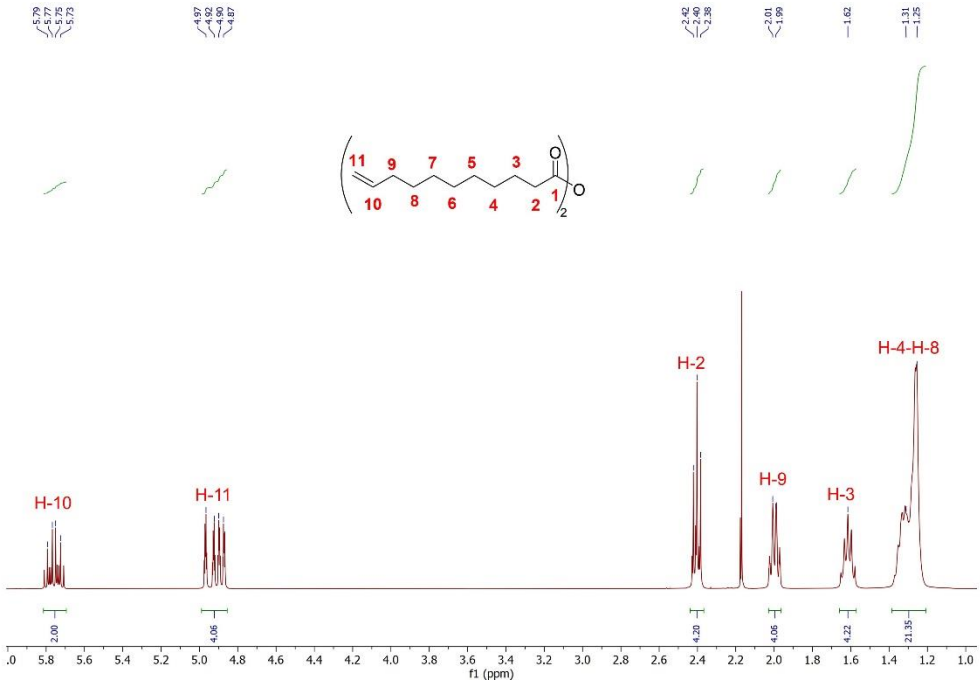

Figure S3: ^{1}H NMR spectrum of 10-undecenoic acid anhydride (residual $CDCl_3$ signal at 7.26 ppm).

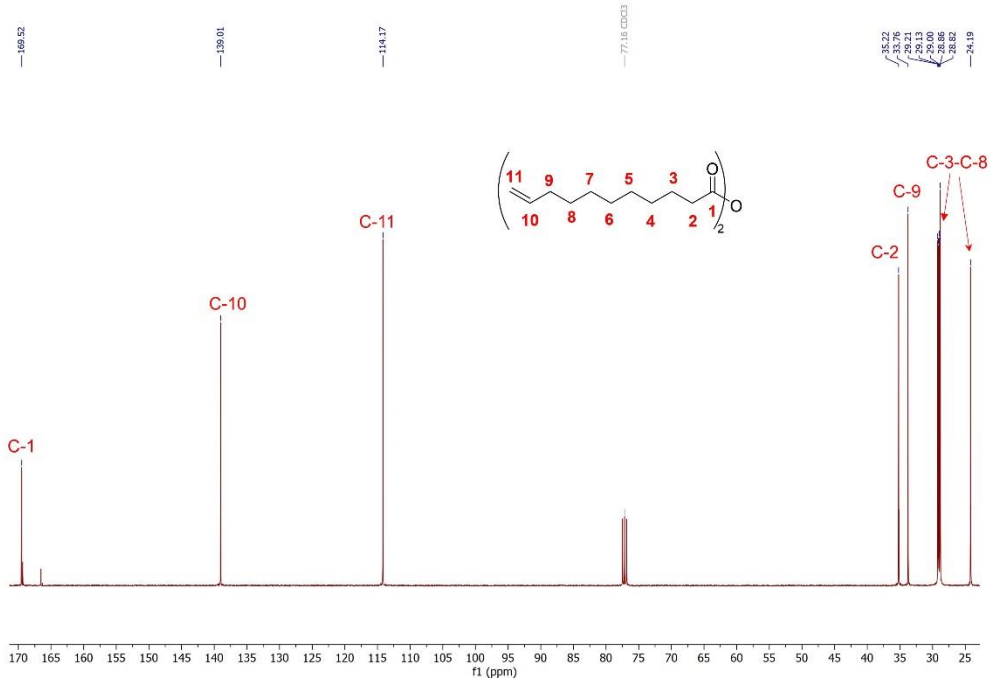

Figure S4: $^{13}C\{^{1}H\}$ NMR spectrum of 10-undecenoic acid anhydride (residual $CDCl_3$ signal at 77.2 ppm).

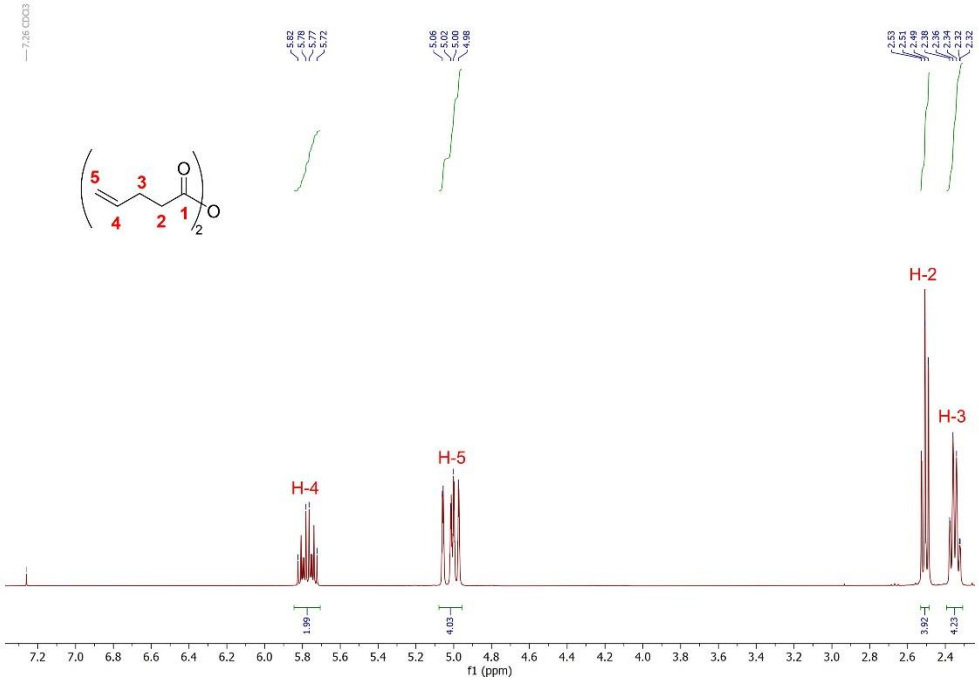

Figure S5: ^{1}H NMR spectrum of 4-pentenoic acid anhydride (residual $CDCl_3$ signal at 7.26 ppm).

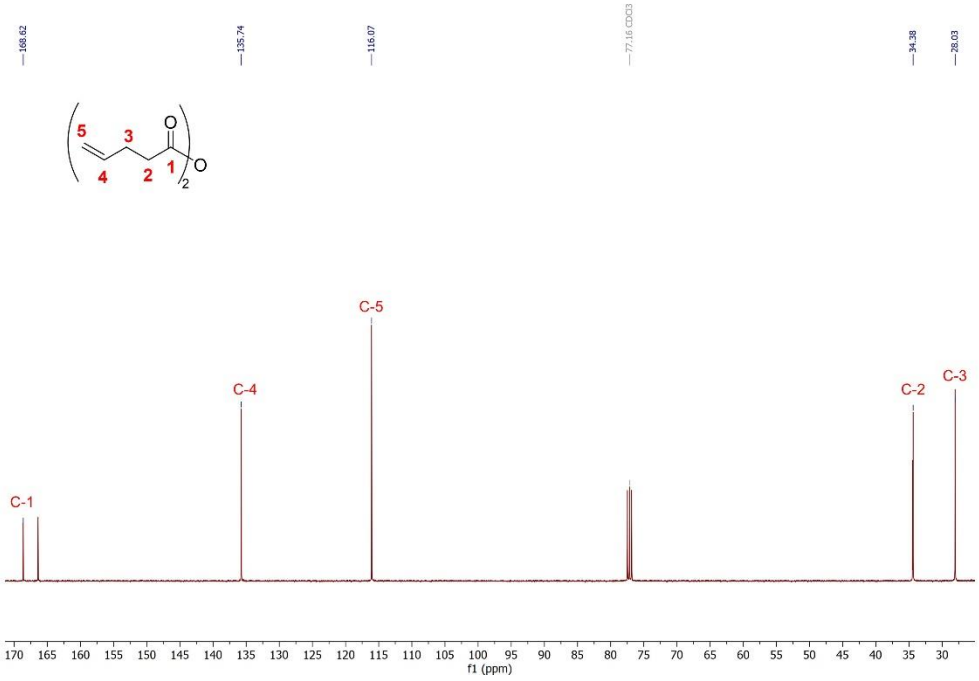

Figure S6: ^{1}H NMR spectrum of 4-pentenoic acid anhydride (residual $CDCl_3$ signal at 7.26 ppm).

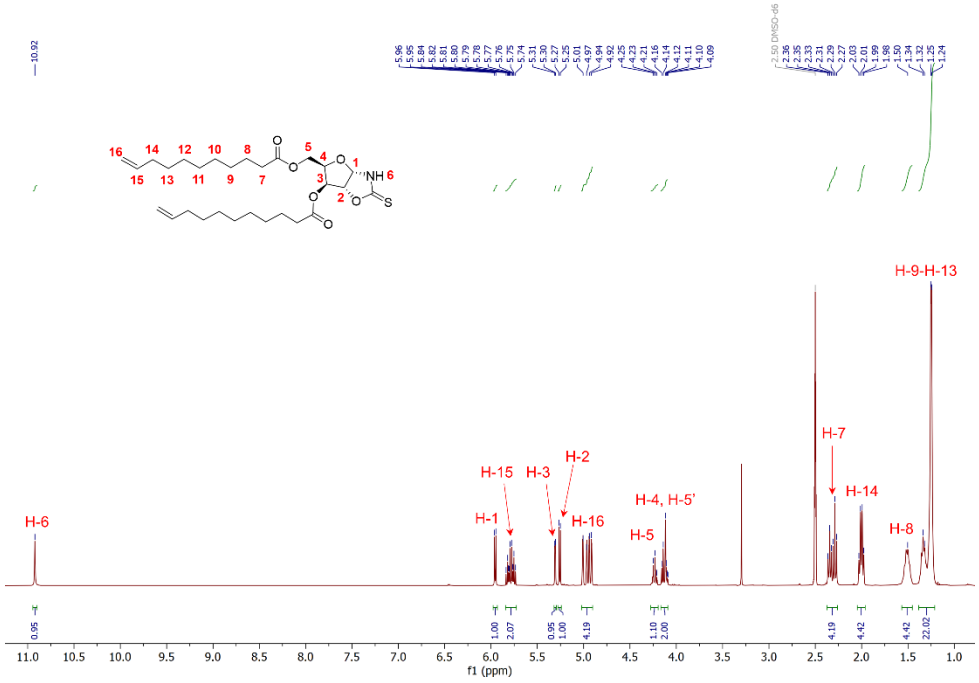

Figure S7: ^{1}H NMR spectrum of monomer **1a** (residual $(CD_3)_2SO$ signal at 2.50 ppm).

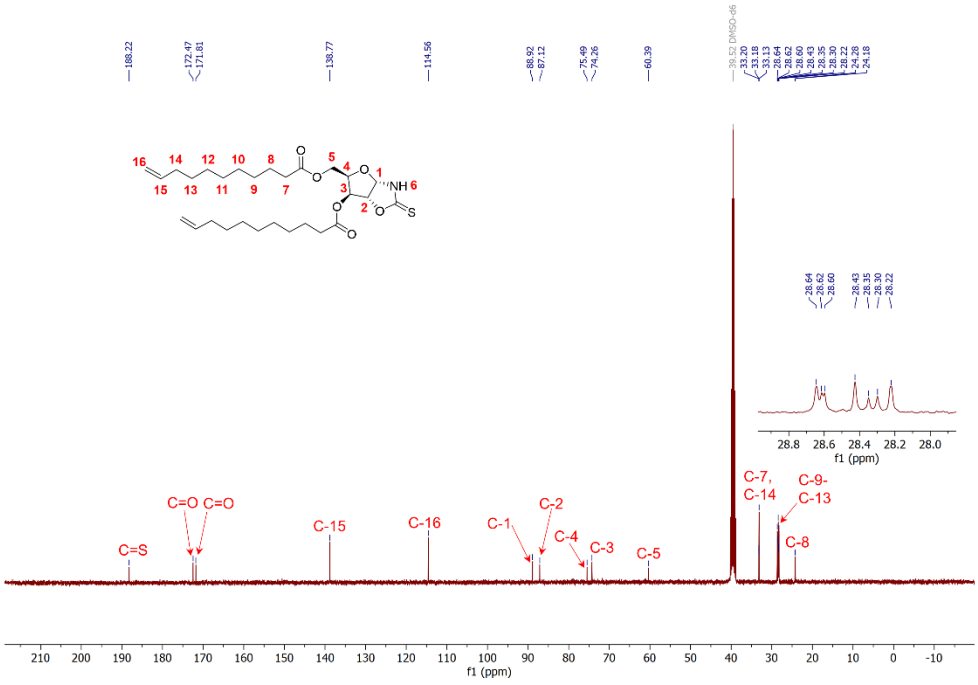

Figure S8: $^{13}C\{^{1}H\}$ NMR spectrum of monomer **1a** (residual $(CD_3)_2SO$ signal at 2.50 ppm).

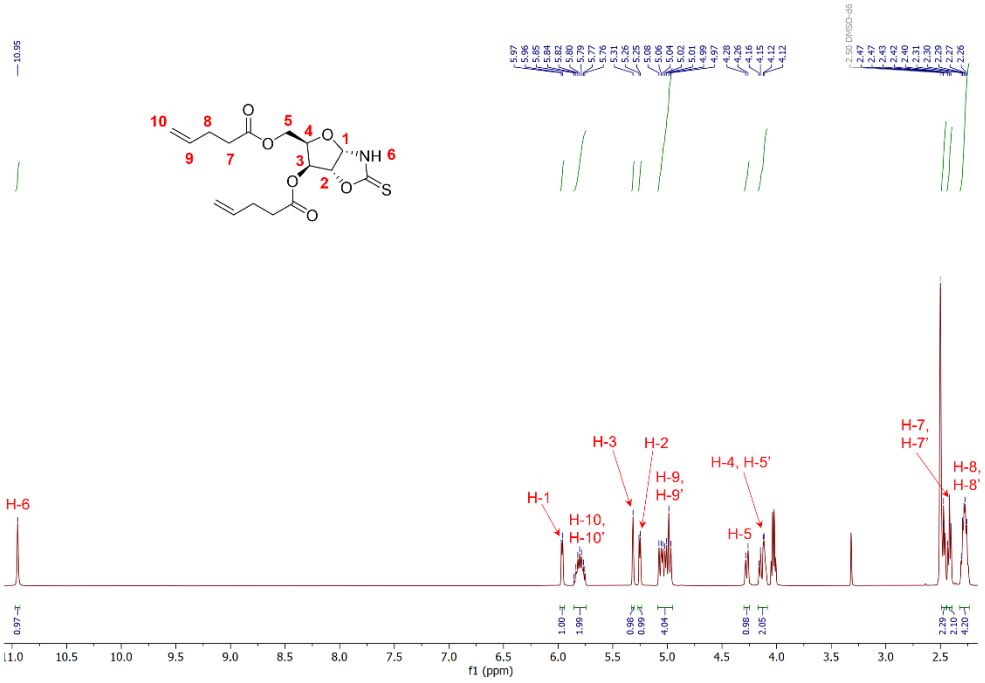

Figure S9: ^{1}H NMR spectrum of monomer **2a** (residual $(CD_3)_2SO$ signal at 2.50 ppm).

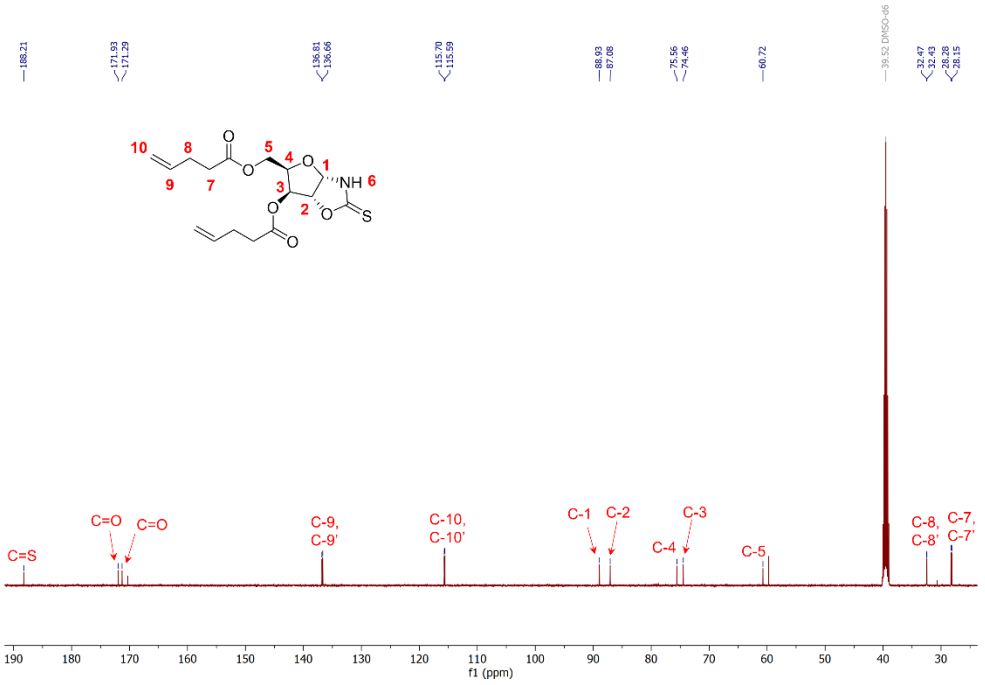

Figure S10: $^{13}C\{^{1}H\}$ NMR spectrum of monomer **2a** (residual $(CD_3)_2SO$ signal at 39.5 ppm).

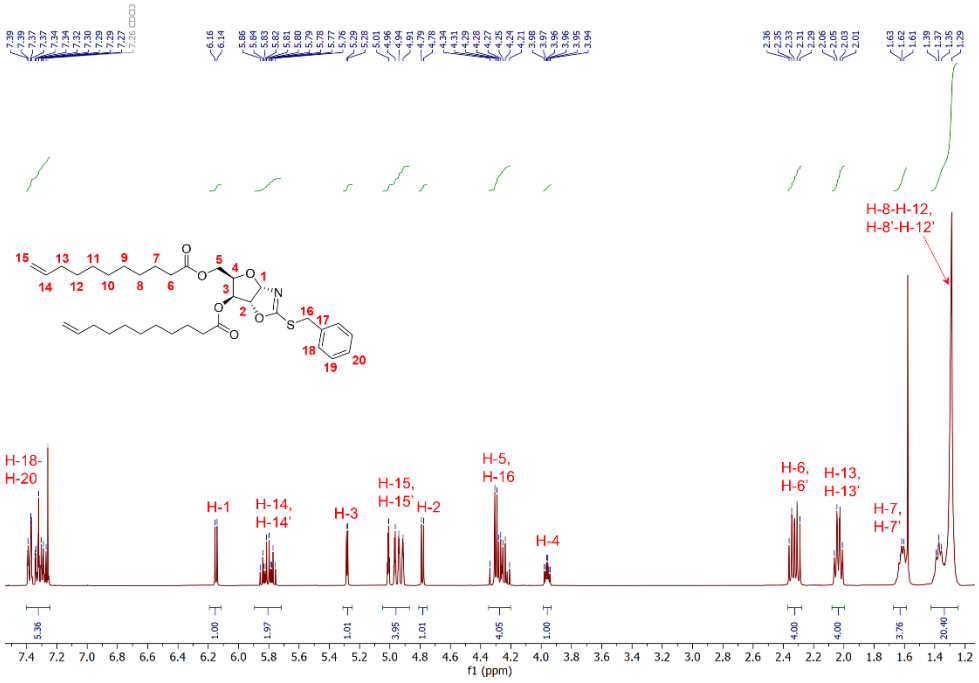

Figure S11: ^{1}H NMR spectrum of monomer **1b** (residual $CDCl_3$ signal at 7.26 ppm).

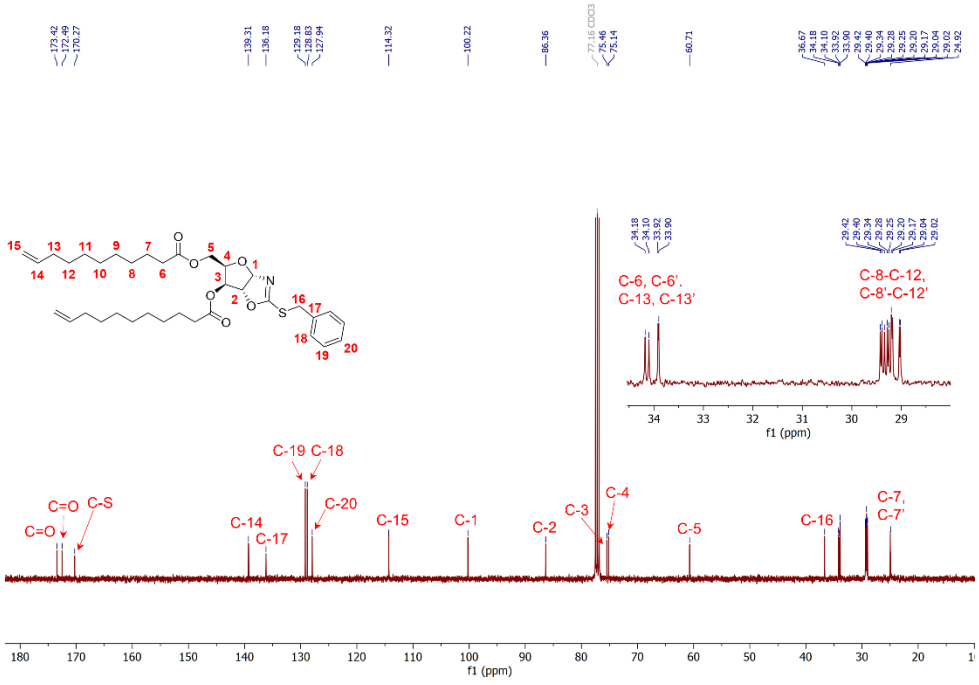

Figure S12: $^{13}C\{^{1}H\}$ NMR spectrum of monomer **1b** (residual $CDCl_3$ signal at 77.2 ppm).

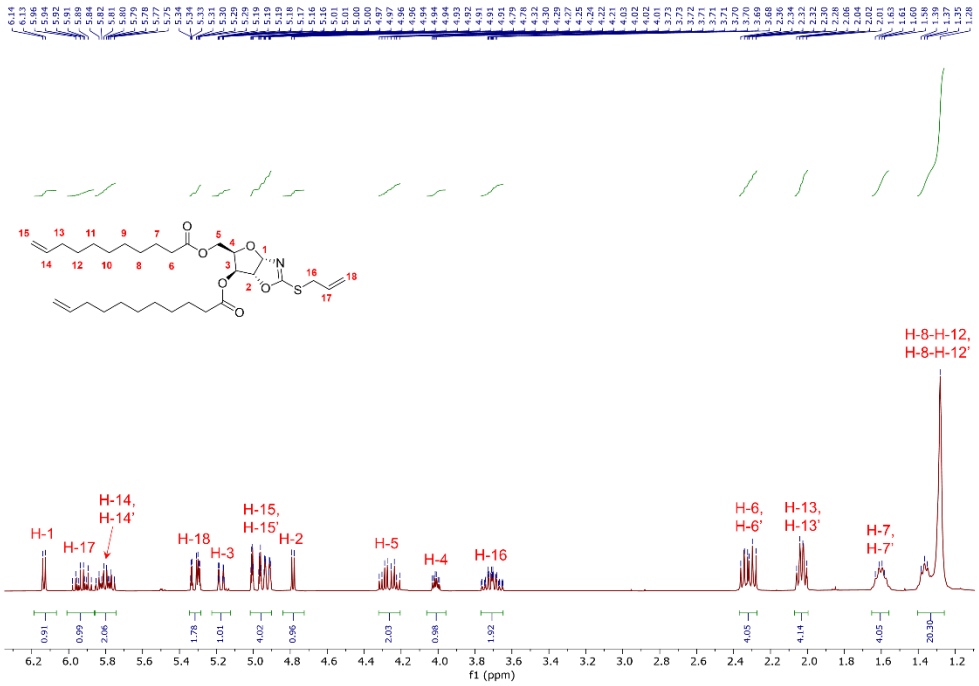

Figure S13: ^{1}H NMR spectrum of monomer **1c** (residual $CDCl_3$ signal at 7.26 ppm).

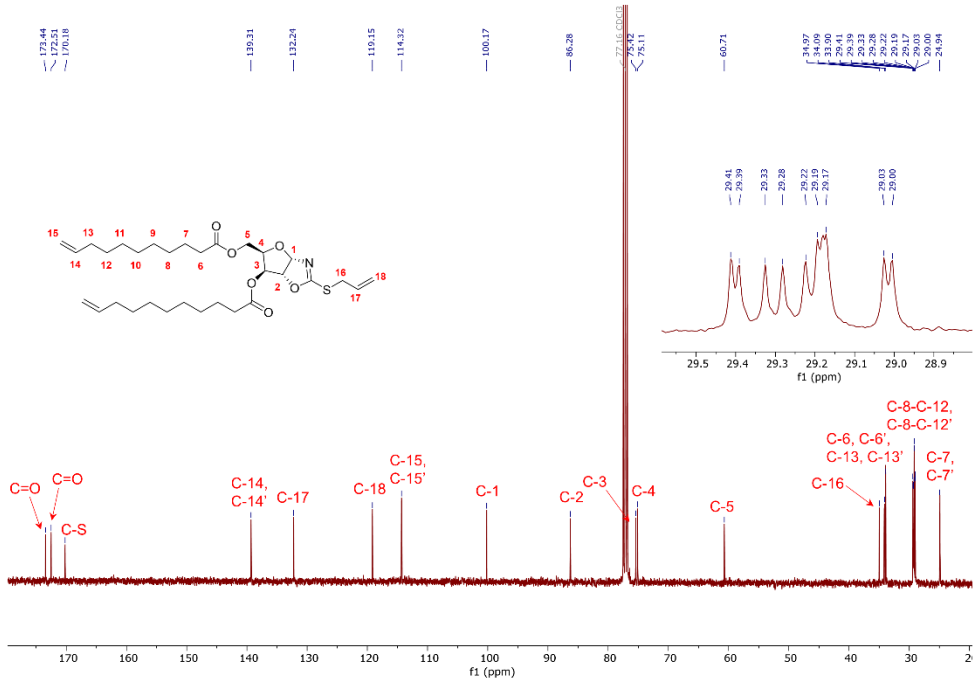

Figure S14: $^{13}C\{^{1}H\}$ NMR spectrum of monomer **1c** (residual $CDCl_3$ signal at 77.2 ppm).

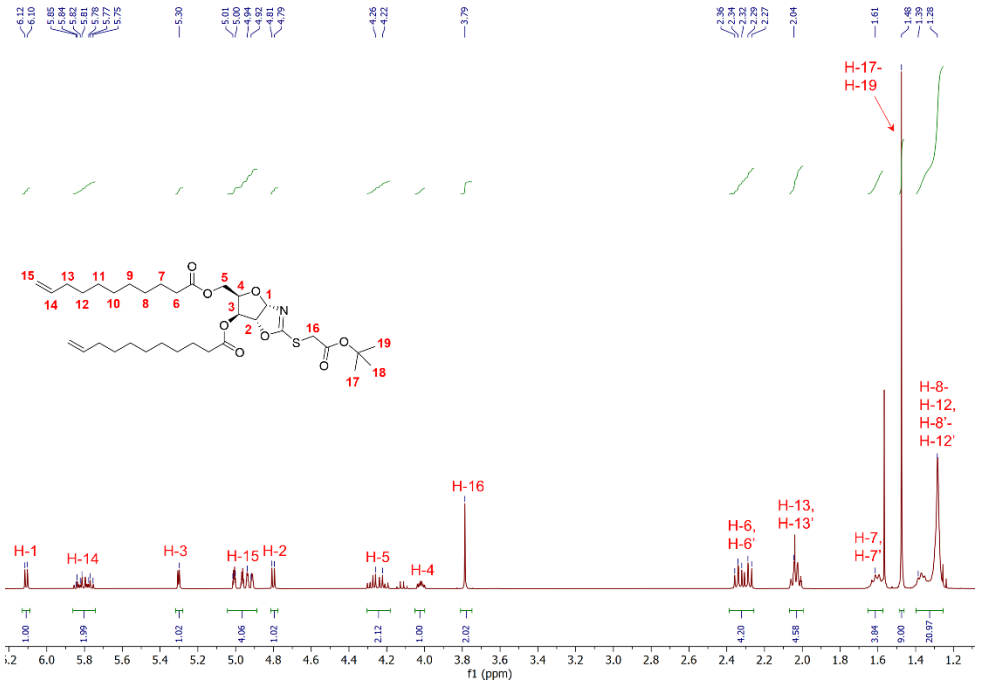

Figure S15: ^{1}H NMR spectrum of monomer **1d** (residual $CDCl_3$ signal at 7.26 ppm).

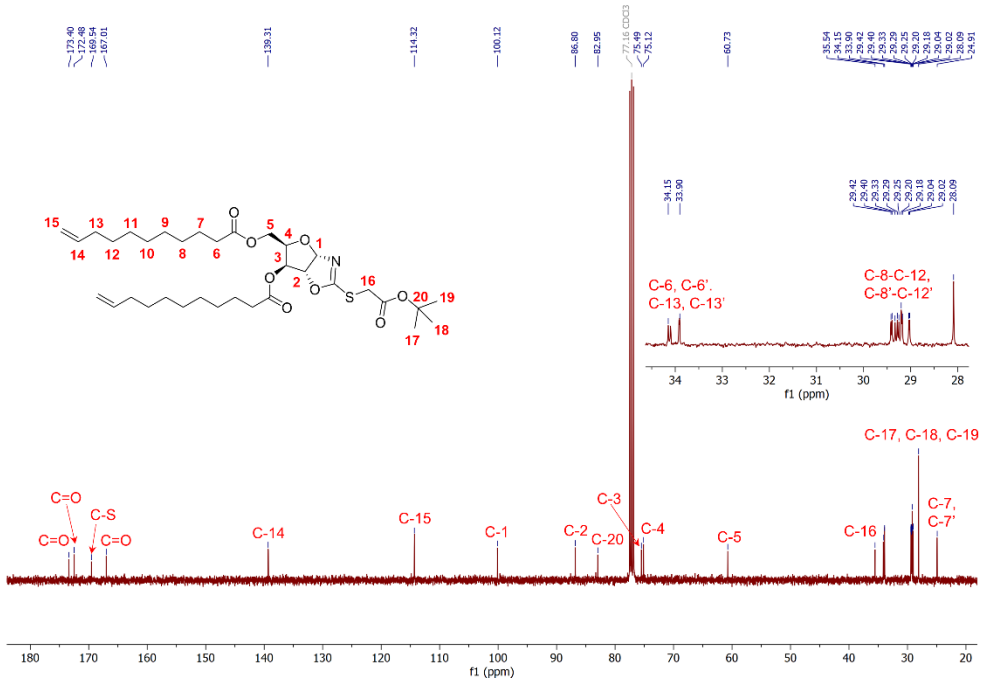

Figure S16: $^{13}C\{^{1}H\}$ NMR spectrum of monomer **1d** (residual $CDCl_3$ signal at 77.2 ppm).

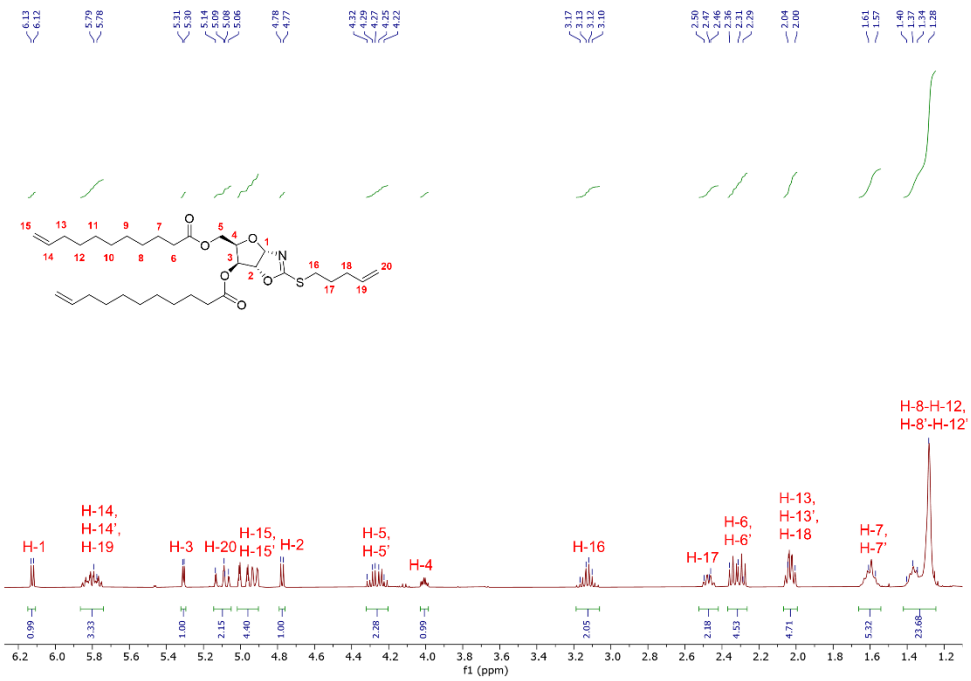

Figure S17: ^{1}H NMR spectrum of monomer **1e** (residual $CDCl_3$ signal at 7.26 ppm).

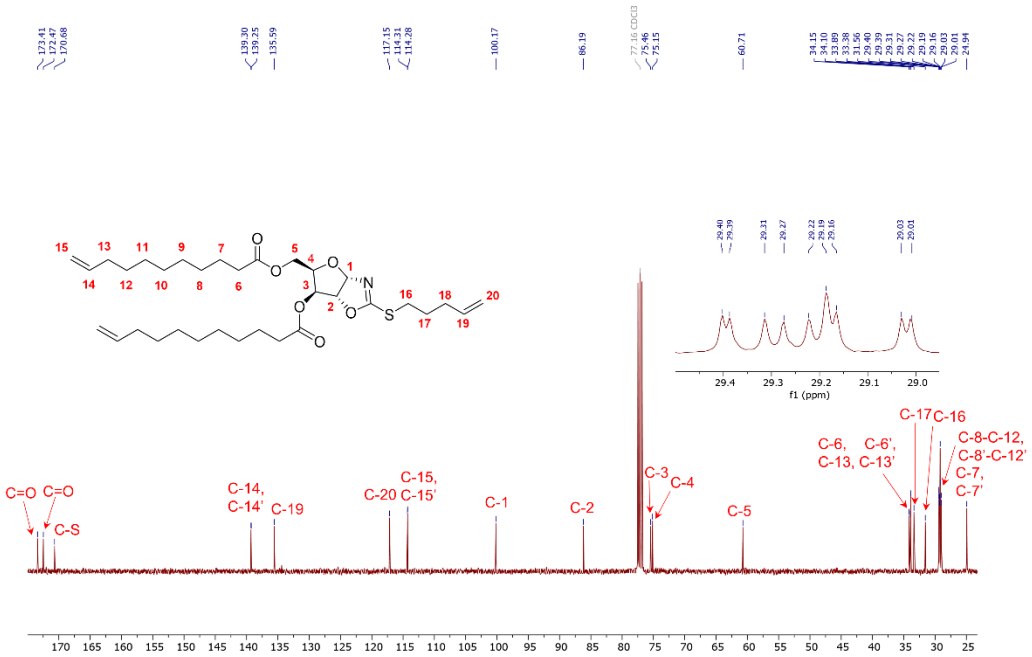

Figure S18: $^{13}C\{^{1}H\}$ NMR spectrum of monomer **1e** (residual $CDCl_3$ signal at 77.2 ppm).

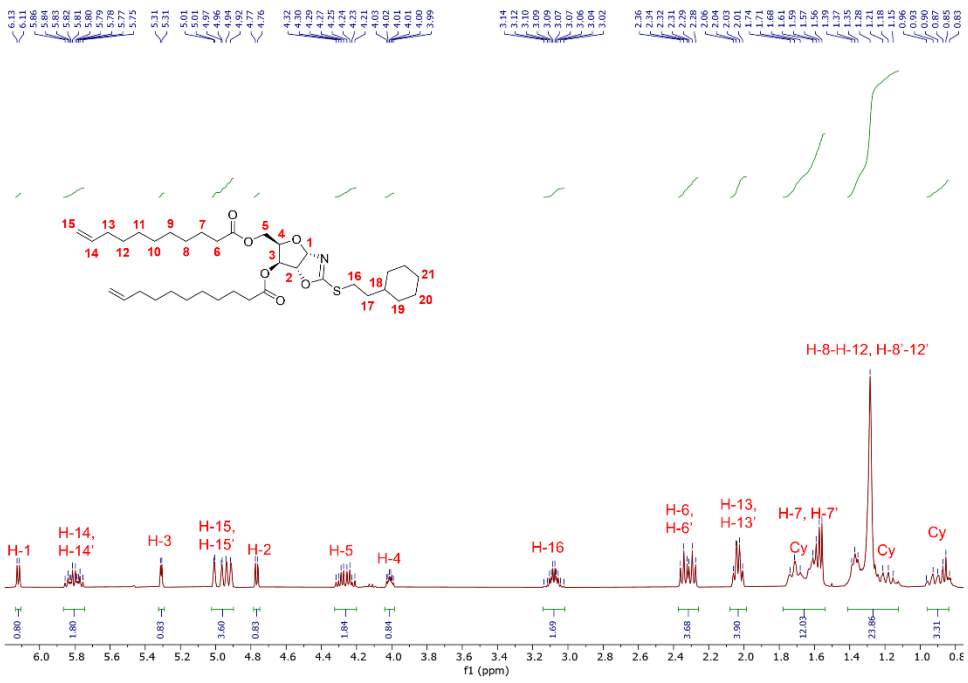

Figure S19: ^{1}H NMR spectrum of monomer **1f** (residual $CDCl_3$ signal at 7.26 ppm).

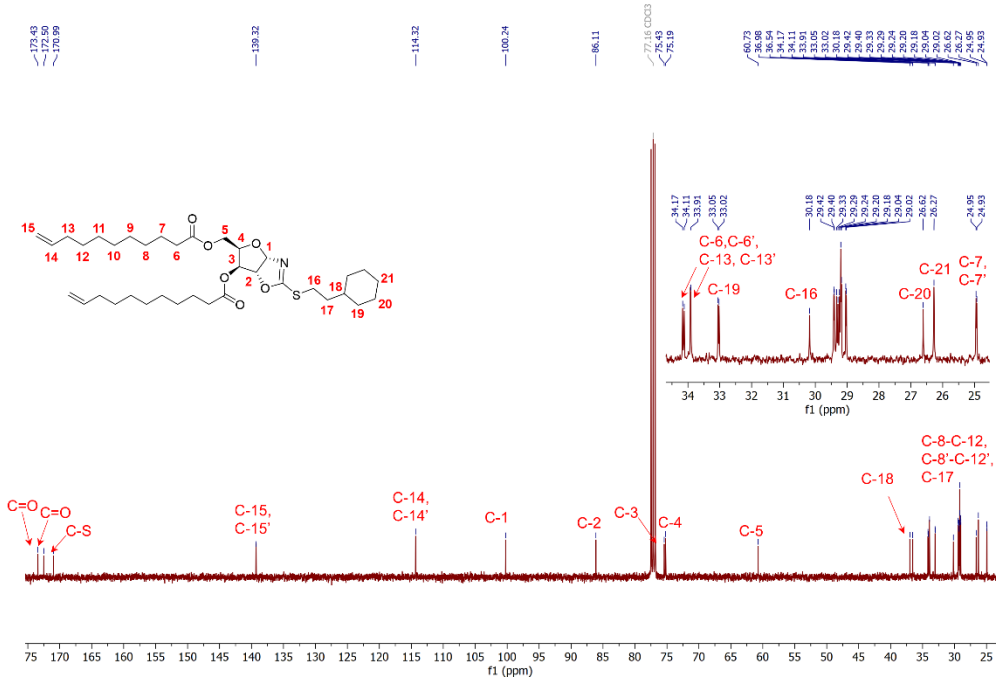

Figure S20: $^{13}C\{^{1}H\}$ NMR spectrum of monomer **1f** (residual $CDCl_3$ signal at 77.2 ppm).

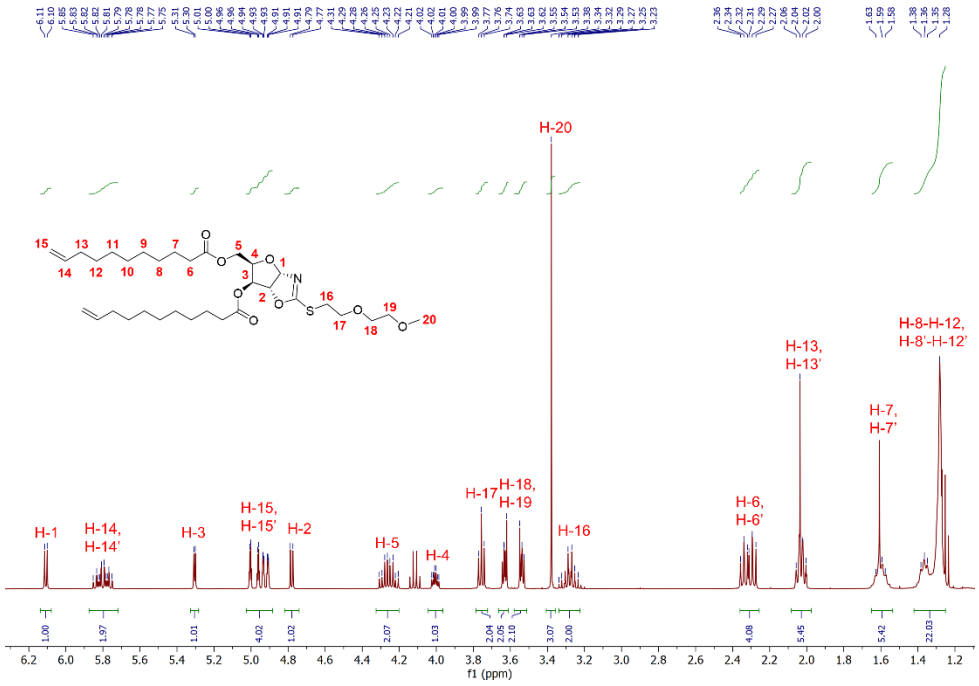

Figure S21: ^{1}H NMR spectrum of monomer **1g** (residual $CDCl_3$ signal at 7.26 ppm).

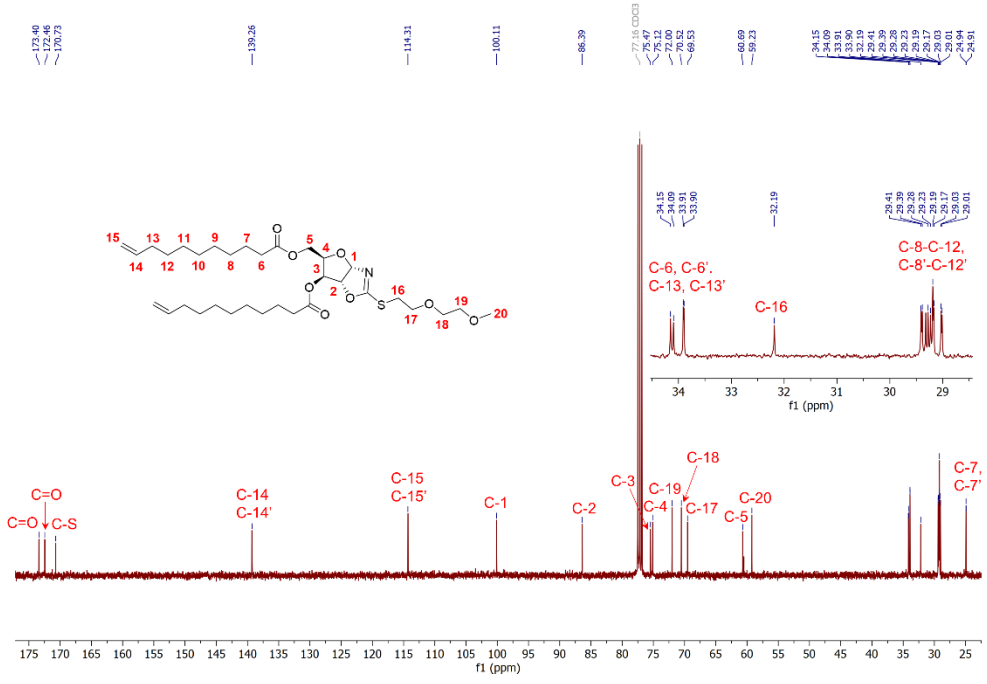

Figure S22: $^{13}C\{^{1}H\}$ NMR spectrum of monomer **1g** (residual $CDCl_3$ signal at 77.2 ppm).

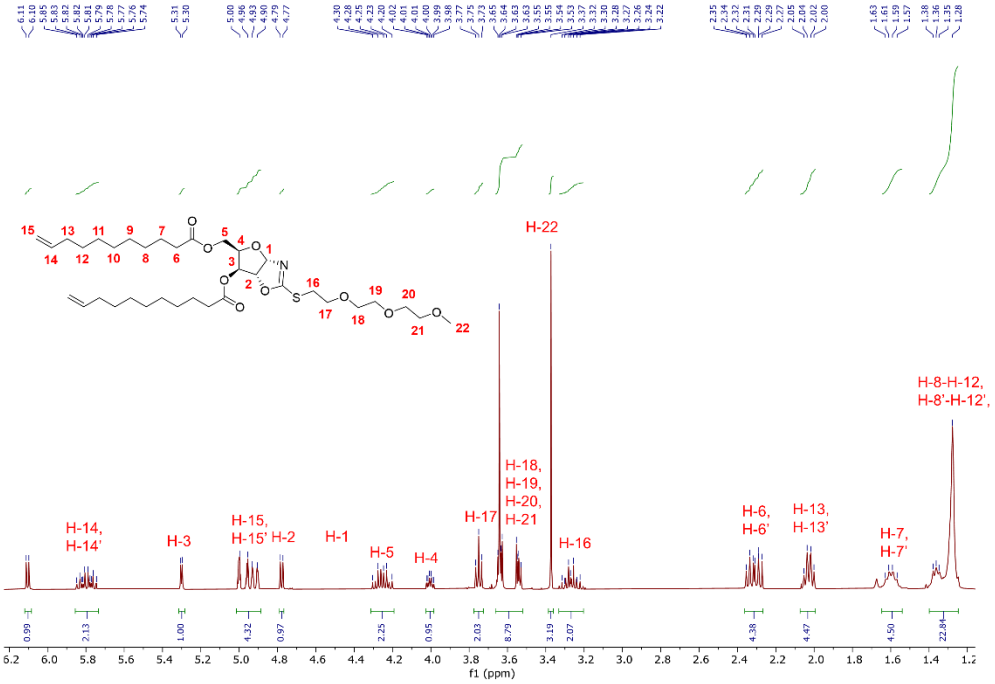

Figure S23: ^{1}H NMR spectrum of monomer **1h** (residual $CDCl_3$ signal at 7.26 ppm).

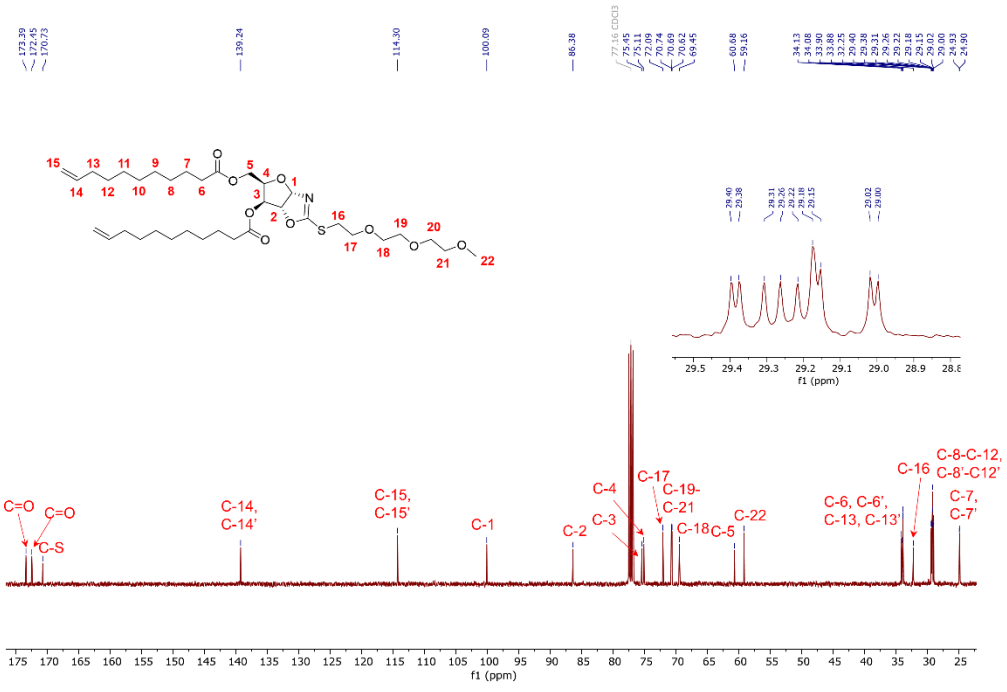

Figure S24: $^{13}C\{^{1}H\}$ NMR spectrum of monomer **1h** (residual $CDCl_3$ signal at 77.2 ppm).

3.2 Polymers

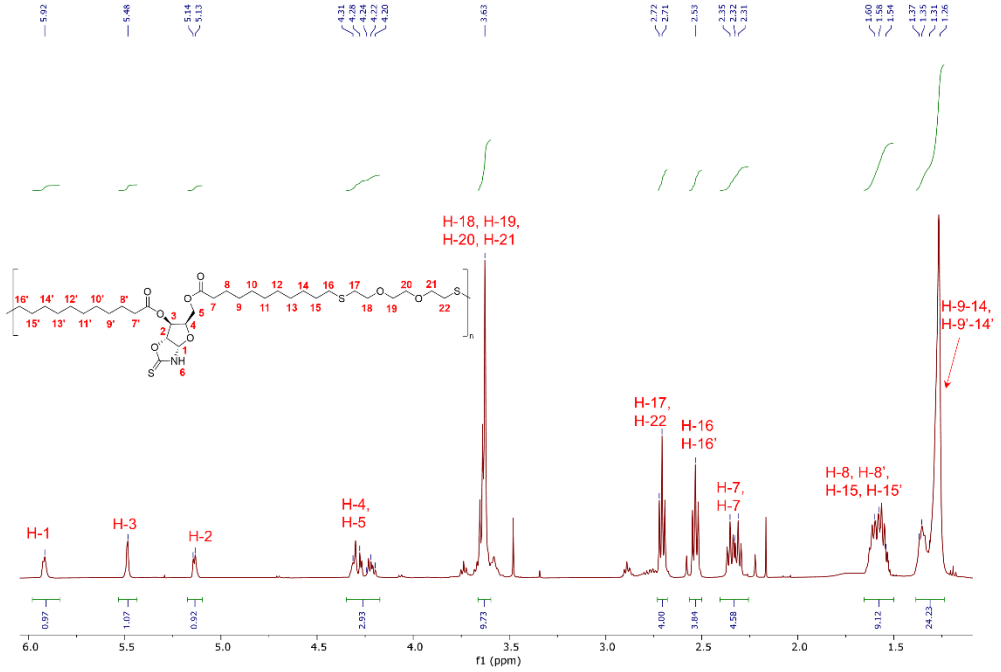

Figure S25: ^{1}H NMR spectrum of poly(**1a**-EDT) (Table 1, entry 1) (residual $CDCl_3$ signal at 7.26 ppm).

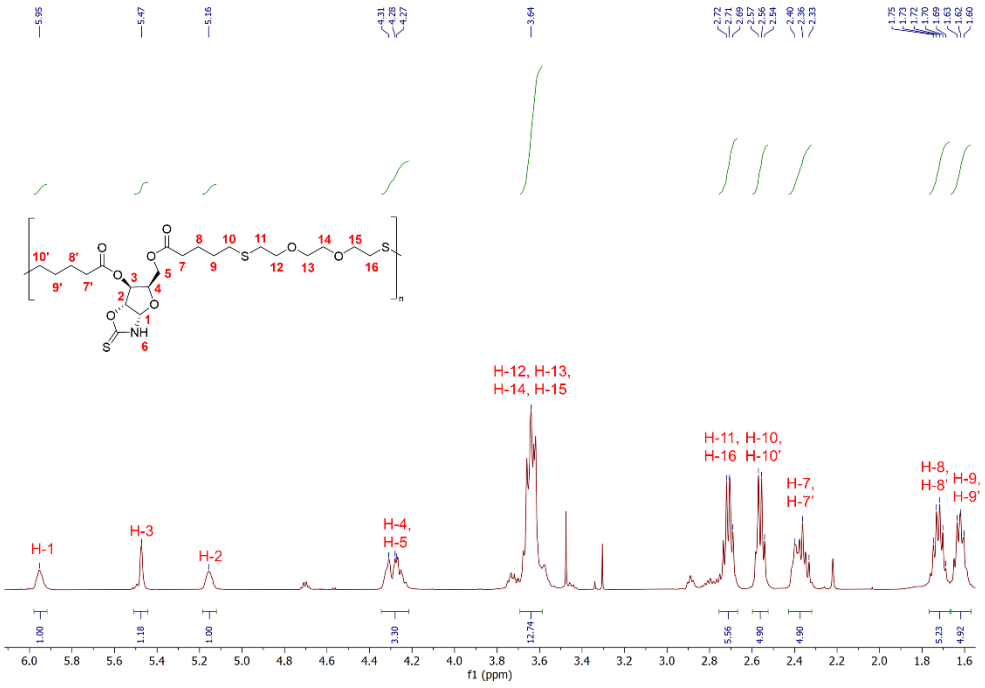

Figure S26: ^{1}H NMR spectrum of poly(**2a**-EDT) (Table 1, entry 2) (residual $CDCl_3$ signal at 7.26 ppm).

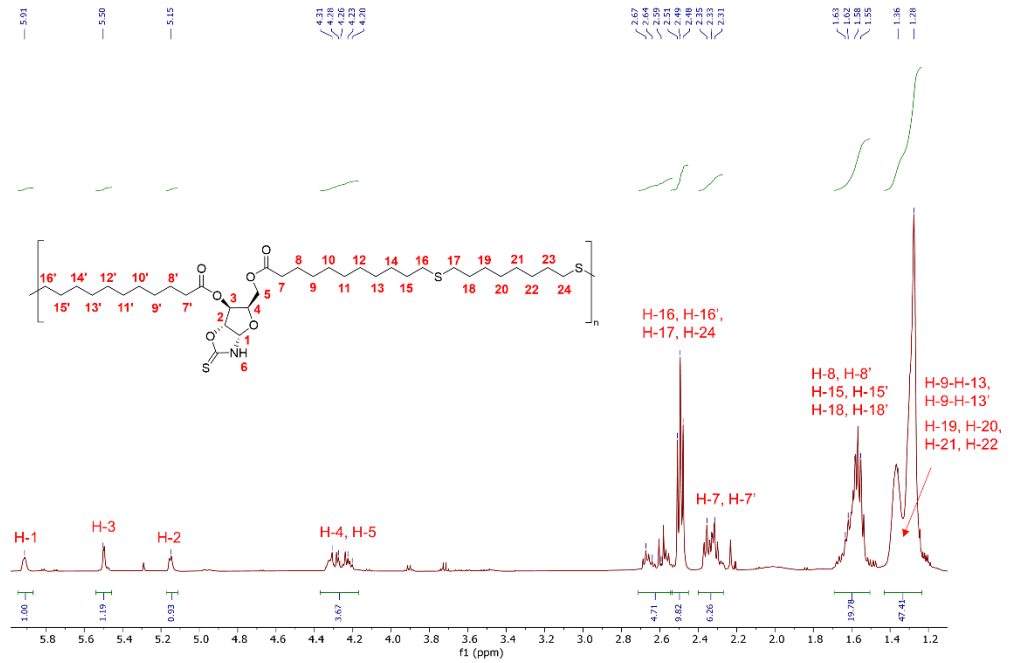

Figure S27: ^{1}H NMR spectrum of poly(**1a**-ODT) (Table 1, entry 3) (residual $CDCl_3$ signal at 7.26 ppm).

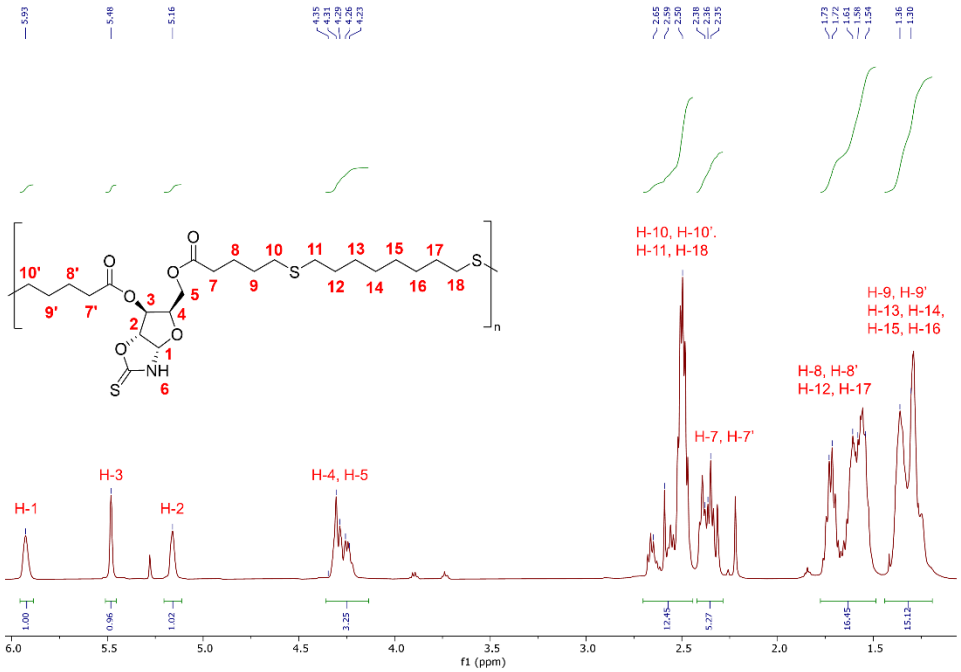

Figure S28: ^{1}H NMR spectrum of poly(**2a**-ODT) (Table 1, entry 4) (residual $CDCl_3$ signal at 7.26 ppm).

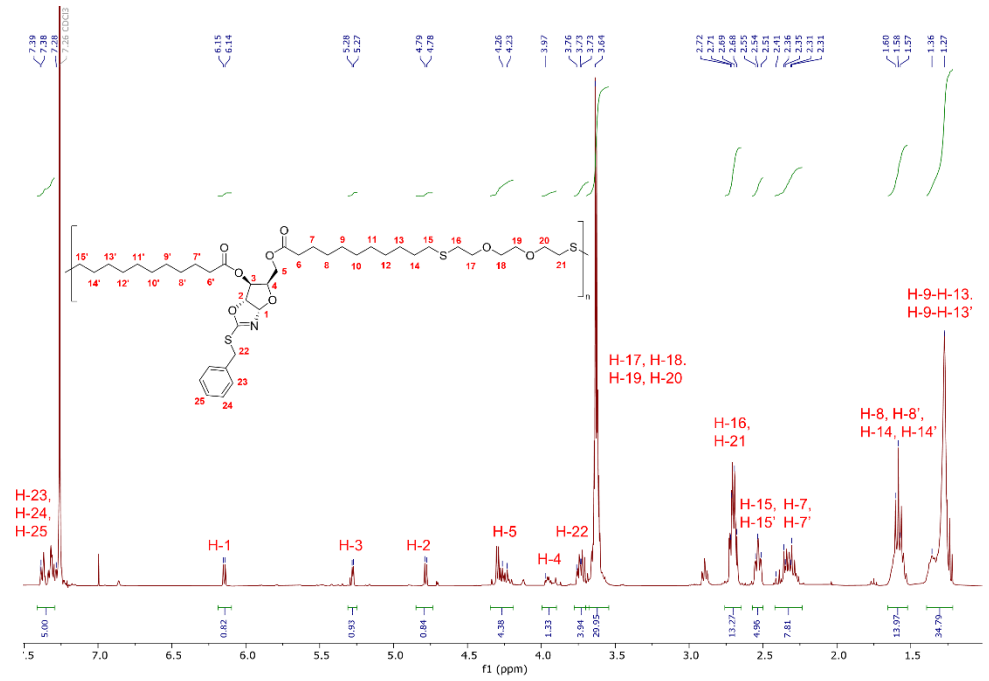

Figure S29: ^{1}H NMR spectrum of Poly(**1b**-EDT) (Table 1, entry 5) (residual $CDCl_3$ signal at 7.26 ppm).

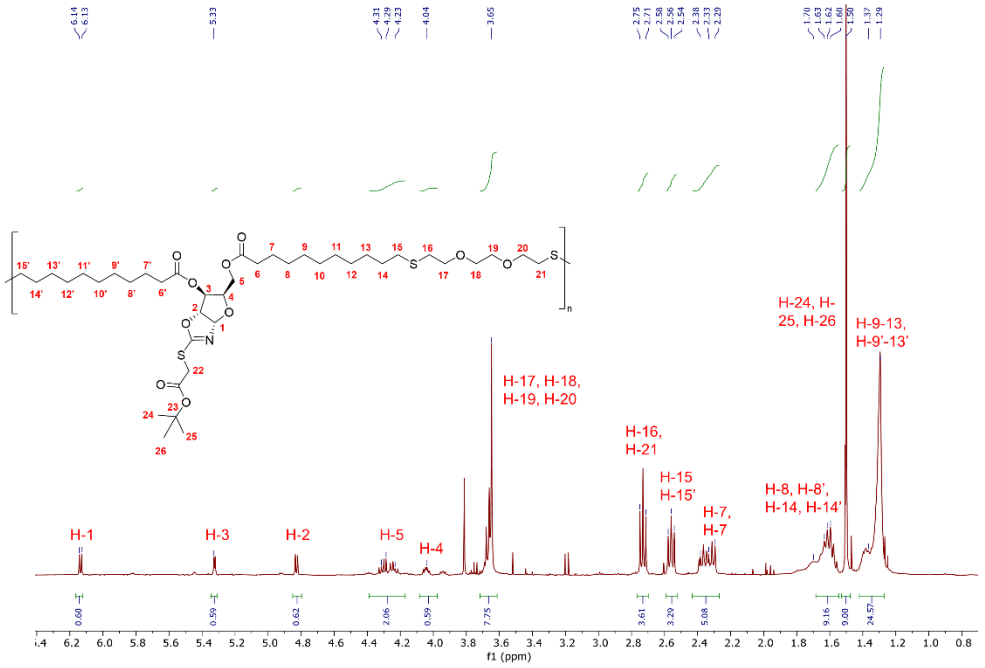

Figure S30: ^{1}H NMR spectrum of Poly(**1d**-EDT) (Table 1, entry 6) (residual $CDCl_3$ signal at 7.26 ppm).

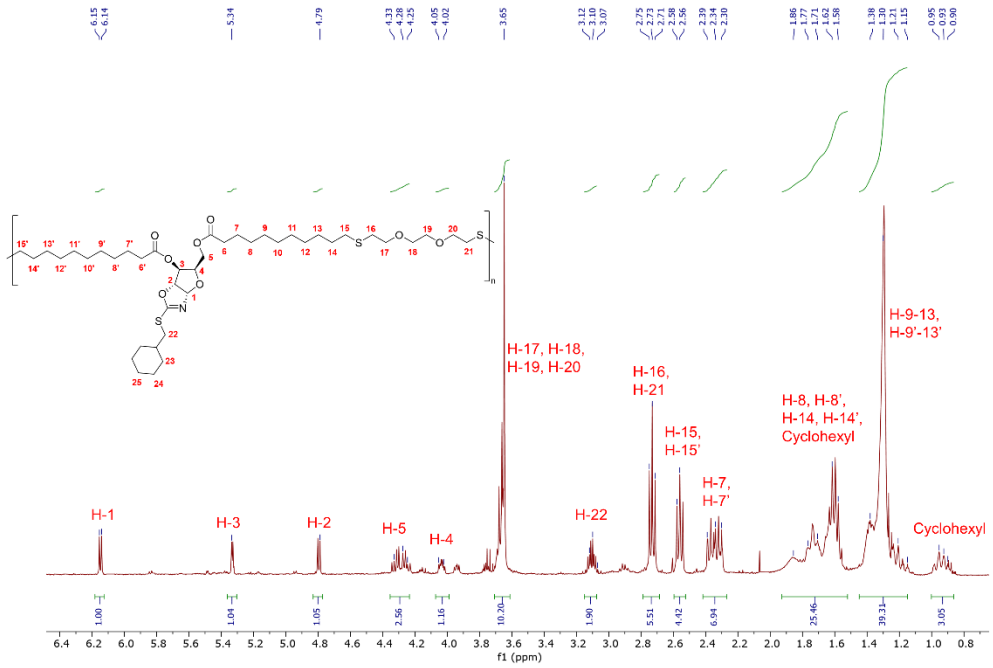

Figure S31: ^{1}H NMR spectrum of poly(**1f**-EDT) (Table 1, entry 7) (residual $CDCl_3$ signal at 7.26 ppm).

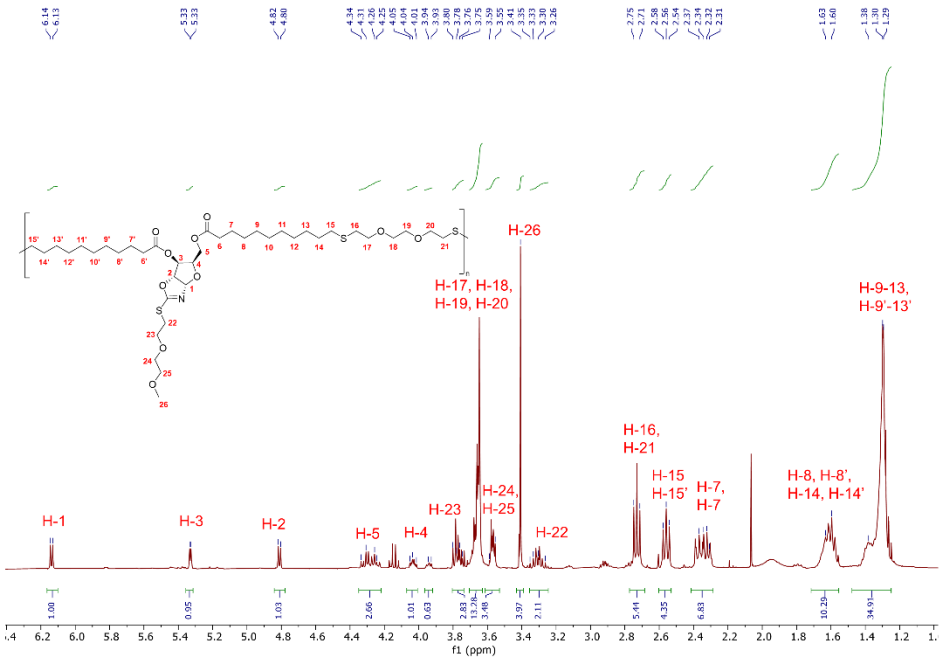

Figure S32: ^{1}H NMR spectrum of poly(**1g**-EDT) (Table 1, entry 8) (residual $CDCl_3$ signal at 7.26 ppm).

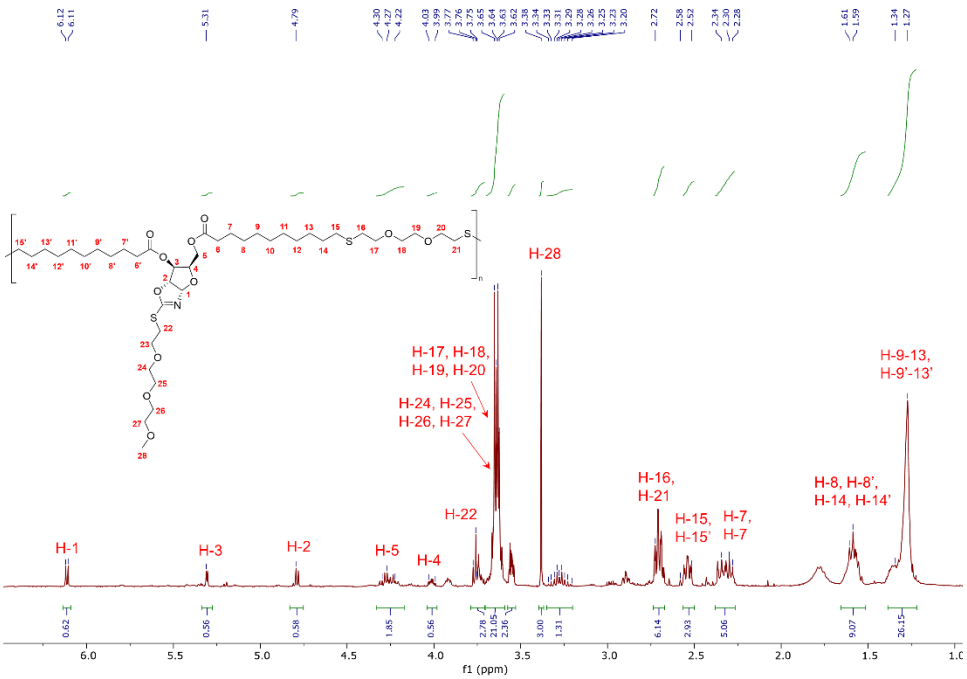

Figure S33: ^{1}H NMR spectrum of poly(**1h**-EDT) (Table 1, entry 9) (residual $CDCl_3$ signal at 7.26 ppm).

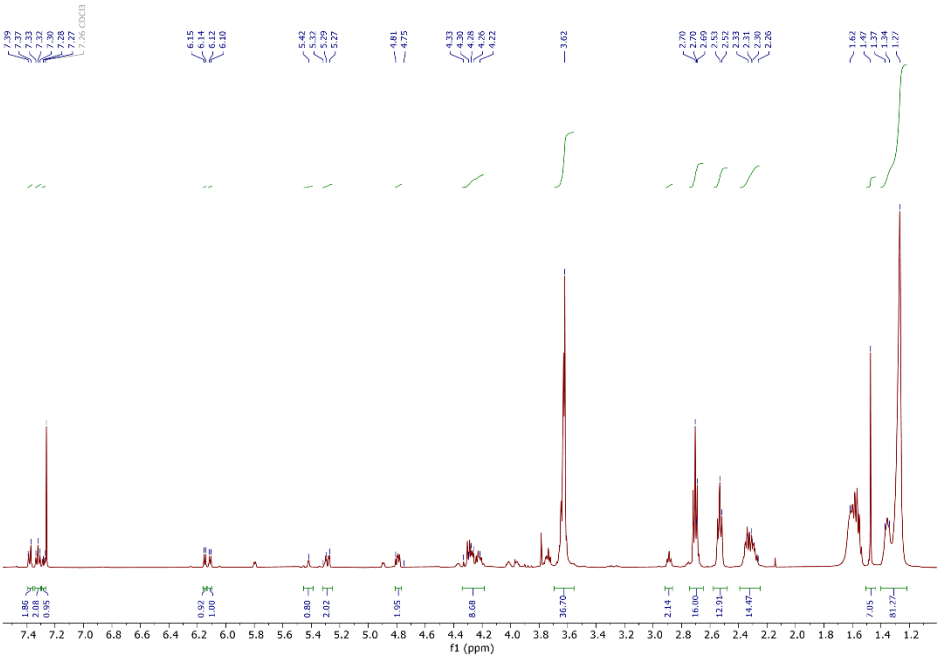

Figure S34: ^{1}H NMR spectrum of poly(**1b**-**1d**-EDT) (Table 1, entry 10) (residual $CDCl_3$ signal at 7.26 ppm).

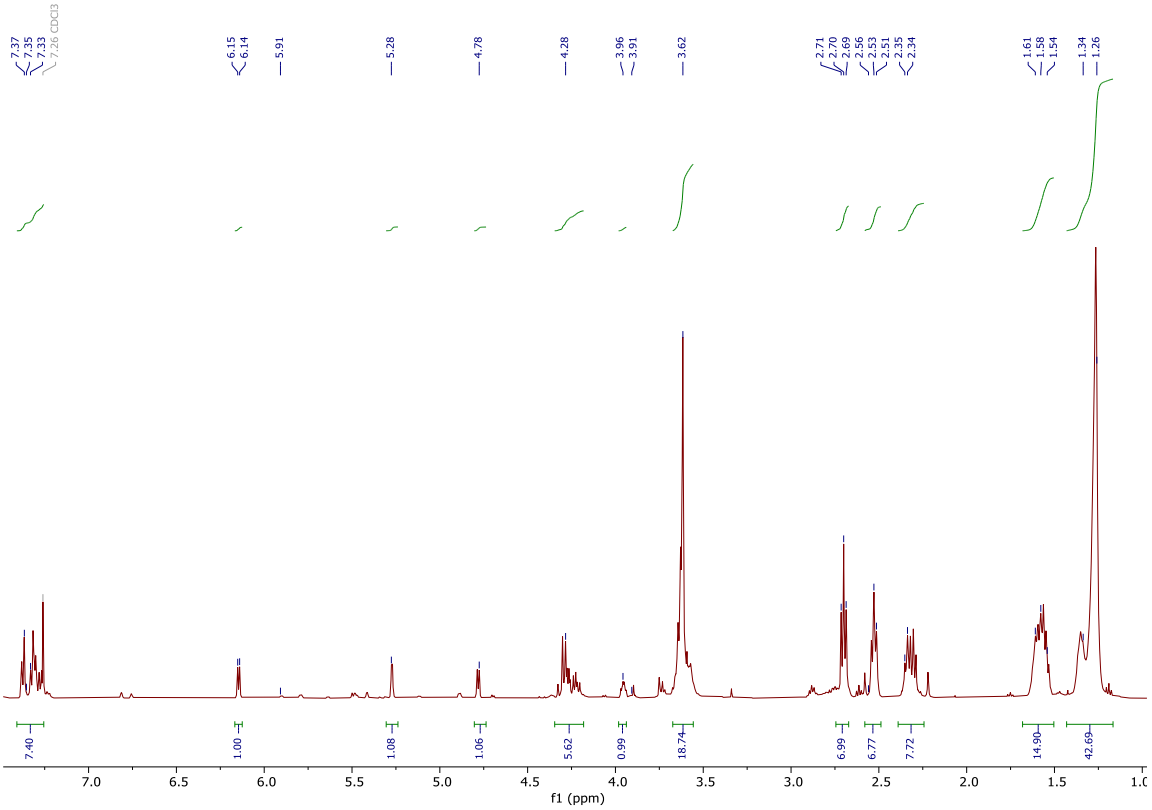

Figure S35: ^{1}H NMR spectrum of 91% benzylated poly(**1a**-EDT) (Table 2, entry 1). Residual $CDCl_3$ signal at 7.26 ppm.

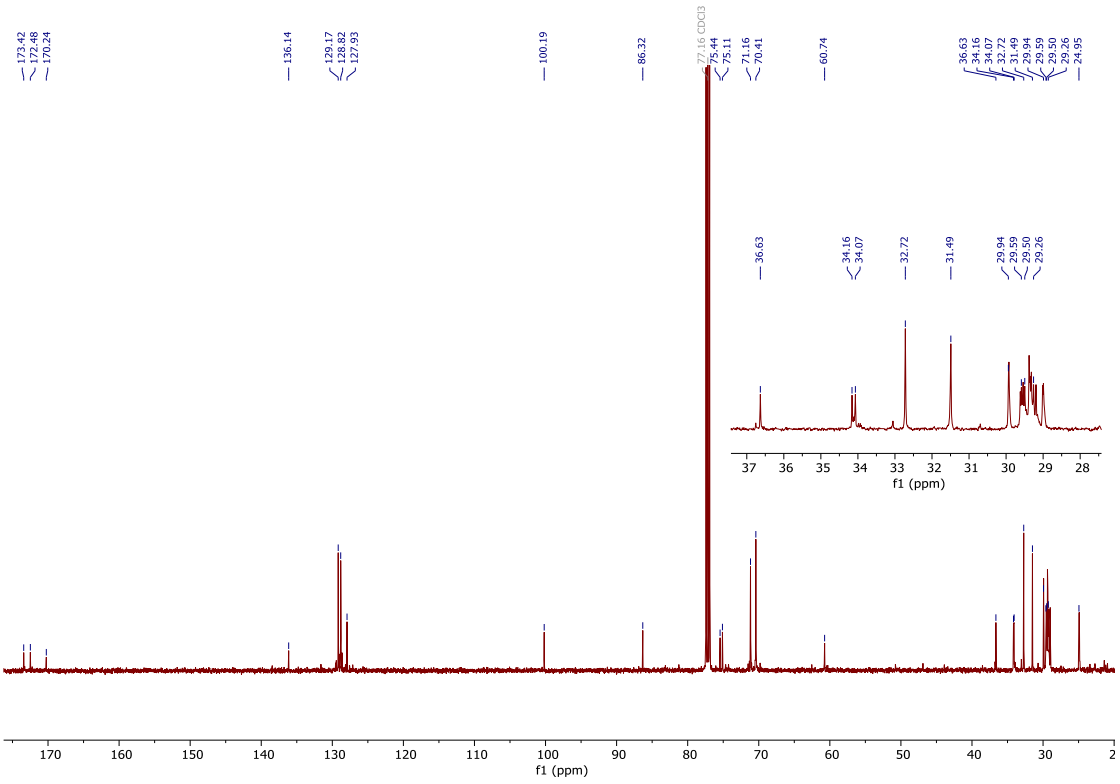

Figure S36: $^{13}C\{^{1}H\}$ NMR spectrum of 91% benzylated poly(**1a**-EDT) (Table 2, entry 1). Residual $CDCl_3$ signal at 77.2 ppm.

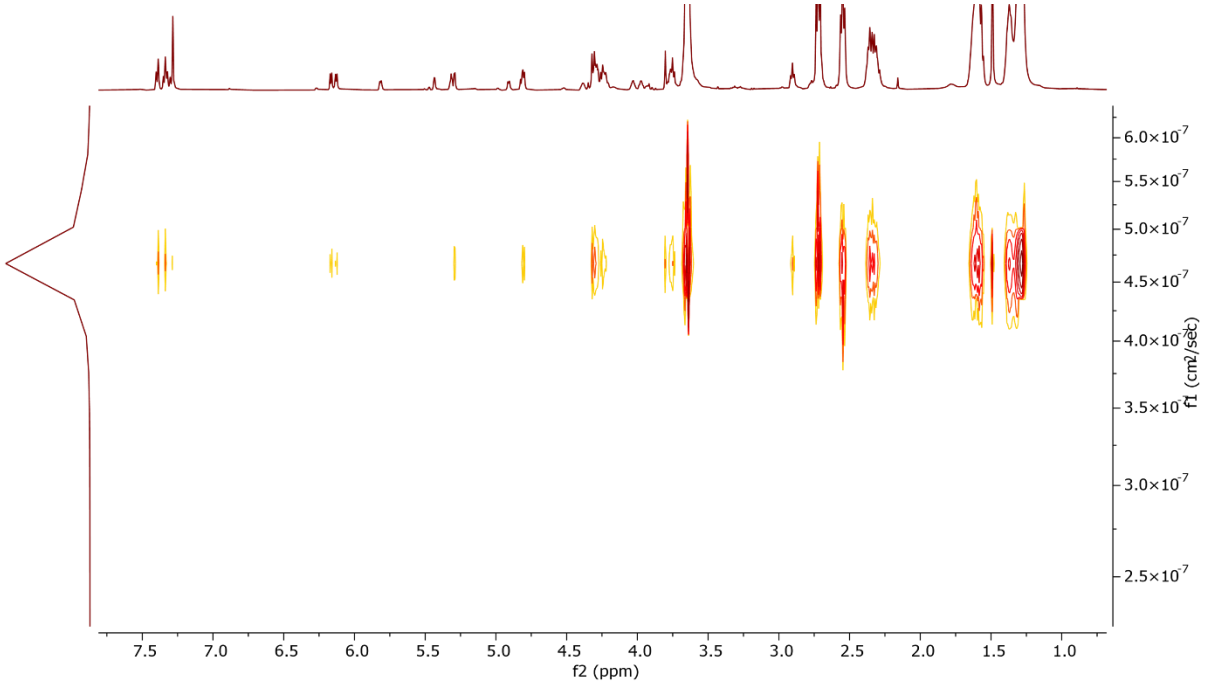

Figure S37: ^{1}H DOSY NMR spectrum of poly(**1b**-**1d**-EDT) (Table 1, entry 10) confirming that the polymer is one species with a diffusion coefficient of 4.67 x 10^{-7} cm^{-2} s^{-1}.

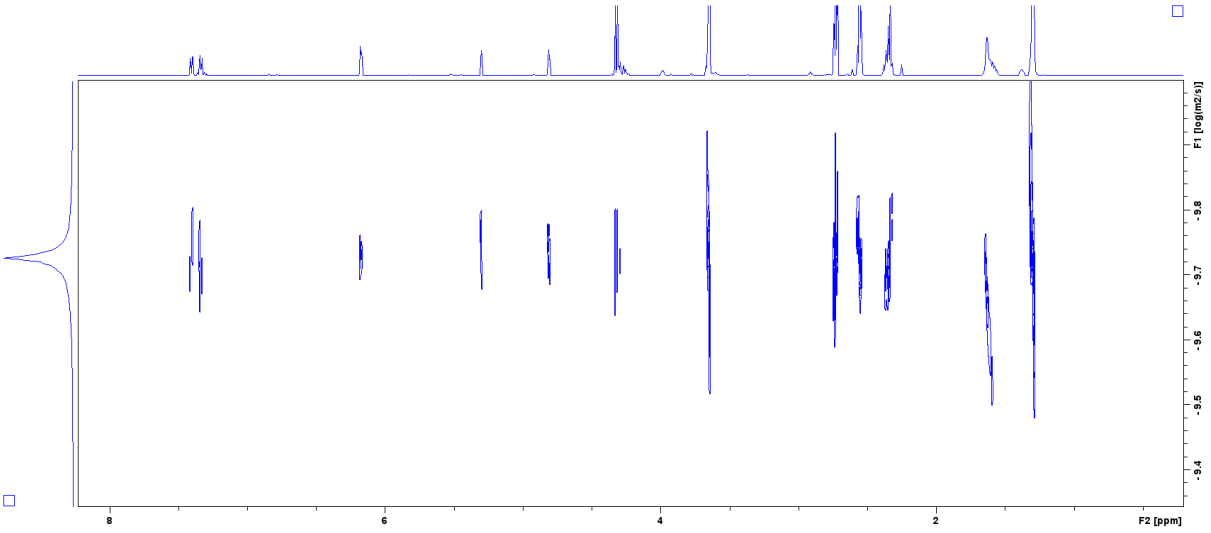

Figure S38: ^{1}H DOSY NMR spectrum of 91% benzylated poly(**1a**-EDT) (Table 2, entry 1) confirming the polymer is one species with a diffusion coefficient of 2.0 x 10^{-7} cm^{-2} s^{-1}.

4. FT-IR Spectra of Compounds

4.1 Small Molecules

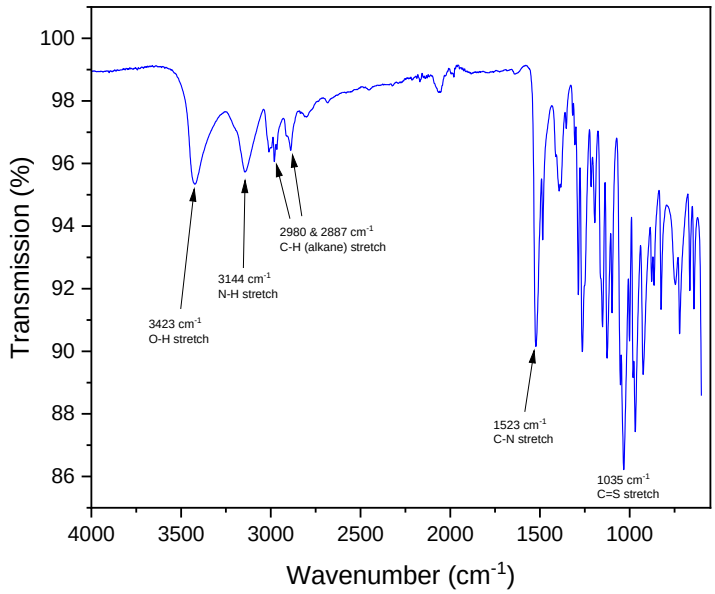

Figure S39: FT-IR spectrum of OZT-xylose.

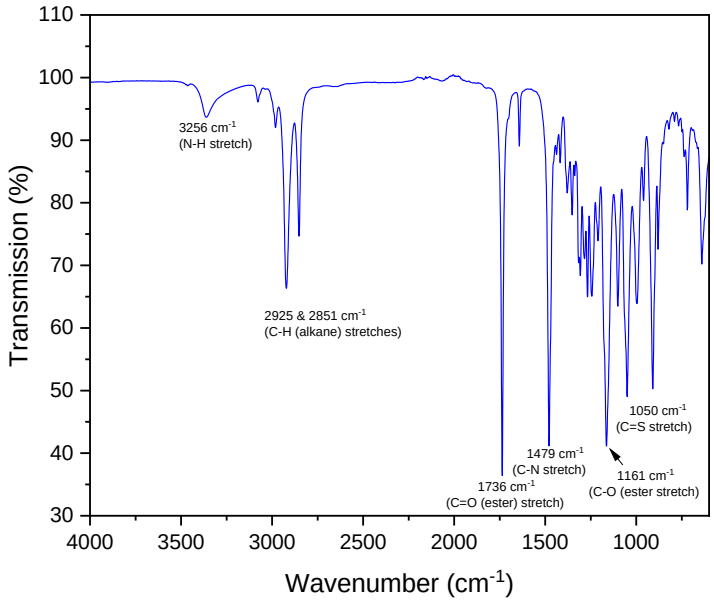

Figure S40: FT-IR spectrum of monomer **1a**.

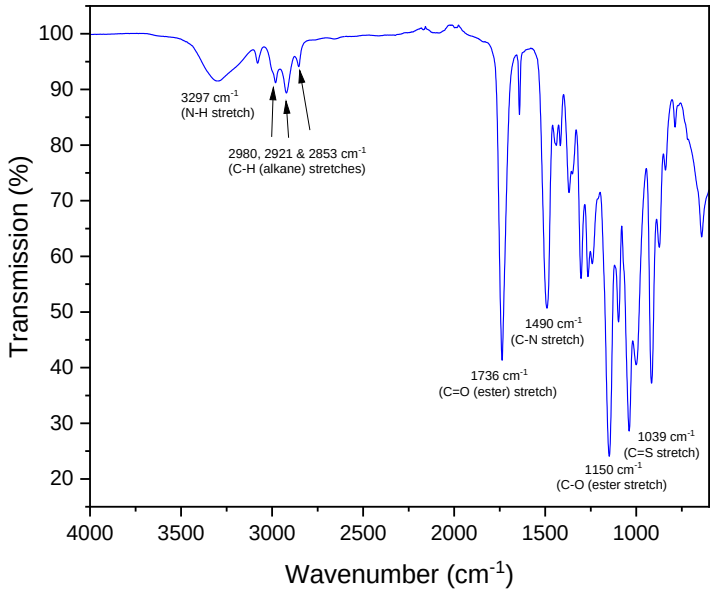

Figure S41: FT-IR spectrum of monomer **2a**.

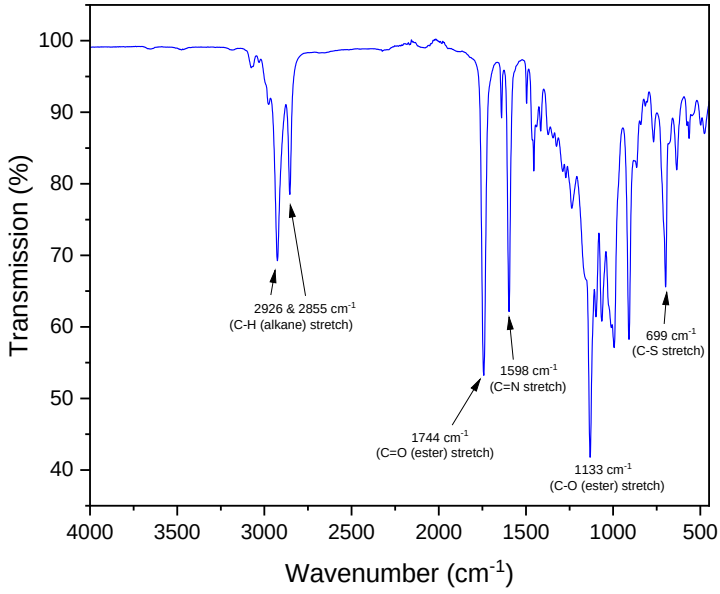

Figure S42: FT-IR spectrum of monomer **1b**.

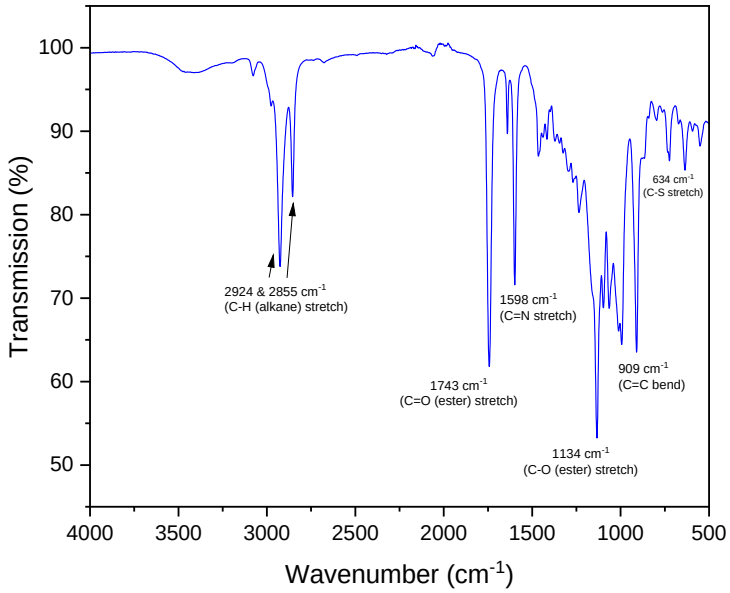

Figure S43: FT-IR spectrum of monomer **1c**.

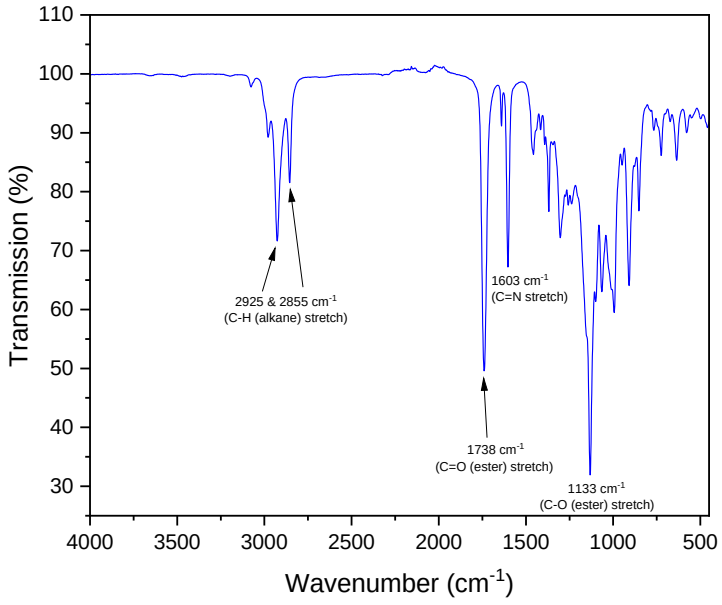

Figure S44: FT-IR spectrum of monomer **1d**.

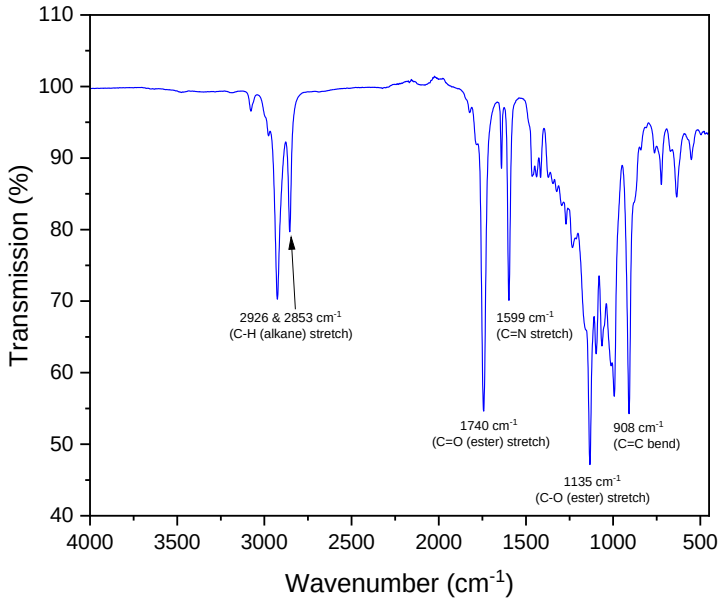

Figure S45: FT-IR spectrum of monomer **1e**.

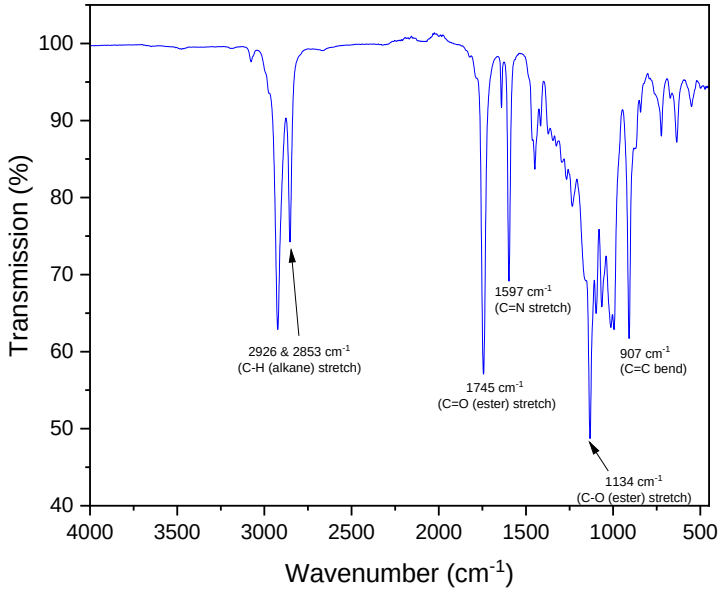

Figure S46: FT-IR spectrum of monomer **1f.**

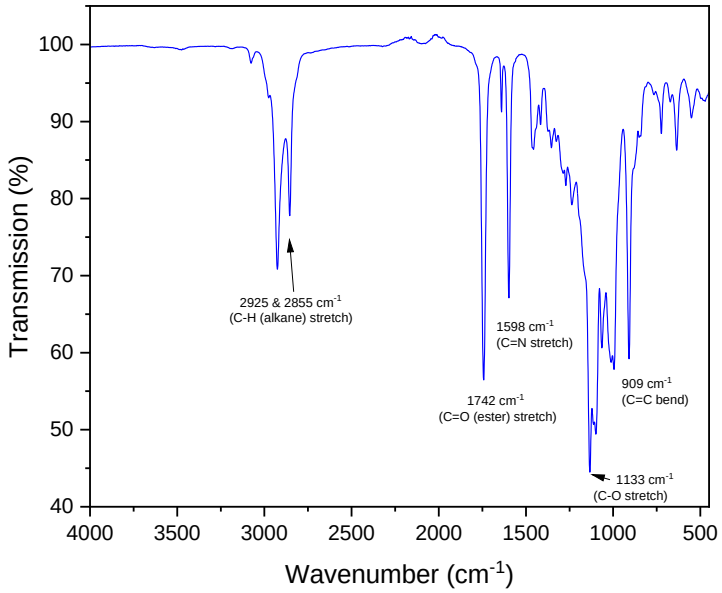

Figure S47: FT-IR spectrum of monomer **1g**.

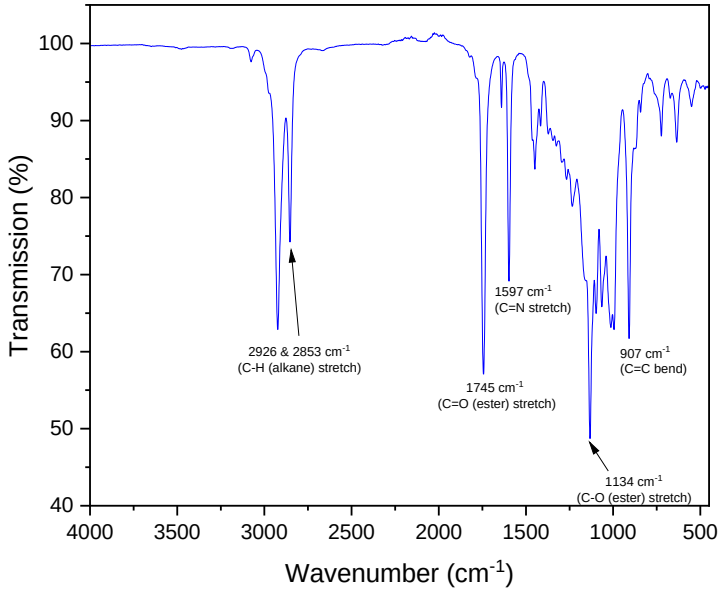

Figure S48: FT-IR spectrum of monomer **1h**.

4.2 Polymers

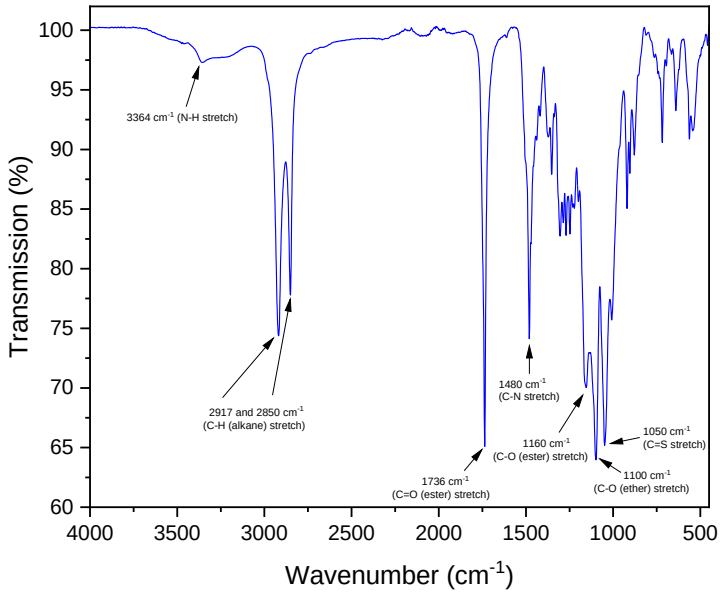

Figure S49: FT-IR spectrum of poly(**1a**-EDT).

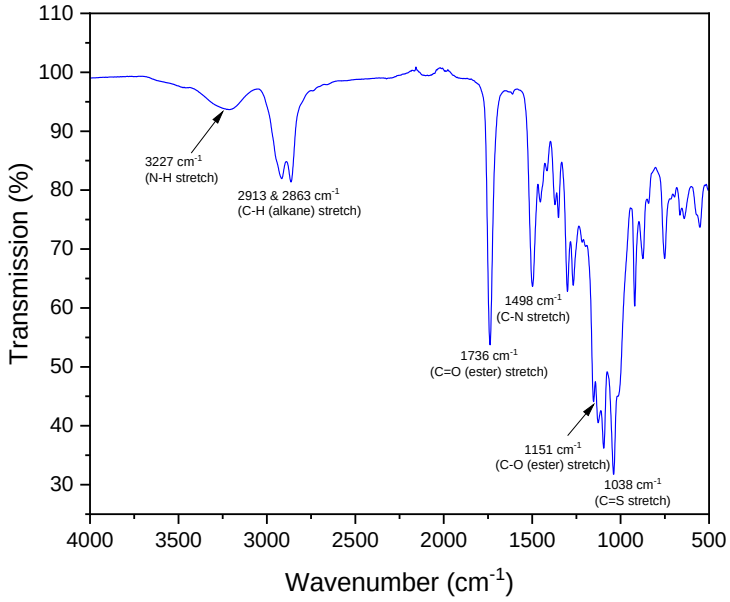

Figure S50: FT-IR spectrum of poly(**2a**-EDT).

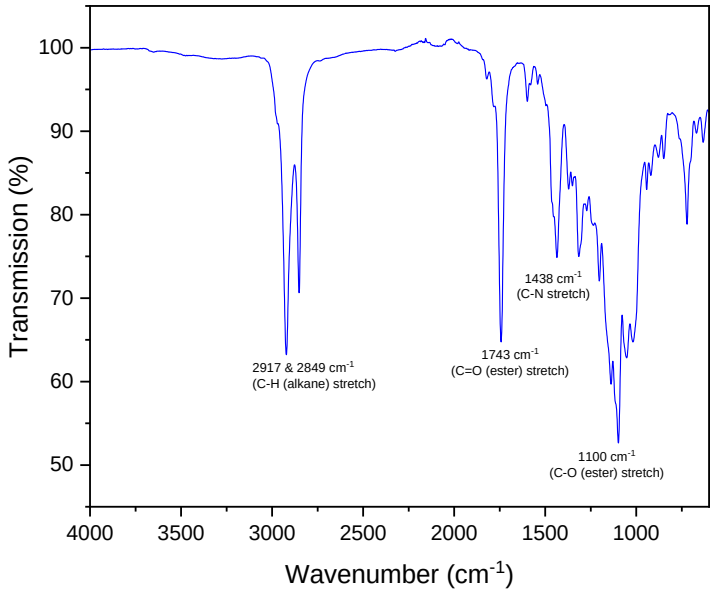

Figure S51: FT-IR spectrum of poly(**1a**-ODT).

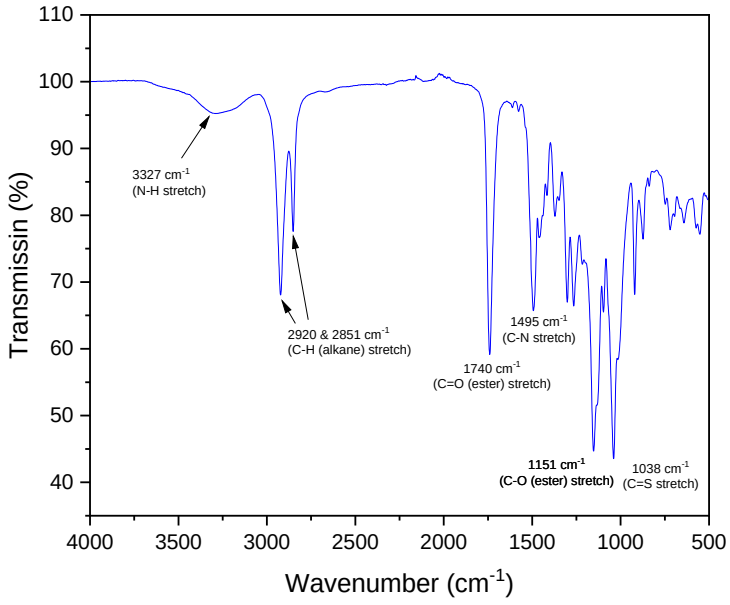

Figure S52: FT-IR spectrum of poly(**2a**-ODT).

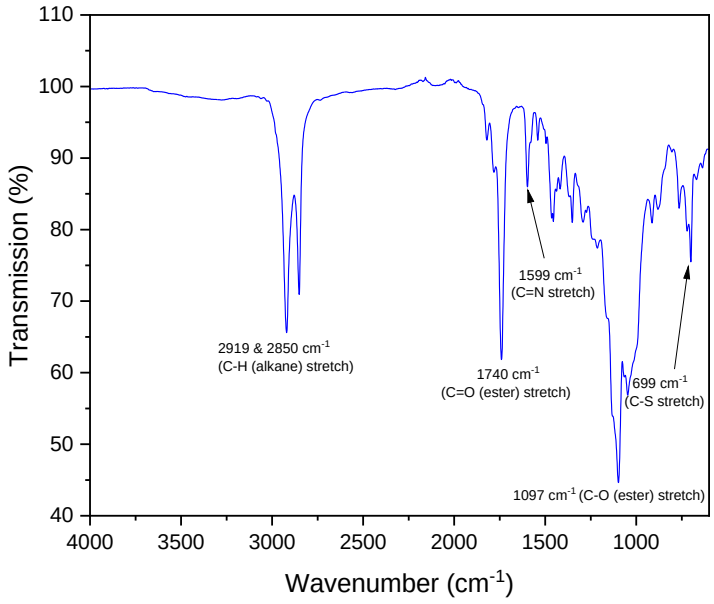

Figure S53: FT-IR spectrum of (poly**1b**-EDT).

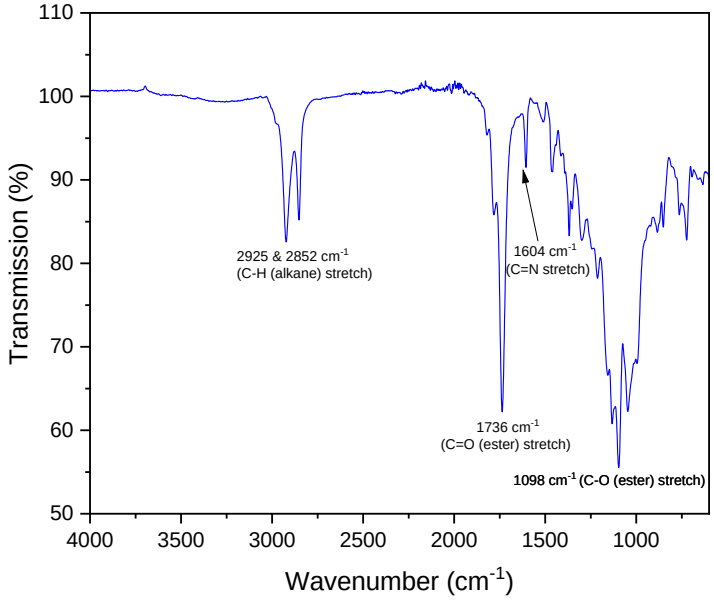

Figure S54: FT-IR spectrum of poly(**1d**-EDT).

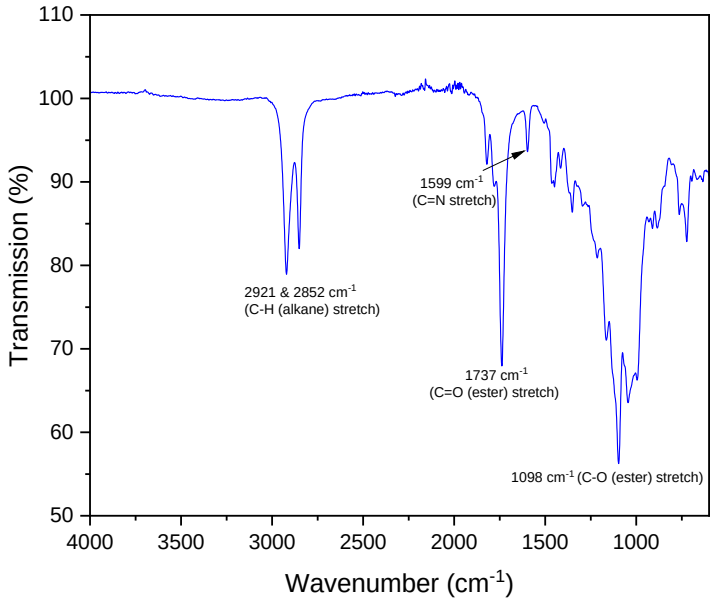

Figure S55: FT-IR spectrum of poly(**1f**-EDT).

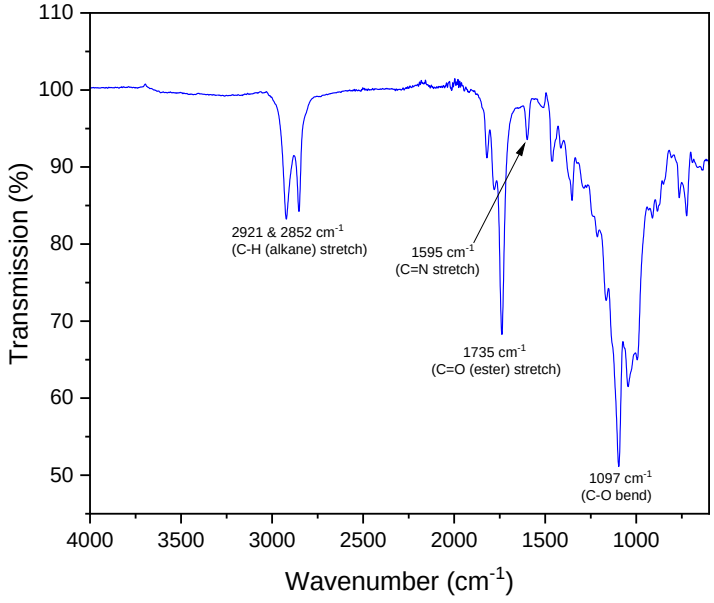

Figure S56: FT-IR spectrum of poly(**1g**-EDT).

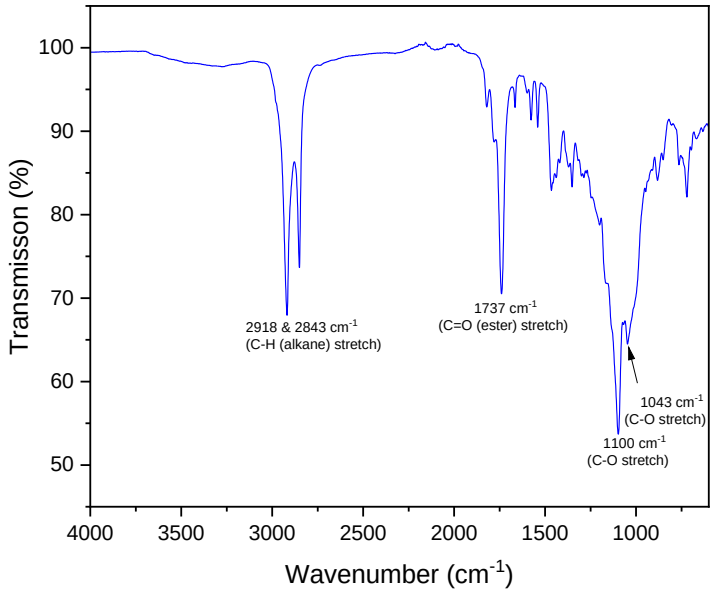

Figure S57: FT-IR spectrum of poly(**1h**-EDT).

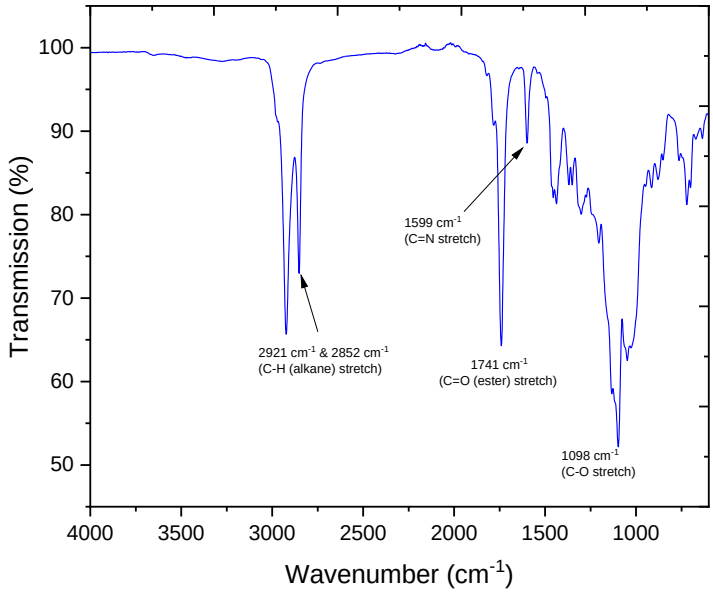

Figure S58: FT-IR spectrum of poly(**1b**-**1d**-EDT).

5. Mass Spectrometry

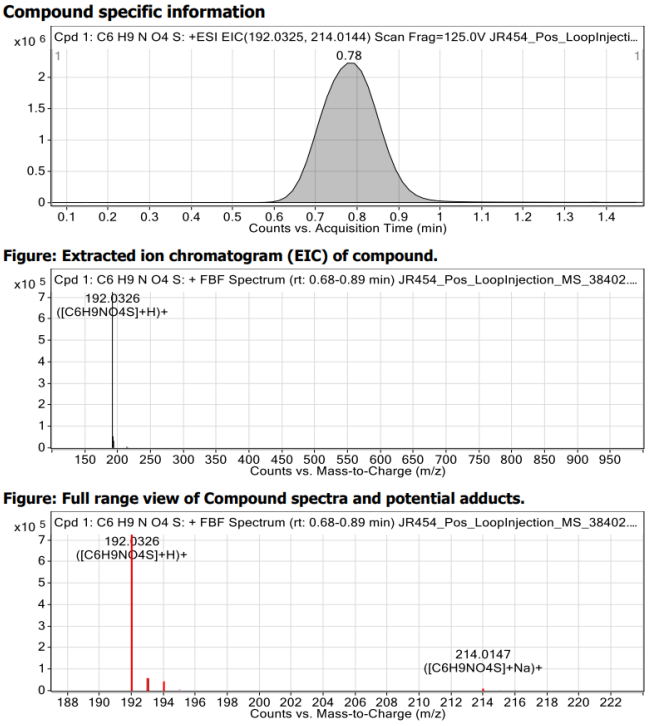

Figure S59: Extracted ion chromatogram (EIC) and full range view of compound spectra for OZT-xylose.

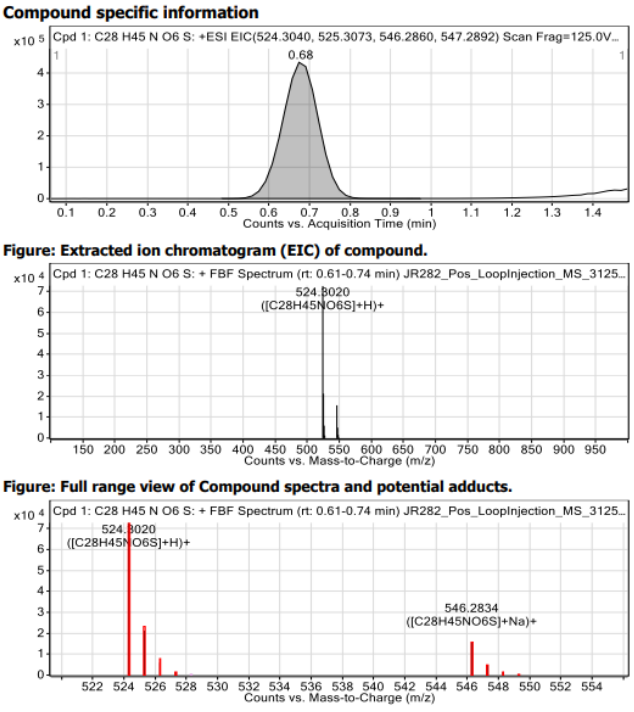

Figure S60: Extracted ion chromatogram (EIC) and full range view of compound spectra for **1a**.

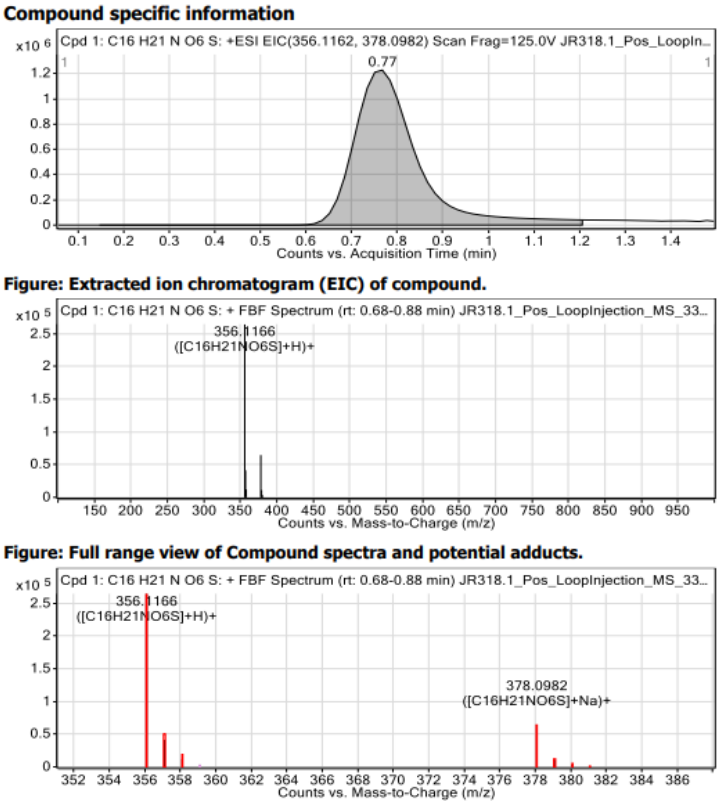

Figure S61: Extracted ion chromatogram (EIC) and full range view of compound spectra for OZT-xylose.

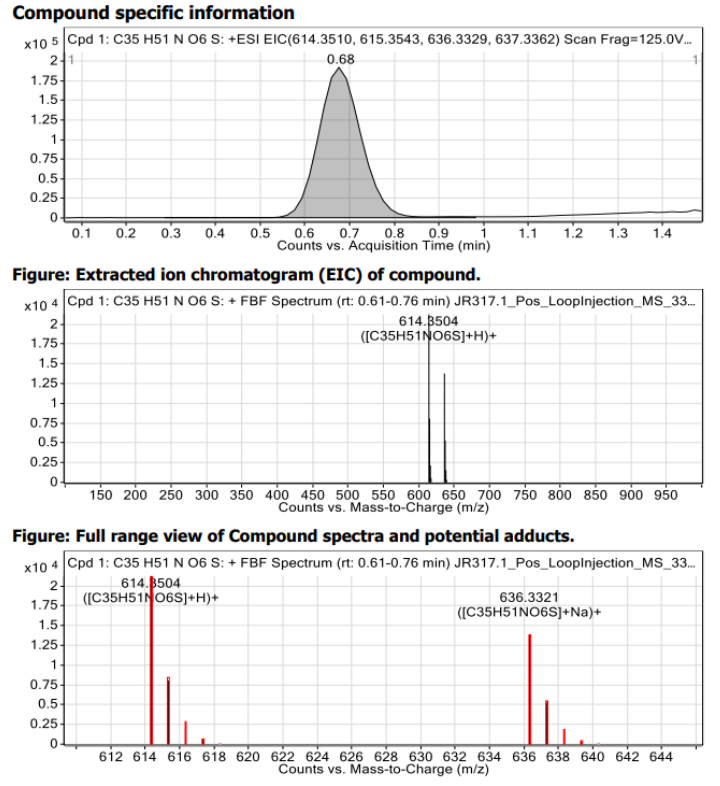

Figure S62: Extracted ion chromatogram (EIC) and full range view of compound spectra for monomer **1b**.

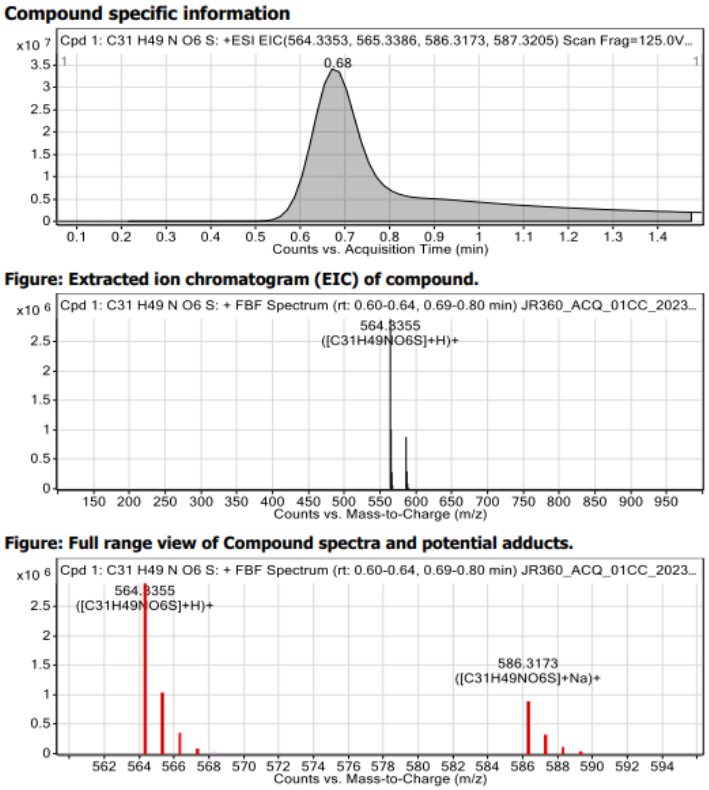

Figure S63: Extracted ion chromatogram (EIC) and full range view of compound spectra for monomer **1c**.

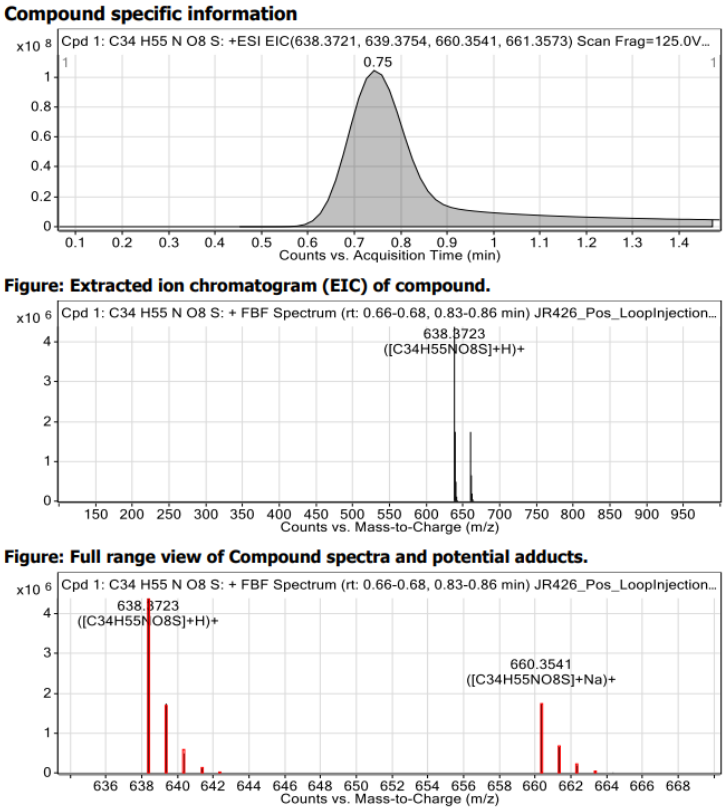

Figure S64: Extracted ion chromatogram (EIC) and full range view of compound spectra for monomer **1d**.

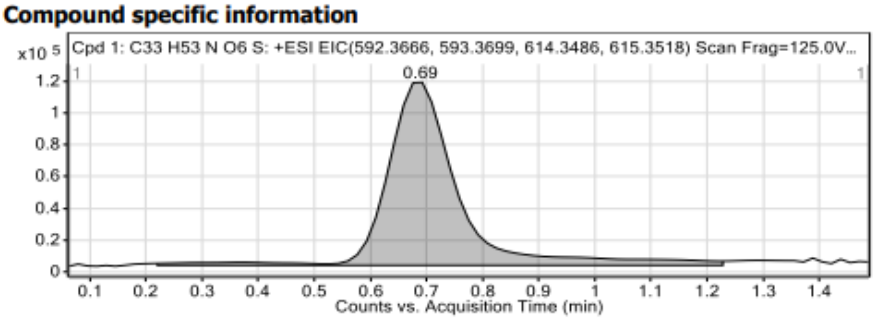

Figure S65: Compound specific information for monomer **1e**.

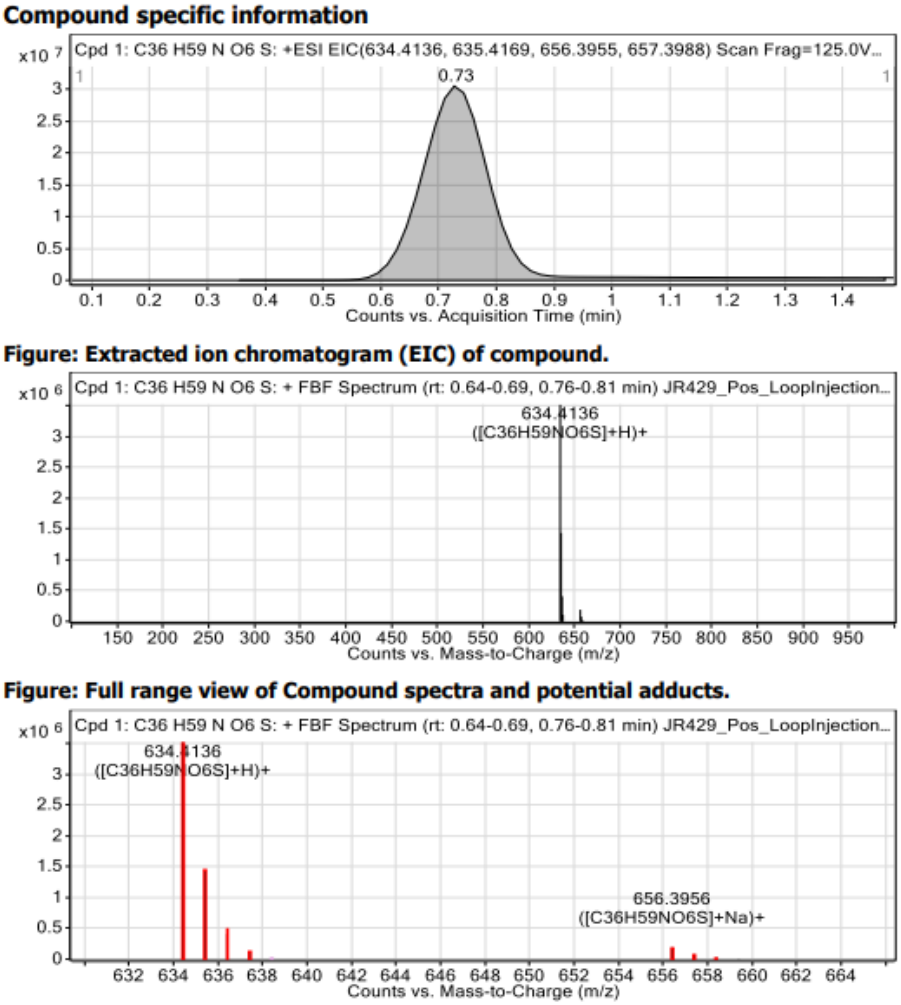

Figure S66: Extracted ion chromatogram (EIC) and full range view of compound spectra for monomer **1f**.

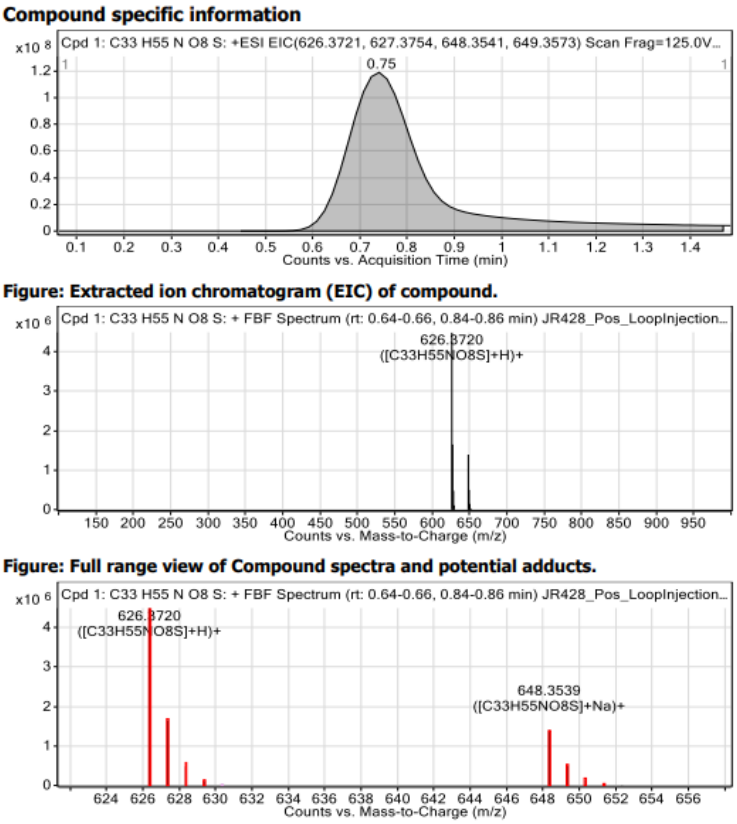

Figure S67: Extracted ion chromatogram (EIC) and full range view of compound spectra for monomer **1g**.

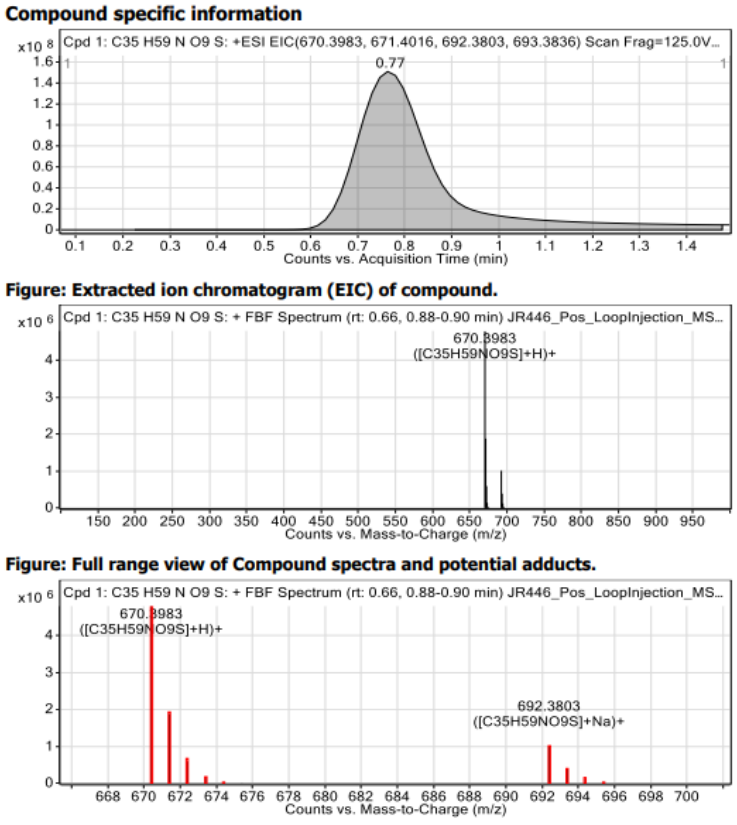

Figure S68: Extracted ion chromatogram (EIC) and full range view of compound spectra for monomer **1h**.

6. Size-Exclusion Chromatography (SEC)

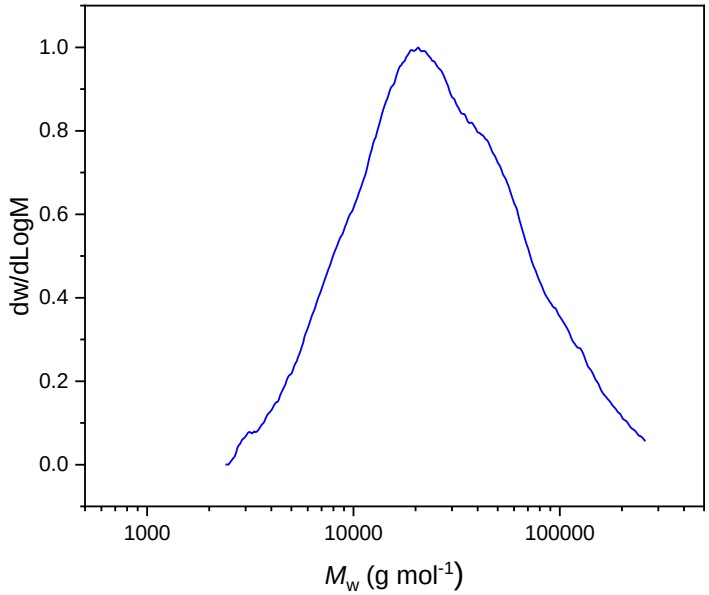

Figure S69: SEC trace of poly(**1a**-EDT) (M_n = 15,000 g mol^{-1}, $Đ_M$ = 2.89, Table 1, entry 1).

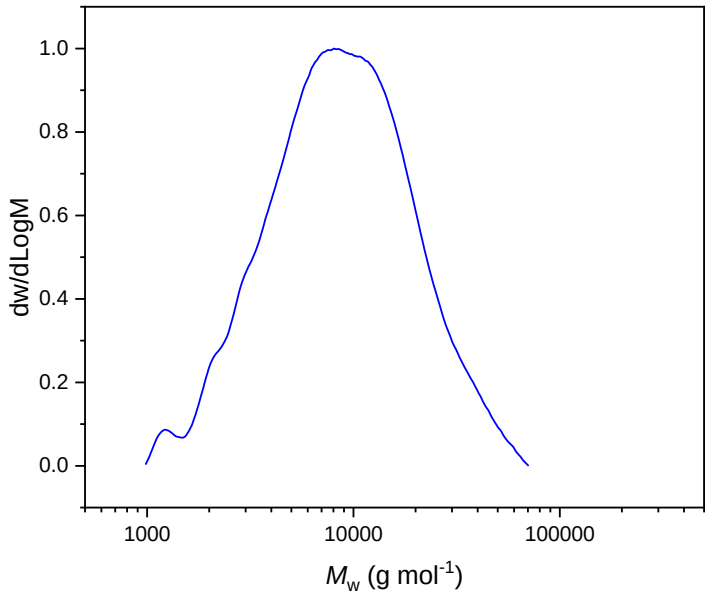

Figure S70: SEC trace of poly(**2a**-EDT) (M_n = 5,900 g mol^{-1}, $Đ_M$ = 2.05, Table 1, entry 2).

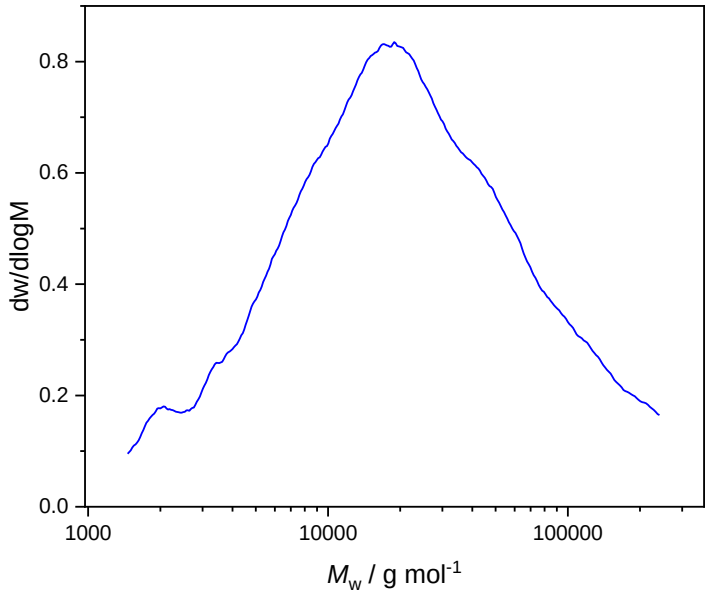

Figure S71: SEC trace of poly(**1a**-ODT) (M_n = 11,000 g mol^{-1}, $Đ_M$ = 3.33, Table 1, entry 3).

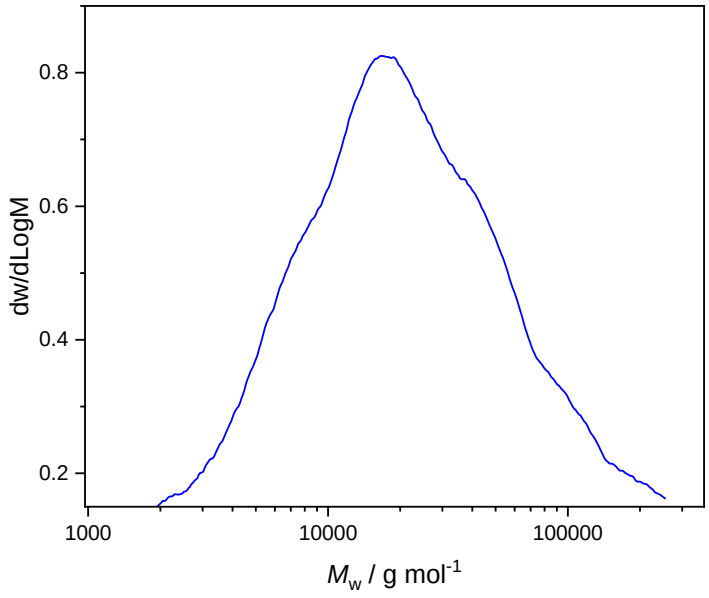

Figure S72: SEC trace of poly(**2a**-ODT) (M_n = 9,500 g mol^{-1}, $Đ_M$ = 3.84, Table 1, entry 4).

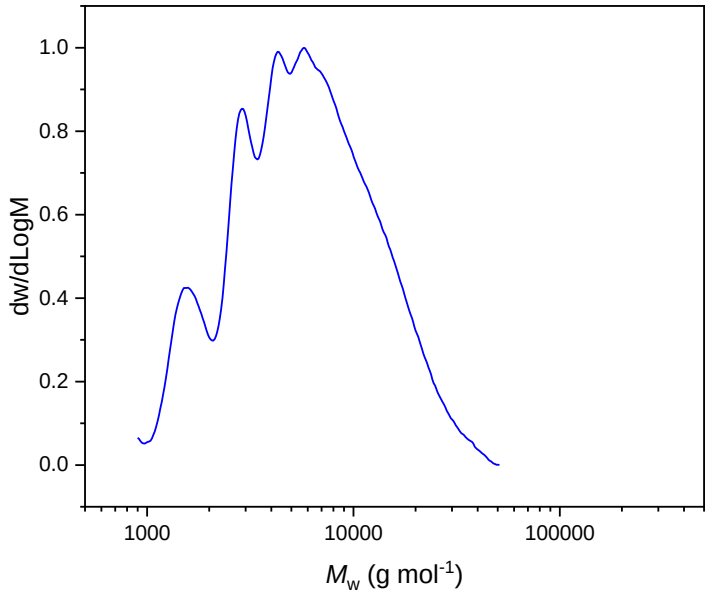

Figure S73: SEC trace of poly(**1b**-EDT) (M_n = 4,200 g mol^{-1}, $Đ_M$ = 1.94, Table 1, entry 5).

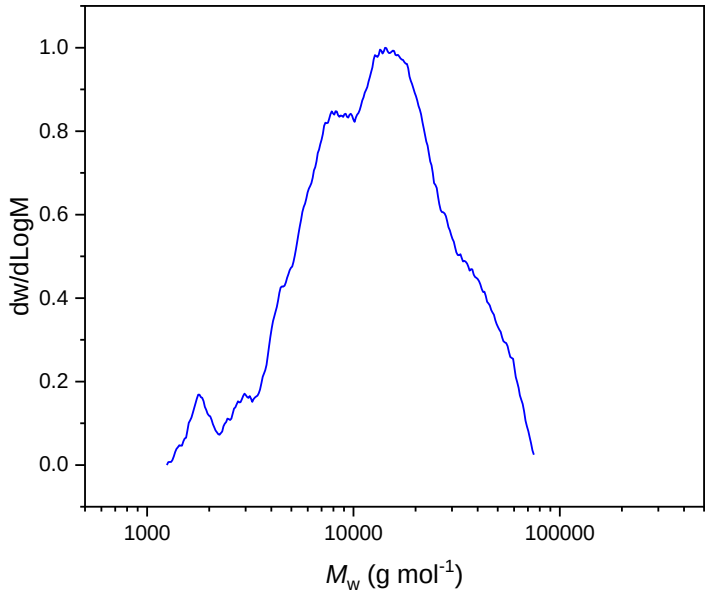

Figure S74: SEC trace of poly(**1d**-EDT) (M_n = 8,900 g mol^{-1}, $Đ_M$ = 1.95, Table 1, entry 6).

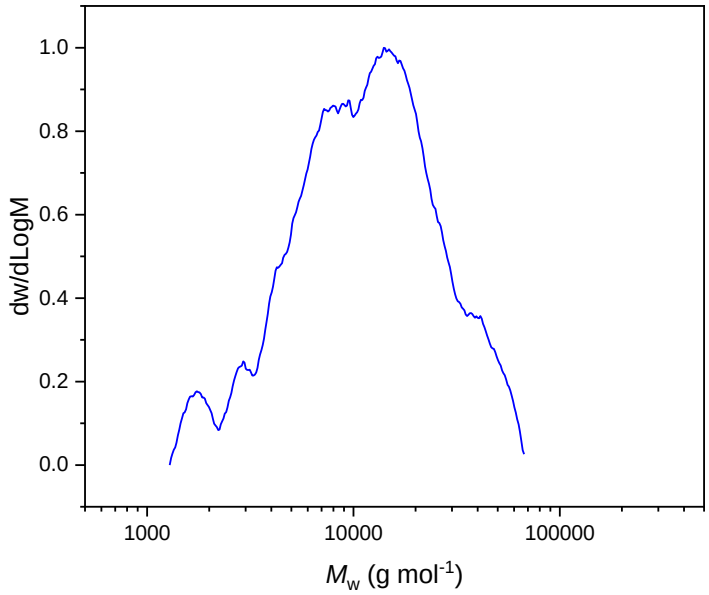

Figure S75: SEC trace of poly(**1f**-EDT) (M_n = 7,600 g mol^{-1}, $Đ_M$ = 2.01, Table 1, entry 7).

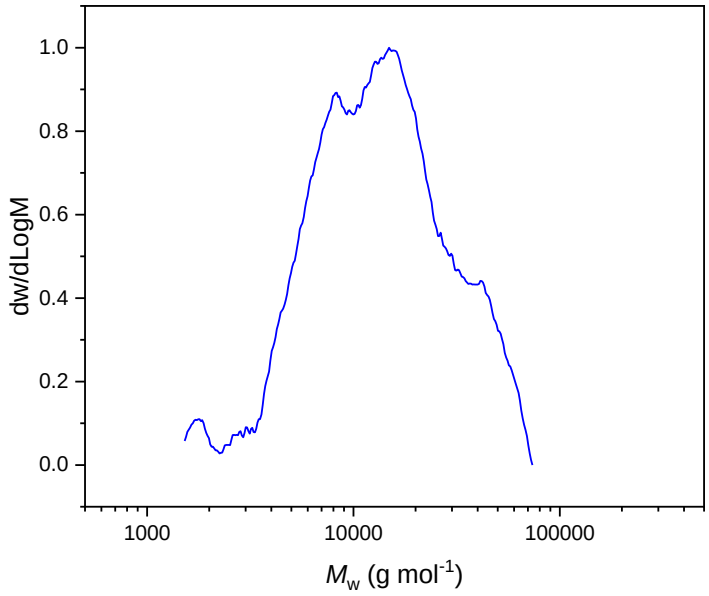

Figure S76: SEC trace of poly(**1g**-EDT) (M_n = 9,400 g mol^{-1}, $Đ_M$ = 1.84, Table 1, entry 8).

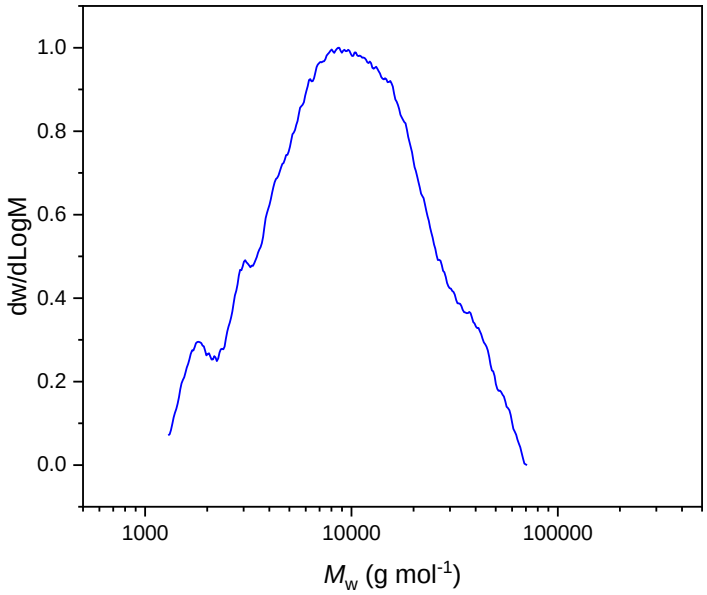

Figure S77: SEC trace of poly(**1h**-EDT) (M_n = 6,400 g mol^{-1}, $Đ_M$ = 2.12, Table 1, entry 9).

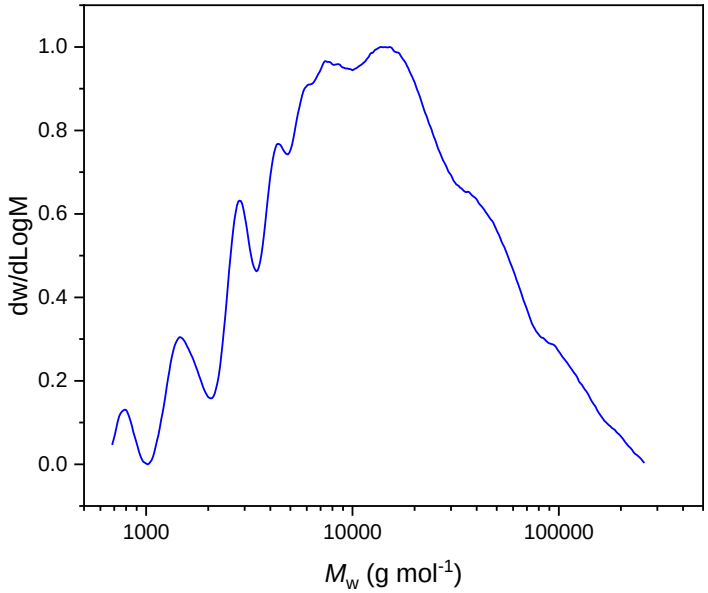

Figure S78: SEC trace of poly(**1b**-**1d**-EDT) (M_n = 6,400 g mol^{-1}, $Đ_M$ = 2.12, Table 1, entry 10).

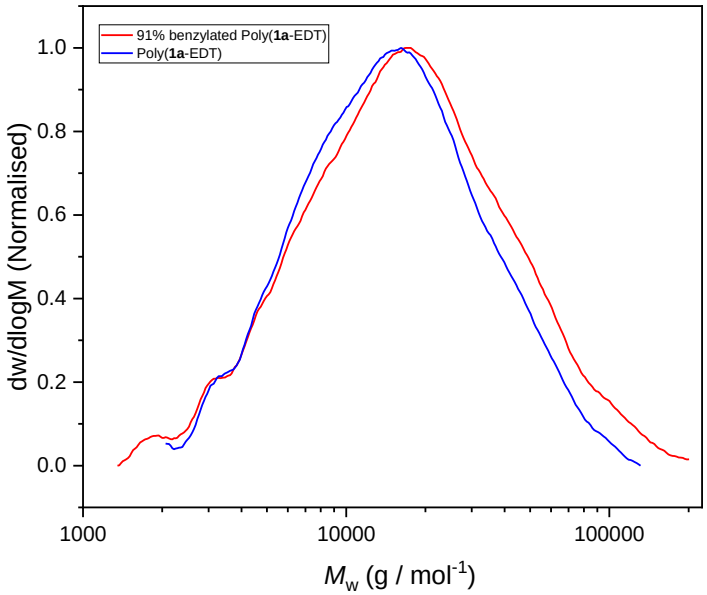

Figure S79: Stacked SEC traces of poly(**1a**-EDT) and 91% benzylated poly(**1a**-EDT).

7. DSC Thermograms

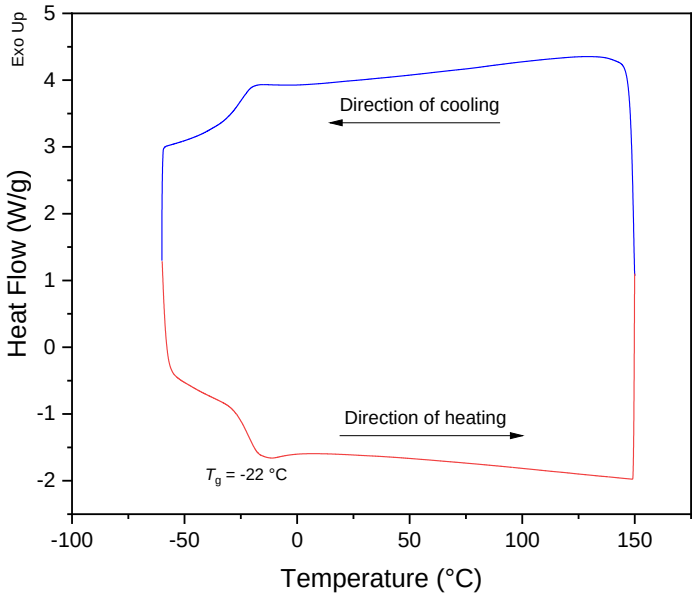

Figure S80: DSC thermogram showing the second cooling and heating cycle between –60 and 150 °C of a sample of poly(**1a**-EDT) ($M_{n,\,SEC}$ = 15,000 g mol^{-1}, $Đ_M$ = 2.89, Table 1, entry 1). $\boldsymbol{T_g}$ = –22 °C.

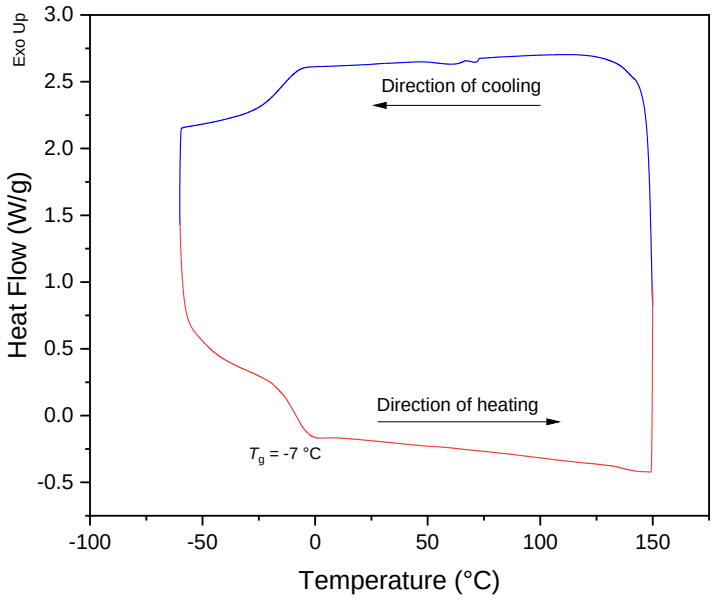

Figure S81: DSC thermogram showing the second cooling and heating cycle between –60 and 150 °C of a sample of poly(**2a**-EDT) ($M_{n,\,SEC}$ = 5,900 g mol^{-1}, $Đ_M$ = 2.05, Table 1, entry 2). $\boldsymbol{T_g}$ = –7 °C.

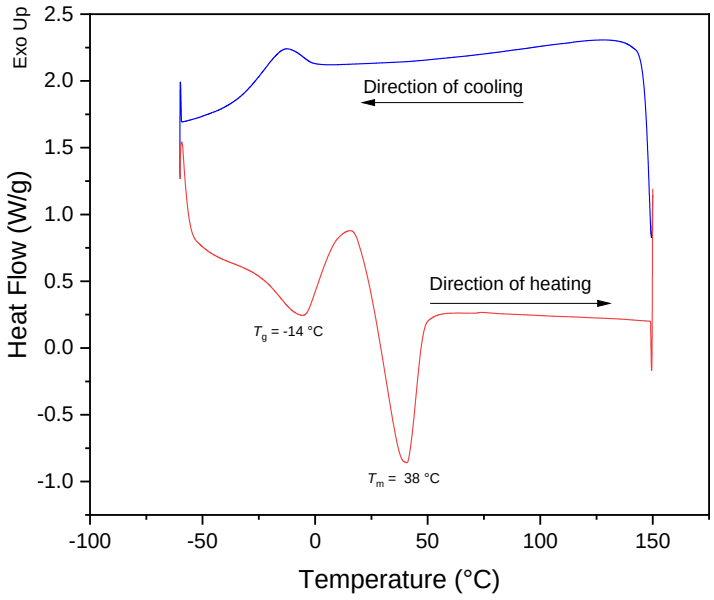

Figure S82*:* DSC thermogram showing the second cooling and heating cycle between –60 and 150 °C of a sample of poly(**1a**-ODT) ($M_{n,\,SEC}$ = 11,000 g mol^{-1}, $Đ_M$ = 3.33, Table 1, entry 3). $\boldsymbol{T_g}$ = –14 °C. $\boldsymbol{T_m}$ = 38 °C.

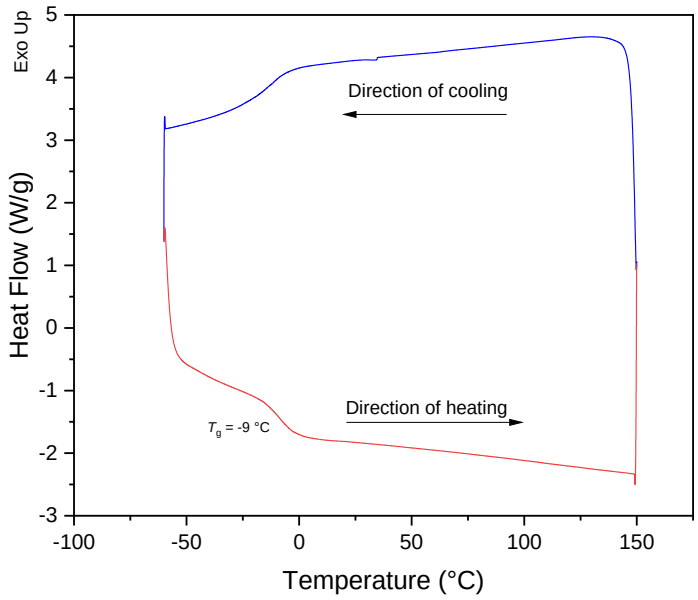

Figure S83: DSC thermogram showing the second cooling and heating cycle between –60 and 150 °C of a sample of poly(**2a**-ODT) ($M_{n,\,SEC}$ = 9,500 g mol^{-1}, $Đ_M$ = 3.84, Table 1, entry 4). $\boldsymbol{T_g}$ = –9 °C.

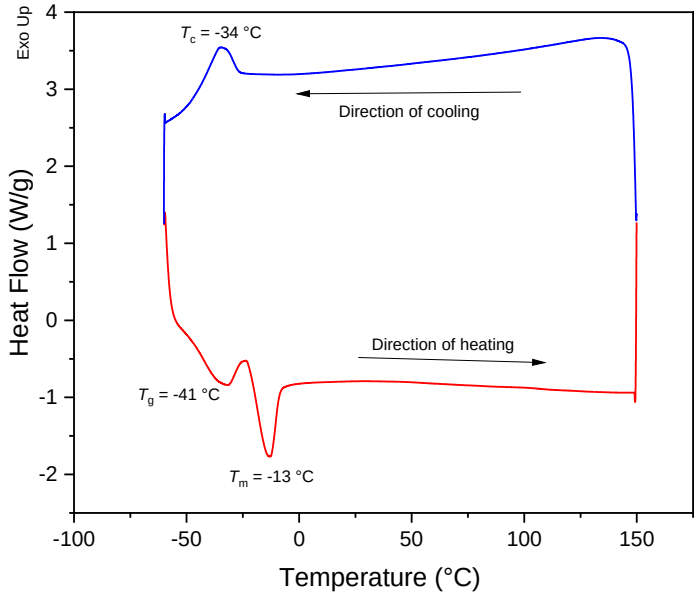

Figure S84: DSC thermogram showing the second cooling and heating cycle between –60 and 150 °C of a sample of poly(**1b**-EDT) ($M_{n,\,SEC}$ = 4,200 g mol^{-1}, $Đ_M$ = 1.94, Table 1, entry 5). $\boldsymbol{T_g}$ = –41 °C, $\boldsymbol{T_m}$ = –13 °C, $\boldsymbol{T_c}$ = –34 °C.

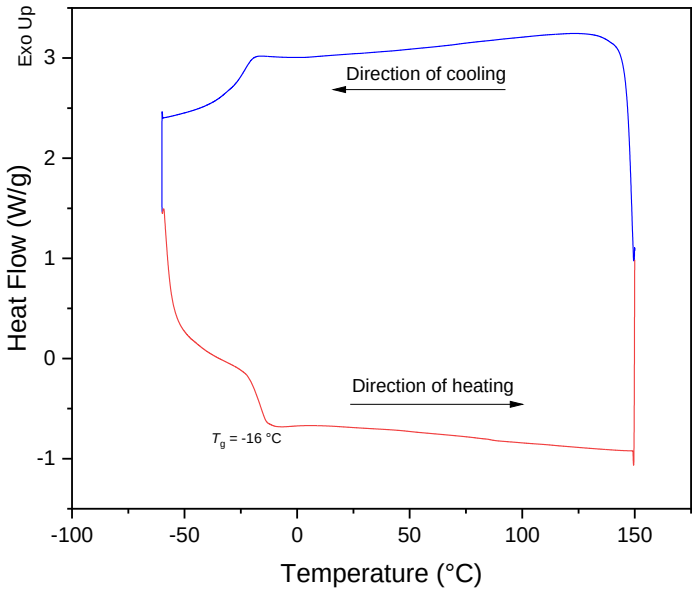

Figure S85: DSC thermogram showing the second cooling and heating cycle between –60 and 150 °C of a sample of poly(**1d**-EDT) ($M_{n,\,SEC}$ = 8,900 g mol^{-1}, $Đ_M$ = 1.95, Table 1, entry 6). $\boldsymbol{T_g}$ = –16 °C.

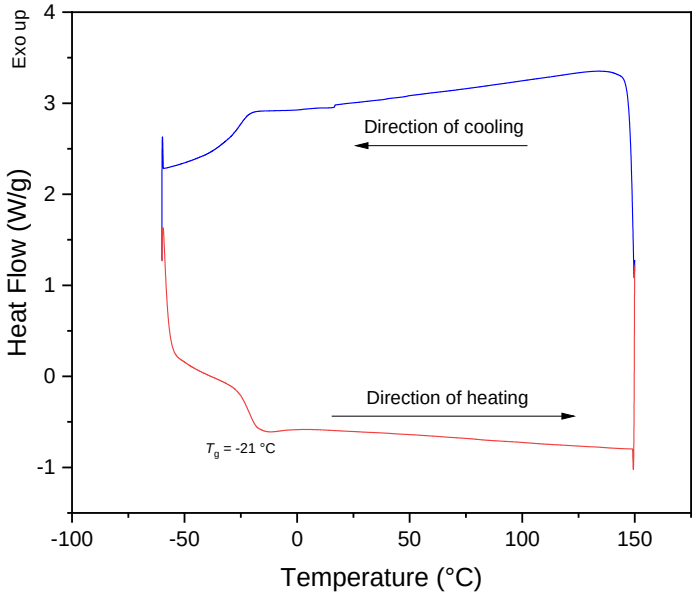

Figure S86: DSC thermogram showing the second cooling and heating cycle between –60 and 150 °C of a sample of poly(**1f**-EDT) ($M_{n,\,SEC}$ = 7,600 g mol^{-1}, $Đ_M$ = 2.01, Table 1, entry 7). $\boldsymbol{T_g}$ = –21 °C.

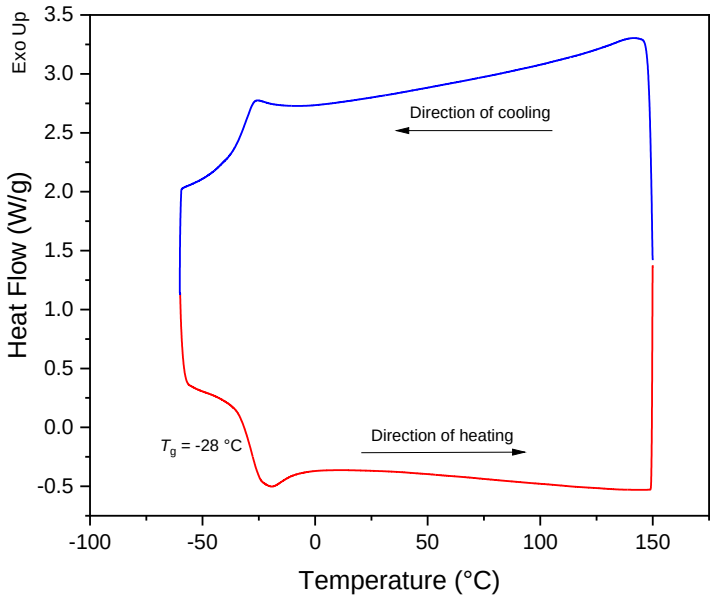

Figure S87*:* DSC thermogram showing the second cooling and heating cycle between –60 and 150 °C of a sample of poly(**1g**-EDT) ($M_{n,\,SEC}$ = 9,400 g mol^{-1}, $Đ_M$ = 1.84, Table 1, entry 8). $\boldsymbol{T_g}$ = –28 °C.

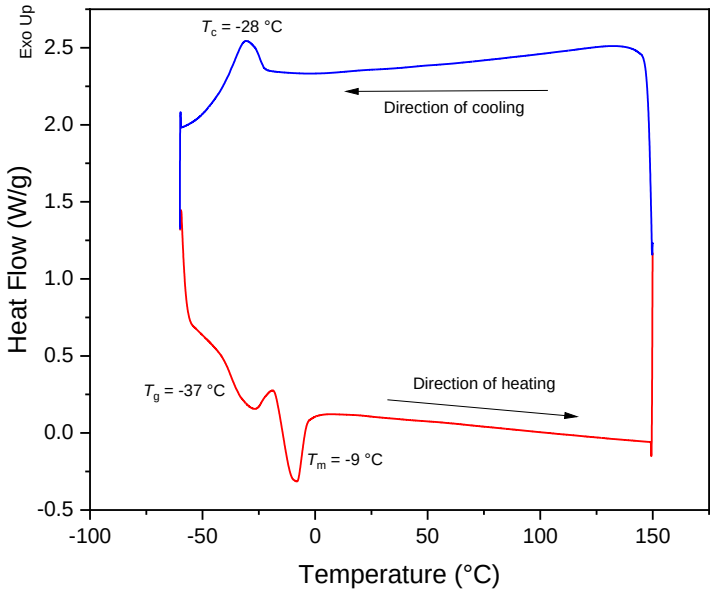

Figure S88: DSC thermogram showing the second cooling and heating cycle between -60 and 150 °C of a sample of poly(**1h**-EDT) ($M_{n,\,SEC}$ = 6,400 g mol^{-1}, $Đ_M$ = 2.12, Table 1, entry 9). $\boldsymbol{T_g}$ = –37 °C, $\boldsymbol{T_c}$ = –28 °C, $\boldsymbol{T_m}$ = –9 °C.

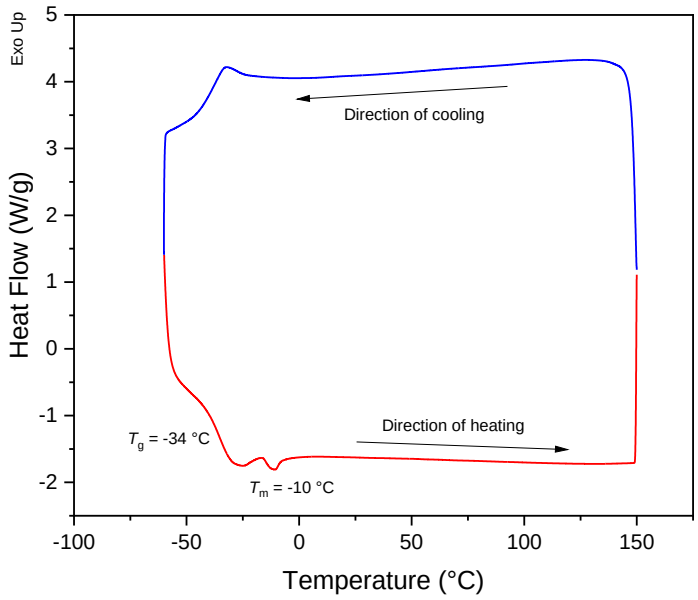

Figure S89: DSC thermogram showing the second cooling and heating cycle between –60 and 150 °C of a sample of poly(**1b-1d**-EDT) ($M_{n,\,SEC}$ = 6,400 g mol^{-1}, $Đ_M$ = 2.12, Table 1, entry 10). $\boldsymbol{T_g}$ = –34 °C, $\boldsymbol{T_m}$ = –10 °C.

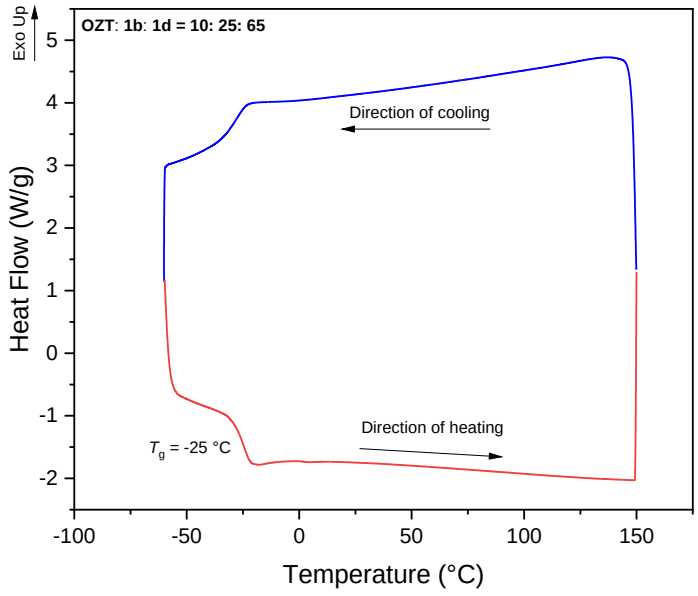

Figure S90: DSC thermogram showing the second cooling and heating cycle between –60 and 150 °C of the polymer produced from one-pot “tandem” functionalisation with equimolar ratio of BnBr and *t*BuBrAc.

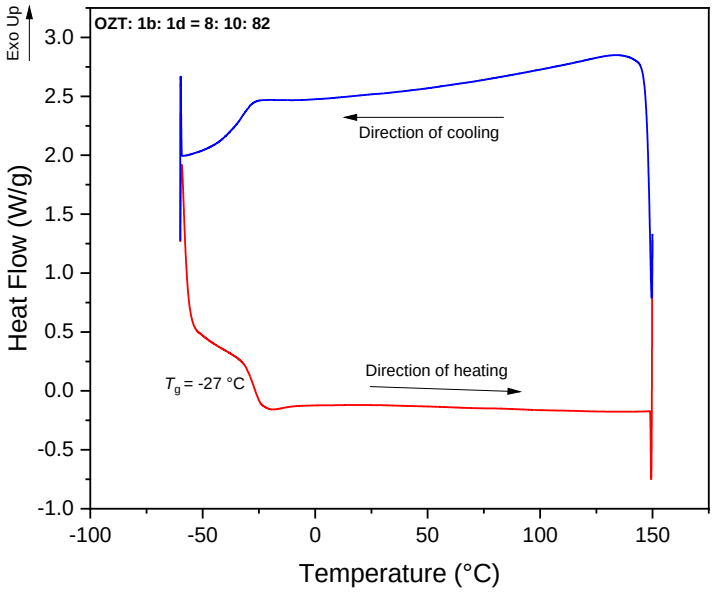

Figure S91: DSC thermogram showing the second cooling and heating cycle between –60 and 150 °C of the polymer produced from one-pot "tandem" functionalisation with ratio of BnBr and *t*BuBrAc = 0.25:0.75.

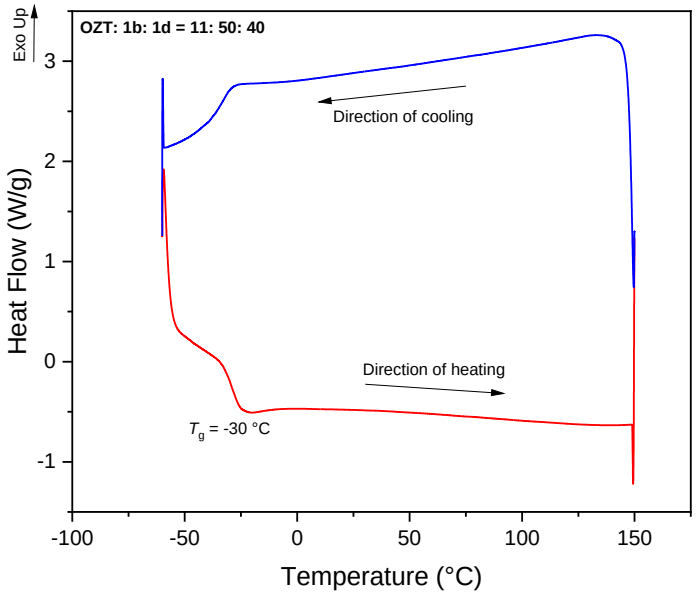

Figure S92: DSC thermogram showing the second cooling and heating cycle between –60 and 150 °C of the polymer produced from one-pot "tandem" functionalisation with ratio of BnBr and *t*BuBrAc = 0.75:0.25.

8. Thermogravimetric Analysis (TGA)

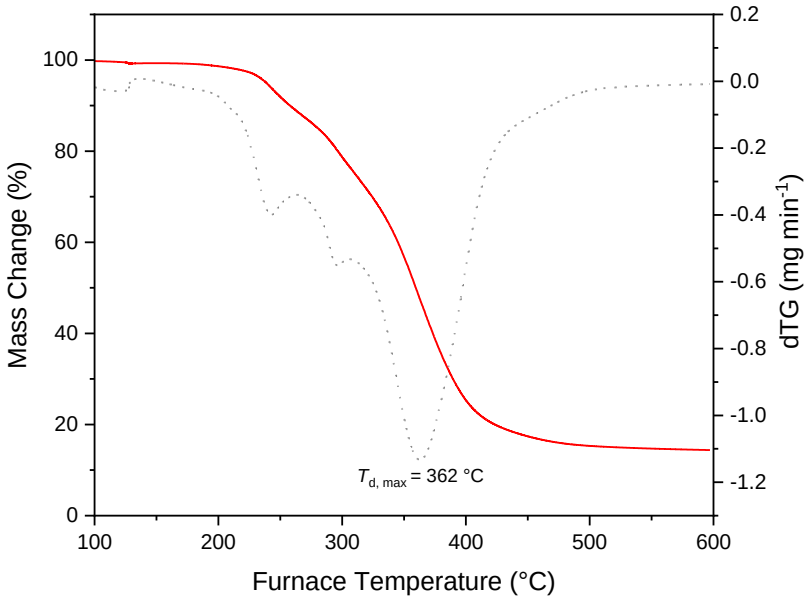

Figure S93: TGA trace of poly(**1a**-EDT) ($M_{n,\,SEC}$ = 15,000 g mol^{-1}, $Đ_M$ = 2.89, Table 1, entry 1). Obtained values: $T_{d,\,5\%}$ = 239 °C and $T_{d,\,max}$ = 362 °C with 14% char remaining at 600 °C.

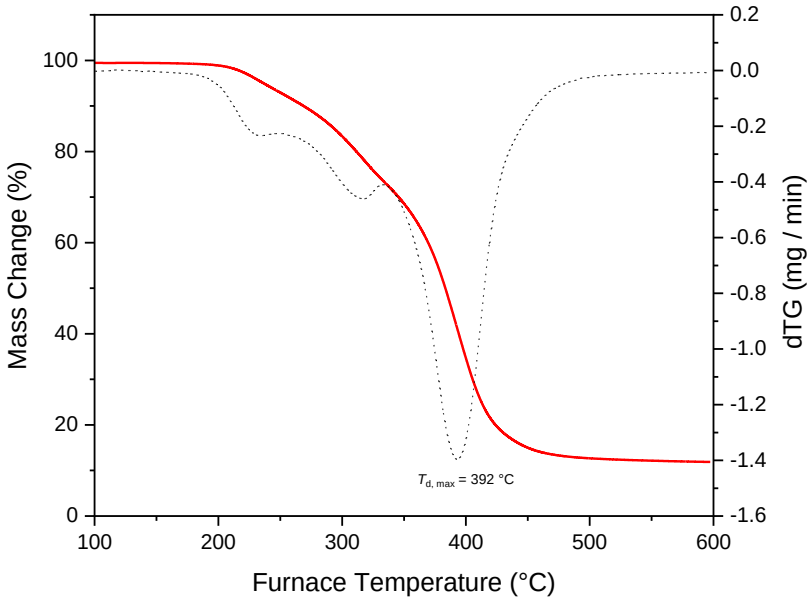

Figure S94: TGA trace of poly(**1a**-ODT) ($M_{n,\,SEC}$ = 11,000 g mol^{-1}, $Đ_M$ = 3.33, Table 1, entry 2). Obtained values: $T_{d,\,5\%}$ = 236 °C and $T_{d,\,max}$ = 392 °C with 12% char remaining at 600 °C.

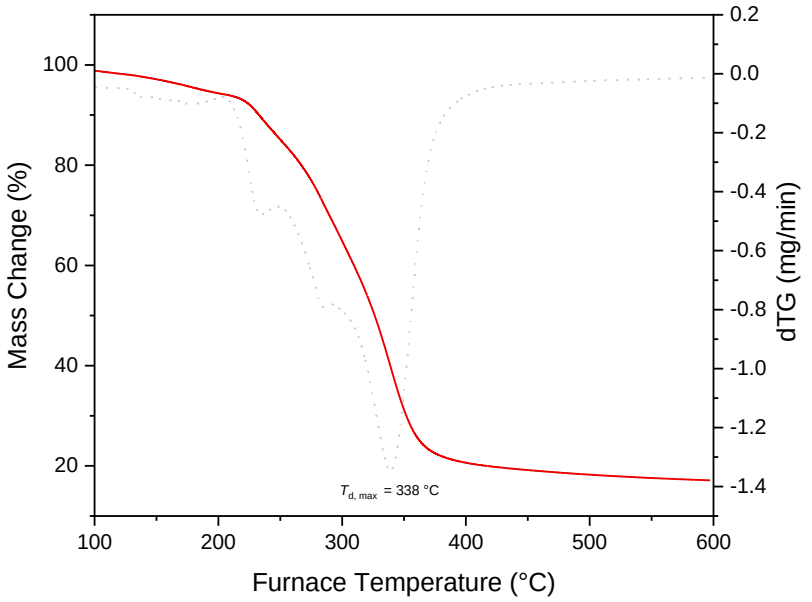

Figure S95: TGA trace of poly(**2a**-EDT) ($M_{n, SEC}$ = 5,900 g mol^{-1}, $Đ_M$ = 2.05, Table 1, entry 3). Obtained values: $\boldsymbol{T_{d, 5\%}}$ = 188 °C and $\boldsymbol{T_{d, max}}$ = 338 °C with 16% char remaining at 600 °C.

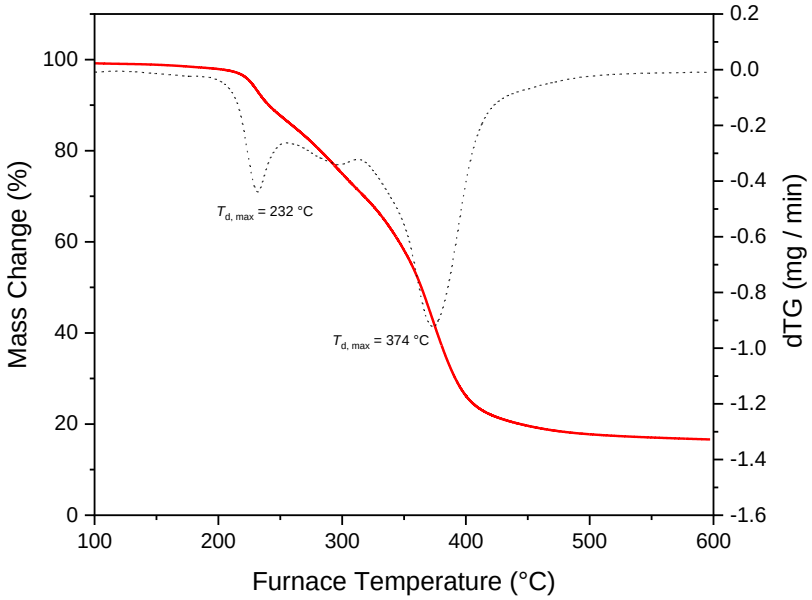

Figure S96: TGA trace of poly(**2a**-ODT) ($M_{n, SEC}$ = 9,500 g mol^{-1}, $Đ_M$ = 3.84, Table 1, entry 4). Obtained values: $\boldsymbol{T_{d, 5\%}}$ = 226 °C and $\boldsymbol{T_{d, max}}$ = 232 °C and 374 °C with 16% char remaining at 600 °C.

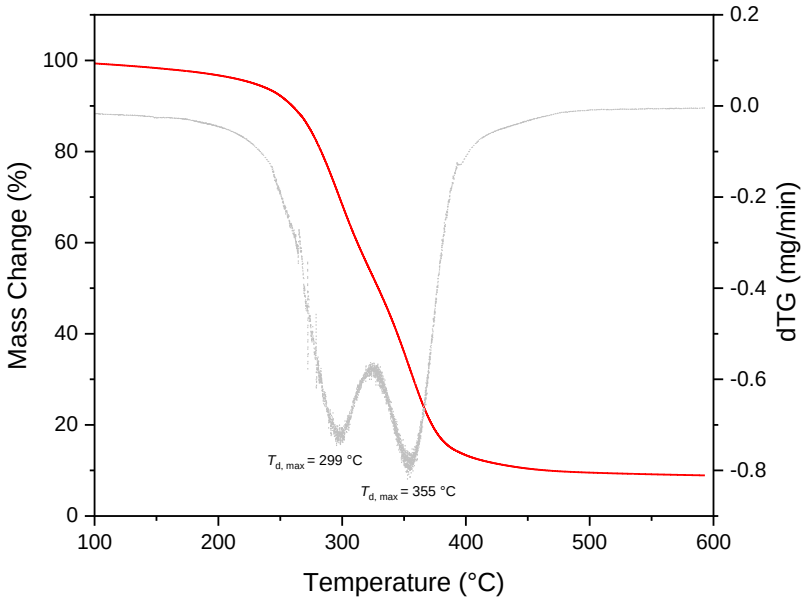

Figure S97: TGA trace of poly(**1b**-EDT) ($M_{n, SEC}$ = 4,200 g mol^{-1}, $Đ_M$ = 1.94, Table 1, entry 5). Obtained values: $\boldsymbol{T_{d, 5\%}}$ = 228 °C and $\boldsymbol{T_{d, max}}$ = 299 °C and 355 °C with 9% char remaining at 600 °C.

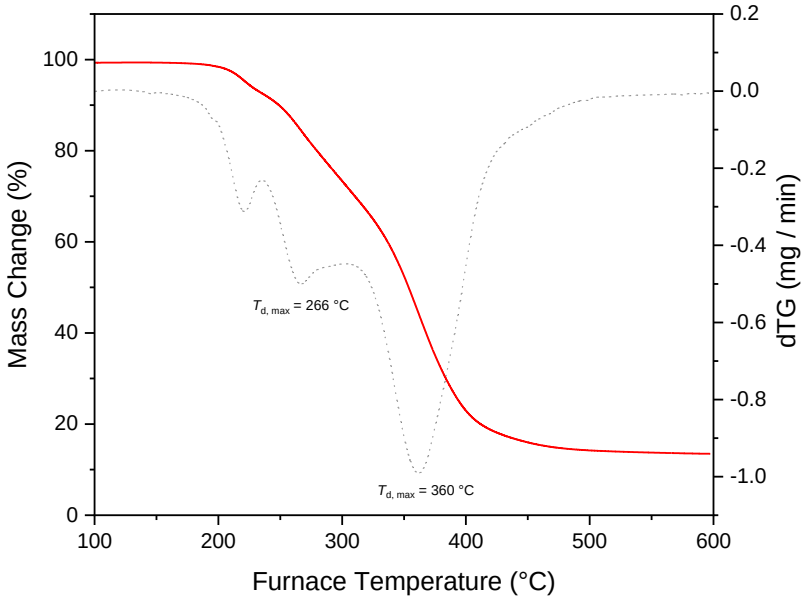

Figure S98*:* TGA trace of poly(**1d**-EDT) ($M_{n, SEC}$ = 8,900 g mol^{-1}, $Đ_M$ = 1.95, Table 1, entry 6). Obtained values: $\boldsymbol{T_{d, 5\%}}$ = 222 °C and $\boldsymbol{T_{d, max}}$ = 266 °C and 360 °C with 13% char remaining at 600 °C.

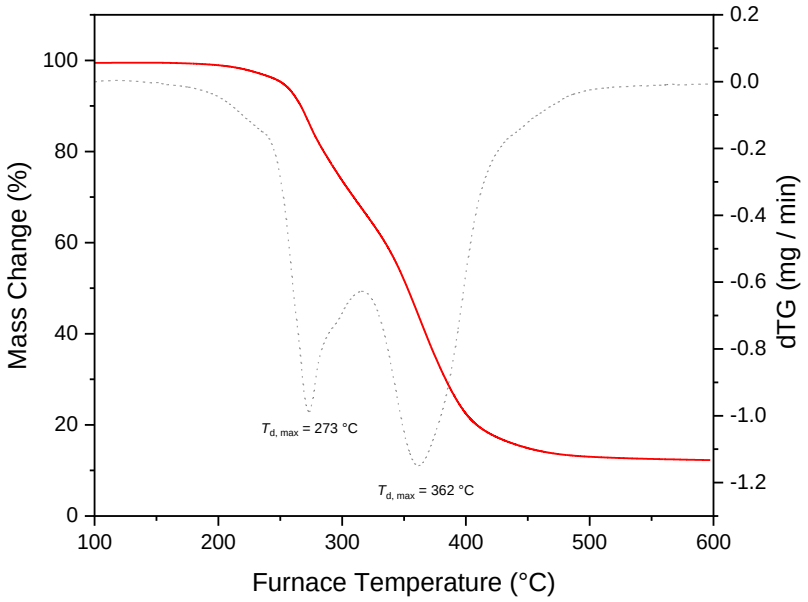

Figure S99: TGA trace of poly(**1f**-EDT) ($M_{n, SEC}$ = 7,600 g mol^{-1}, $Đ_M$ = 2.01, Table 1, entry 7). Obtained values: $\mathbf{T_{d, 5\%}}$ = 251 °C and $\mathbf{T_{d, max}}$ = 273 °C and 362 °C with 12% char remaining at 600 °C.

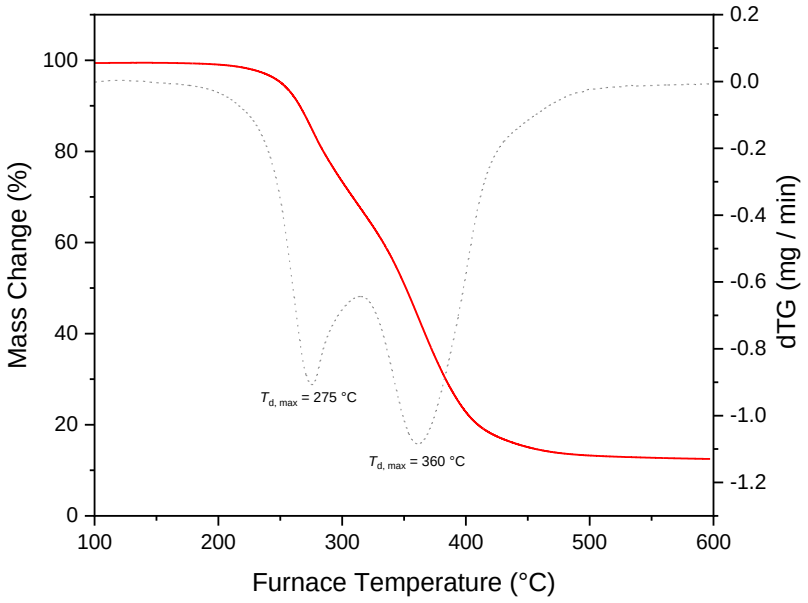

Figure S100: TGA trace of poly(**1g**-EDT) ($M_{n, SEC}$ = 9,400 g mol^{-1}, $Đ_M$ = 1.84, Table 1, entry 8). Obtained values: $\boldsymbol{T_{d, 5\%}}$ = 250 °C and $\boldsymbol{T_{d, max}}$ = 275 °C and 360 °C with 12% char remaining at 600 °C.

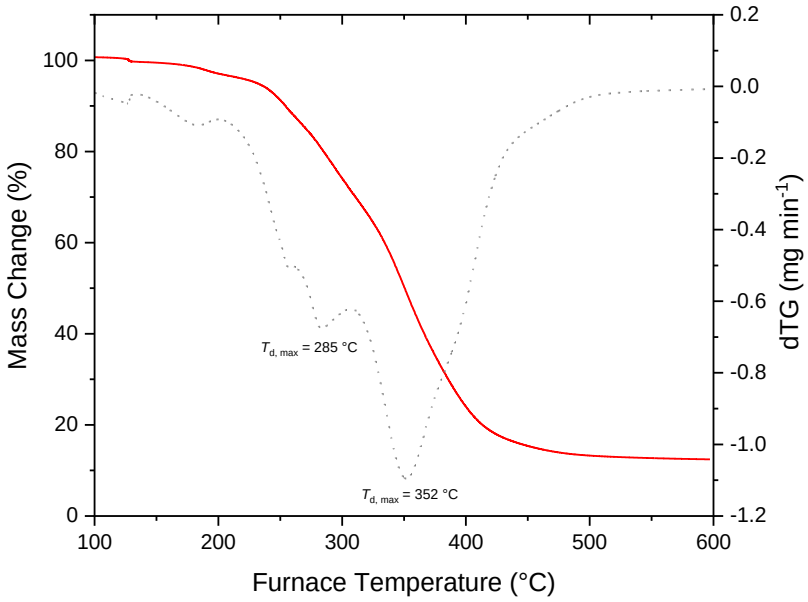

Figure S101*:* TGA trace of poly(**1h**-EDT) ($M_{n,\,SEC}$ = 6,400 g mol^{-1}, $Đ_M$ = 2,12, Table 1, entry 9). Obtained values: $T_{d,\,5\%}$ = 231 °C, $T_{d,\,max}$ = 285 °C and 352 °C with 14% char remaining at 600 °C.

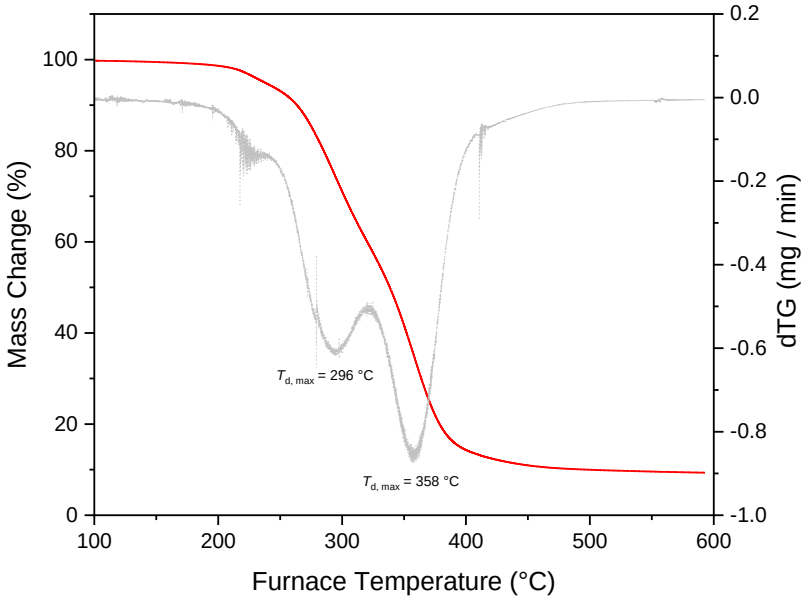

Figure S102: TGA trace of poly(**1b**-**1d**-EDT) ($M_{n,\,SEC}$ = 6,000 g mol^{-1}, $Đ_M$ = 4.85, Table 1, entry 10). Obtained values: $T_{d,\,5\%}$ = 237 °C and $T_{d,\,max}$ = 296 °C and 358 °C with 10% char remaining at 600 °C.

9. Additional Chemical Reaction Data

Table S1: Yield information of the poly(ester-thioethers) prepared in this work.

Polymer	Theoretical Yield / g	Isolated Yield / g	Percentage Yield / %
Poly(1a-EDT)	1.30	1.28	98
Poly(1a-ODT)	0.549	0.378	69
Poly(2a-EDT)	0.476	0.289	61
Poly(2a-ODT)	0.417	0.378	91
Poly(1b-EDT)	0.161	0.110	68
Poly(1d-EDT)	0.207	0.087	42
Poly(1f-EDT)	0.147	0.075	51
Poly(1g-EDT)	0.138	0.076	55
Poly(1h-EDT)	0.254	0.178	70

Table S2: S-alkylation of OZT functional group of **1a** with benzyl bromide under different reaction conditions.

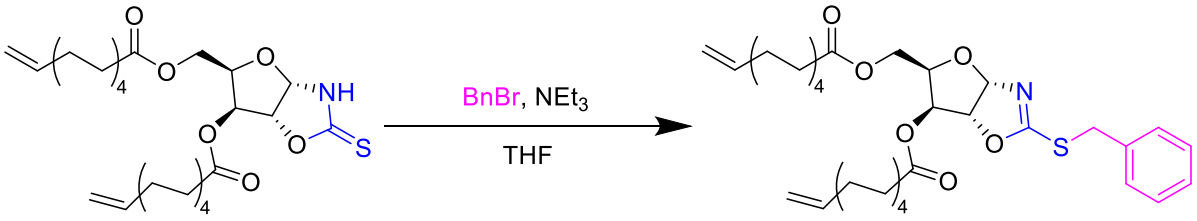

1a **1b**

Entry[a]	[1a] / mol L^{-1}	BnBr / equiv.	NEt_3 / equiv.	Solvent	Conversion / %[c]
1[b]	0.10	2.0	4.0	THF	70
2	0.25	2.0	4.0	THF	88
3	0.50	2.0	4.0	THF	94
4	1.00	2.0	4.0	THF	94
5	0.50	1.0	4.0	THF	71
6	0.50	1.2	4.0	THF	76
7	0.50	1.5	4.0	THF	84
8	0.50	2.0	2.0	THF	87
9	0.50	2.0	3.0	THF	85

[a]Reaction conditions unless otherwise stated: BnBr (1.0 – 2.0 equiv.), NEt_3 (2.0 – 4.0 equiv.), 0 °C addition of BnBr before allowing to warm to room temperature for 24 hours. [b]Literature reported reaction conditions for similar compounds from cited reference[5]. [c]Determined by the relative integration of anomeric protons of **1a** (5.89 ppm) and **1b** (6.13 ppm) from a crude sample of the reaction mixture.

Table S3: The effect of irradiation time on the alternating thiol-ene co-polymerisation of **1a** and 2,2-(ethylenedioxy)diethanethiol (EDT).

Entry[a]	Irradiation Time[b] / h	Conv.[c] / %	$M_{n\,(SEC)}$ [d] / g mol^{-1}	$Đ_M$[e]
1	1	100	4600	1.41
2	2	100	4300	1.40
3	3	100	4700	2.85
4	4	100	4000	1.23
5	5	100	3800	1.27
6	6	100	4900	1.28
7	7	100	3800	1.26

[a] Reaction conditions unless otherwise stated: 1.00 equiv. OZT-xylose diene, 1.00 equiv. of dithiol, 0.10 equiv. of IG819, $CHCl_3$ (0.5 M *w.r.t.* **1a**), [b] UV irradiation (λ = 365 nm) unless otherwise stated. [c] Determined by the disappearance of olefin signals (5.83-5.73 (ddt, 2H, *J* = 16.9, 10.2, 6.6 Hz, H-15) and (5.03 – 4.89 (m, 4H, H-16)). [d] Calculated by SEC relative to polystyrene standards in THF eluent. [e] $Đ_M = M_w/M_n$ as calculated by SEC.

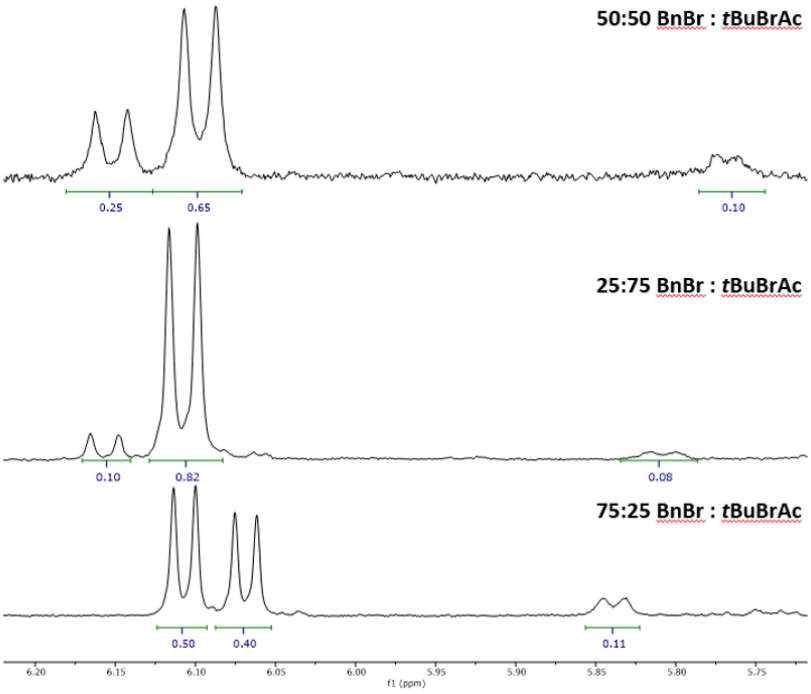

Figure S103: ^{1}H NMR of concurrent functionalisation reactions between region 6.20-5.75 ppm in $CDCl_3$.

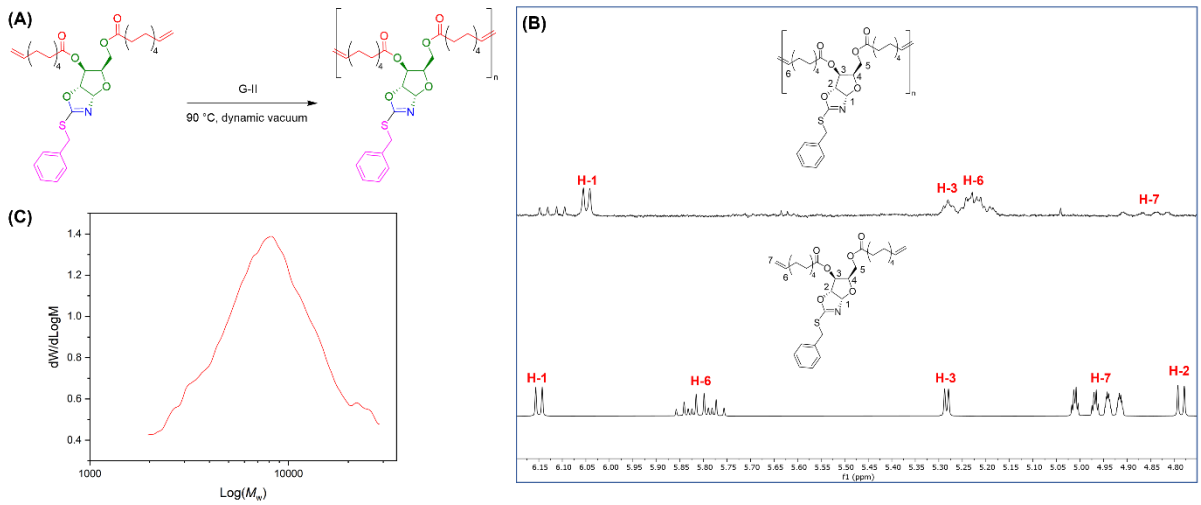

Figure S104: A). Reaction scheme for the ADMET polymerisation of monomer **1b**. **B).** ^{1}H NMR spectra (400 MHz, CDI_3) of poly(**1b**) (top) and **1b** (bottom) between the region of 6.15–4.80 ppm showing the disappearance of signals corresponding to the terminal olefin bonds of **1b** (5.86–5.77 and 5.01–4.91 ppm) and formation of the internal olefin bond H-6 (5.24–5.19 ppm). **C).** SEC trace of poly**(1b)** (6,100 g mol^{-1}, $Đ$ = 1.52) relative to polystyrene standards using a THF eluent.

References

1. J. Girniene, D. Gueyrard, A. Tatibouët, A. Sackus and P. Rollin, *Tetrahedron Lett.*, 2001, **42**, 2977-2980.

2. L. M. Lillie, W. B. Tolman and T. M. Reineke, *Polym. Chem.*, 2017, **8**, 3746-3754.

3. M. Piccini, J. Lightfoot, B. C. Dominguez and A. Buchard, *ACS Appl. Polym. Mater.*, 2021, **3**, 5870-5881.

4. M. Piccini, D. J. Leak, C. J. Chuck and A. Buchard, *Polym. Chem.*, 2020, **11**, 2681-2691.

5. M. Domingues, J. Jaszczyk, M. I. Ismael, J. A. Figueiredo, R. Daniellou, P. Lafite, M. Schuler and A. Tatibouët, *Eur. J. Org. Chem.*, 2020, **2020**, 6109-6126.